ELECTROSPINNING of BIOCOMPATIBLE POLYMERIC NANOFIBERS FUNCTIONALIZED with CYCLODEXTRIN INCLUSION COMPLEX

A THESIS

SUBMITTED TO THE MATERIALS SCIENCE AND NANOTECHNOLOGY

PROGRAM OF GRADUATE SCHOOL OF ENGINEERING AND SCIENCE

OF BILKENT UNIVERSITY

IN PARTIAL FULFILLMENT OF THE REQUIREMENTS

FOR THE DEGREE OF

MASTER OF SCIENCE

By

Zeynep Aytaç

August, 2012

I certify that I have read this thesis and that in my opinion it is fully adequate, in scope and in quality, as a thesis of the degree of Master of Science.

……

Assist. Prof. Dr. Tamer Uyar (Advisor)

I certify that I have read this thesis and that in my opinion it is fully adequate, in scope and in quality, as a thesis of the degree of Master of Science.

……

Assist. Prof. Dr. Turgay Tekinay

I certify that I have read this thesis and that in my opinion it is fully adequate, in scope and in quality, as a thesis of the degree of Master of Science.

……

Assist. Prof. Dr. Fatih Büyükserin

Approved for the Graduate School of Engineering and Science:

……

Prof. Dr. Levent Onural

Director of the Graduate School of Engineering and Science

ABSTRACT

ELECTROSPINNING of BIOCOMPATIBLE POLYMERIC NANOFIBERS FUNCTIONALIZED with CYCLODEXTRIN INCLUSION COMPLEX

Zeynep Aytaç

M.S. in Materials Science and Nanotechnology

Supervisor: Assist. Prof. Dr. Tamer Uyar

August, 2012

Electrospinning is a simple, versatile and cost-effective method to produce nanofibers. Electrospun nanofibers have high surface area to volume ratio and nanoporous structure. Moreover, electrospun nanofibers could be functionalized with additives to extend their application areas. Cyclodextrins (CDs) are cyclic oligosaccharides and have truncated-cone shape structure. Due to their hydrophobic cavity, CDs have ability to form inclusion complex (IC) with a variety of molecule. In our study, we functionalized electrospun nanofibers with CDs and CD-ICs.

In the first part, we successfully produced hydroxypropyl cellulose- (HPC), carboxymethyl cellulose- (CMC) and alginate-based nanofibers via electrospinning. Then we functionalized these nanofibers with CDs. The morphological characterizations of nanofibers were performed through scanning electron microscopy (SEM). Here, we have combined the properties of both electrospun nanofibers and CDs, and these nanofibers could be used in drug delivery, wound healing and tissue engineering applications.

In the second part, we prepared IC of sulfisoxazole (SFS) (hydrophobic drug) with hydroxypropyl-beta-cyclodextrin (HPβCD) (SFS/HPβCD-IC). Then electrospinning of SFS/HPβCD-IC incorporating hydroxypropyl cellulose (HPC) nanofibers were performed (SFS/HPβCD-IC-HPC-NFs). In the third part of our study, we produced IC of α-tocopherol (α-TC) (antioxidant molecule) with beta-cyclodextrin (β-CD) (α-TC/β-CD-IC); and polycaprolactone (PCL) nanofibers incorporating α-TC/β-CD-IC was obtained via electrospinning (α-TC/β-CD-PCL-NFs). In the fourth part, IC of allyl isothiocyanate (AITC) (antibacterial compound) with β-CD (AITC/β-CD-IC) was produced. The electrospinning of AITC/β-CD-IC incorporating polyvinyl alcohol (PVA) nanofibers was carried out (AITC/β-CD-IC-PVA-NFs). In the fifth part, IC of quercetin (QU) (antioxidant molecule) with β-CD (QU/β-CD-IC) was prepared; and polyacrylic acid (PAA) nanofibers incorporating QU/β-CD-IC was obtained via electrospinning (QU/β-CD-IC-PAA-NFs). The structural and thermal characterizations of SFS/HPβCD-IC-HPC-NFs, α-TC/β-CD-PCL-NFs, AITC/β-CD-IC-PVA-NFs and QU/β-CD-IC-PAA-NFs were carried out by scanning electron microscopy (SEM), X-ray diffraction (XRD), differential scanning calorimetry (DSC) and thermogravimetric analysis (TGA). The amount of released molecules were determined via liquid chromatography-mass spectroscopy (LC-MS) for SFS/HPβCD-IC-HPC-NFs; high performance liquid chromatography (HPLC) for α-TC/β-CD-PCL-NFs and QU/β-CD-IC-PAA-NFs and gas chromatography-mass spectrometry (GC-MS) for AITC/β-CD-IC-PVA-NFs. The antioxidant activity of α-TC/β-CD-PCL-NFs and QU/β-CD-IC-PAA-NFs was investigated by using 2,2-diphenyl-1-picrylhydrazyl (DPPH) radical scavenging assay. Moreover, α-TC/β-CD-PCL-NFs released great proportion of α-TC after exposing UV light. Thus, α-TC/β-CD-PCL-NFs exhibited quite high photostability. The antibacterial activity of AITC/β-CD-IC-PVA-NFs was evaluated by colony counting method against Escherichia coli (E.coli) and Staphylococcus aureus (S.aureus). In brief, we concluded that SFS/HPβCD-IC-HPC-NFs, α-TC/β-CD-PCL-NFs, AITC/β-CD-IC-PVA-NFs and QU/β-CD-IC-PAA-NFs are promising materials for drug delivery and wound healing applications.

Keywords: electrospinning, nanofibers, biopolymers, cyclodextrin, inclusion complex, sulfisoxazole, α-tocopherol, allyl isothiocyanate, quercetin, controlled release.

ÖZET

ELEKTROEĞİRME YÖNTEMİ İLE SİKLODEKSTRİN İNKLÜZYON KOMPLEKSLERİYLE FONKSİYONLAŞTIRILMIŞ BİYOUYUMLU NANOLİFLERİN ÜRETİLMESİ

Zeynep Aytaç

Yüksek Lisans, Malzeme Bilimi ve Nanoteknoloji Bölümü

Tez Yöneticisi: Yard. Doç. Dr. Tamer Uyar

Ağustos, 2012

Elektroeğirme nanolif elde etmek için basit, verimli ve maliyeti düşük bir yöntemdir. Elektroeğirme yöntemiyle elde edilen nanolifler yüksek yüzey alanına ve nano boyutta gözenekli yapıya sahiptir. Dahası, bu nanolifler uygulama alanlarını genişletmek amacıyla katkı maddeleri ile fonksiyonel hale getirilebilirler. Siklodekstrinler (CD), kesik koni şeklindeki siklik oligosakkaritlerdir. Hidrofobik kaviteleri sayesinde, pek çok molekülle inklüzyon kompleksi (IC) oluşturabilirler. Çalışmalarımızda, elektroeğirme yöntemiyle elde edilen nanolifleri CD ve CD-IC ile fonksiyonel hale getirdik.

İlk kısımda, hidroksipropil selüloz (HPC), karboksimetil selüloz (CMC) ve aljinat nanoliflerini elektroeğirme yöntemi ile başarıyla ürettik. Daha sonra bu nanolifleri CD'lerle fonksiyonel hale getirdik. Bu nanoliflern morfolojik karakterizasyonları taramalı electron mikroskobu (SEM) yardımıyla yapıldı. Burada, elektroeğirme ile üretilen nanoliflerin ve CD'lerin özelliklerini

birleştirmiş olduk. Bu nanolifler ilaç salımı, yara iyileştirme ve doku mühendisliği alanlarında kullanılabilirler.

İkinci kısımda, sülfisoksazol (SFS) (hidrofik ilaç) ile hidroksipropil-beta-siklodekstrin (HPβCD) inklüzyon kompleksini (IC) (SFS/HPβCD-IC) hazırladık. Daha sonra SFS/HPβCD-IC içeren hidroksipropil selüloz (HPC) nanolifleri elektroeğirme yöntemiyle üretildi. Çalışmamızın üçüncü kısmında, α-tokoferol (α-TC) (antioksidan madde) ile beta-siklodekstrin (β-CD) IC (α-TC/β-CD-IC) ürettik; ve α-TC/β-CD-IC içeren polikprolakton (PCL) nanolifleri elektroeğirme ile elde edildi (α-TC/β-CD-IC-PCL-NFs). Dördüncü kısımda, alil izotiyosiyanat (AITC) (antibakteriyel madde) ile β-CD IC (AITC/β-CD-IC) üretildi. AITC/β-CD-IC içeren polivinil alkol (PVA) nanolifleri elektroeğirme ile üretildi (AITC/β-CD-IC-PVA-NFs). Beşinci kısımda, kuersetin (QU) (antioksidan madde) ile β-CD IC (QU/β-CD-IC) hazırlandı ve QU/β-CD-IC içeren poliakrilik asit (PAA) nanolifleri elektroeğirme ile elde edildi (QU/β-CD-IC-PAA-NFs). SFS/HPβCD-IC-HPC-NFs, α-TC/β-CD-IC-PCL-NFs, AITC/β-CD-IC-PVA-NFs ve QU/β-CD-IC-PAA-NFs'nin yapısal ve ısıl karakterizasyonları taramalı elektron mikroskobu (SEM), X-ışını kırınımı (XRD), diferansiyel tarama kalorimetrisi (DSC) ve termogravimetrik analiz (TGA) ile yapıldı. Nanoliflerden salınan moleküllerin miktarı SFS/HPβCD-IC-HPC-NFs için sıvı kromatografisi-kütle spektrometresi (LC-MS); α-TC/β-CD-IC-PCL-NFs ve QU/β-CD-IC-PAA-NFs için yüksek performanslı sıvı kromatografisi (HPLC) ve AITC/β-CD-IC-PVA-NFs için gaz kromatografisi-kütle spektrometresi (GC-MS) yardımıyla belirlendi. α-TC/β-CD-IC-PCL-NFs ve QU/β-CD-IC-PAA-NFs'nin antioksidan aktivitesi 2 2-difenil-1-pikrilhidrazil (DPPH) radikal temizleme testiyle incelendi. Dahası, α-TC/β-CD-PCL-NFs UV ışığına maruz bırakıldıktan sonra da α-TC'nin büyük bir kısmını salmıştır. Bu nedenle, α-TC/β-CD-IC-PCL-NFs oldukça yüksek fotostabilite göstermiştir. AITC/β-CD-IC-PVA-NFs'nin Escherichia coli (E.coli) and Staphylococcus aureus'a karşı antibakteriyel etkisi koloni sayma metoduyla belirlendi. Kısacası, SFS/HPβCD-IC-HPC-NFs, α-TC/β-CD-IC-PCL-NFs, AITC/β-CD-IC-PVA-

NFs ve QU/β-CD-IC-PAA-NFs'nin ilaç salımı ve yara iyileştirme uygulamalarında gelecek vadeden malzemeler oldukları sonucunda vardık.

Anahtar Kelimeler: elektroeğirme, nanolif, biyopolimer, siklodekstrin, inklüzyon kompleks, sülfisoksazol, α-tokoferol, alil izotiyosiyanat, kuersetin, kontrollü salım.

ACKNOWLEDGEMENT

I would like to express my sincerest gratitude to my supervisor Assist. Prof. Dr. Tamer Uyar for his guidance, support, patience and providing me with an excellent atmosphere for doing research.

I would like to thank the members of my group members Aslı Çelebioğlu, Fatma Kayacı and Yelda Ertaş for their support and valuable friendship.

I would like to thank Asst. Prof. Dr. Turgay Tekinay and his student Özgün Candan Onarman Umu for their collaboration in antibacterial test experiments.

I would like to acknowledge State Planning Organization (DPT) of Turkey for its support to UNAM Institute of Materials Science and Nanotechnology, and The Scientific and Technological Research Council of Turkey (TÜBİTAK) for their financial support.

I would also like to thank my parents, my sister İrem Aytaç and Damla Uzun for their understanding, support and encouragement.

TABLE OF CONTENTS

LIST OF FIGURES

LIST OF TABLES

PART I.

INTRODUCTION

1.1. Electrospinning

Nanofibers with their porous structure and high surface-to-volume ratio are highly promising materials that can be used in various applications. There are many methods to produce nanofibers like drawing, template synthesis, phase separation, self-assembly, electrospinning, etc. [1]. Among these methods, electrospinning is a universal method to produce nanofibers having diameter ranging from 10 nanometers to a few microns [2]. In electrospinning, one can use polymers, polymer blends, sol-gels and ceramic precursors to obtain nanofibers and different structures such as core-shell, hollow, ribbon-like, porous and aligned nanofibers can be produced [3]. Electrospinning is superior to other methods with its relatively low cost, high production rate and simplicity [4]. In addition to unique properties of nanofibers, electrospun nanofibers are easily functionalized with nanoparticles, additives, bioactive agents; therefore, multifunctional electrospun nanofibers can be produced [5].

Electrospinning set-up has three main components; these are high voltage power supply, syringe pump and grounded collector (Figure 1). The basic principle of electrospinning relies on formation of nanofibers through electric field. The solution in a syringe is pumped through the outlet of the spinneret at a controlled rate by means of syringe pump. At the same time, high voltage in 10-30 kV range is applied from high voltage power supply; particles within the solution are charged and create a repulsive force; this results in deformation of drop in cone-shaped named as Taylor cone. When threshold voltage value is surpassed, the repulsive force overcomes the surface tension of the solution and polymer jet is formed in the tip of spinneret. While aforementioned jet going towards the grounded collector, the solvent evaporates and nanofibers are collected on the collector [1,4].

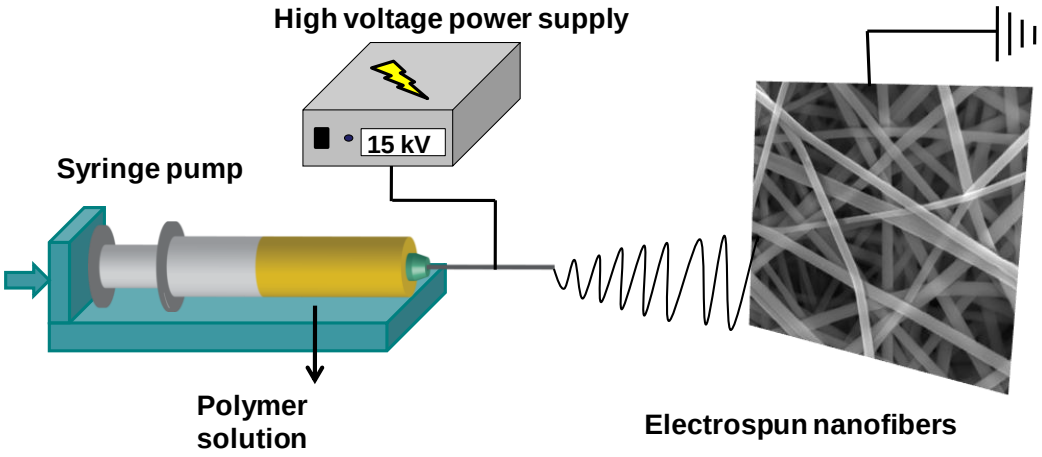

Figure 1. Schematic view of electrospinning.

The history of electrospinning dates back to 1900s; electrical charge was firstly used to spray liquids by Cooley and his studies was patented in 1902 [6-8]. Then, Formhals received a patent which is on electrospinning of polymer filaments [9]. After almost 40 years, Simm et al. produced nanofibers which have diameter below 1μm via electrospinning and this study was patented as well [10]. But until 1990s there was no significant study on this technique. In early 1990s, Reneker's group started to study on electrospinning [11-13] and this technique has gained reputation. Today it is being used by many research groups as well as industries all around the world.

In regard to parameters of electrospinning, there exist three main groups: polymer/solution parameters, processing conditions and environmental conditions [1]. In order to obtain uniform nanofibers with electrospinning, one should optimize all these parameters. First of all, polymer/solution parameters are of vital importance for electrospinning. These are type, molecular weight and molecular weight distribution of the polymer; surface tension, dielectric constant, conductivity, concentration and viscosity of the solution [1]. Initially, molecular weight and concentration are the factors affecting viscosity of the polymer solution. Since certain amount of viscosity is required for a polymer solution to be electrospun, polymer with suitable molecular weight and concentration should be used to obtain electrospun nanofibers. Effect of increasing concentration (viscosity) on electrospinning of carboxymethyl

cellulose (CMC) was shown in Figure 2. Secondly, as conductivity of the solution increases, more charges are formed in the solution, so stretching of the solution increases. As a result, nanofibers with a smaller diameter are obtained. Thirdly, impact of dielectric constant of the solvent should be considered. While the dielectric constant of the solution rises; electrospinnability of solution is improved, and diameter of the solutions reduces. Last but not least, surface tension has an influence on formation of nanofibers from electrospinning. Because in order nanofibers to be formed; surface tension of polymer solution must be overcame by electrical forces [1].

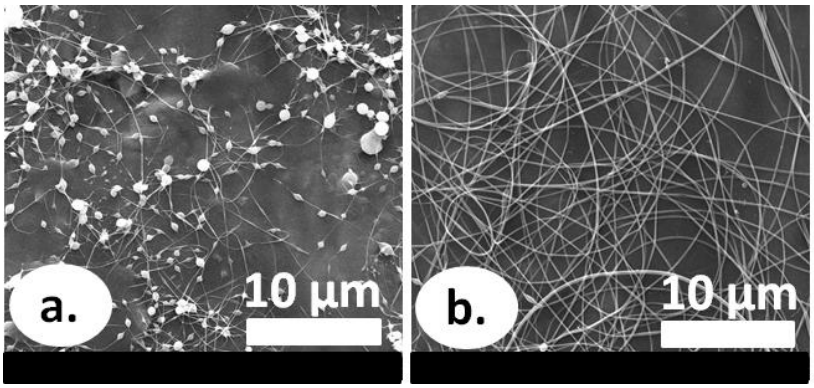

Figure 2. Effect of concentration in electrospinning of carboxymethyl cellulose (CMC)/polyethyleneoxide (PEO) nanofibers: a) 2.25% CMC-0.75%PEO, b) 3% CMC-1%PEO.

On the other hand, process conditions are of secondary significance in the formation of electrospun nanofibers. These are applied voltage, distance from tip of the spinneret to collector, feed rate, needle diameter and type of the collector [1]. Basically, high voltage is required to produce nanofibers by electrospinning. Owing to high voltage, electrostatic force is formed and surface tension of polymer is surpassed. In addition, further increase in applied voltage cause formation of thinner nanofibers in diameter, because of higher electric field caused the higher stretching of solution. On the other hand, decrease in the distance from tip of the spinneret to collector lead to increase in electric field; thus, average fiber diameter decreases. Mostly, low feed rate is preferred rather than high; in order to allow solvent to evaporate. Otherwise, due to the great amount of solution fed towards to the collector, nanofibers are most likely to

coalesce on top of another on the collector without finding time to evaporate. The needle diameter is another factor influences the morphology and uniformity of electrospun nanofibers. First of all, it is important to use suitable needle in diameter according to the viscosity of solution. The smaller needle diameter leads to formation of small polymer droplet in the tip of the spinneret; therefore the surface tension of the so-called droplet is getting higher. So the greater amount of voltage and indirectly more time is needed nanofibers to be obtained. Finally, the collector is covered with a conductive material such as aluminum foil to increase efficiency of nanofibers' deposition on collector. In addition, type of the collector has great contribution to achieve different kinds of structures through the use of electrospinning. For instance, aligned nanofibers could be obtained by using rotating collector in electrospinning system [1].

Lastly, environmental conditions such as temperature, humidity and pressure are of importance on the morphology of nanofibers obtained via electrospinning [1]. To illustrate, temperature rise triggers viscosity and surface tension to decrease; whereas conductivity to increase. So, average fiber diameter decreases with the increasing of temperature [14]. On the other side, the rise in humidity decelerates the evaporation of solvent; therefore average fiber diameter increases. Moreover, porous nanofibrous structure might be formed with the increase in the humidity [15].

Owing to the unique properties of electrospun nanofibers like high surface area to volume ratio, diameters at nanoscale and possibility to produce different structures from various materials; electrospun nanofibers can be used in textile [5], environmental applications (separation membranes, affinity membranes, water filter, air filter) [16]; energy (solar cells, fuel cells, supercapacitors, hydrogen storage, optoelectronics, transistor) [16]; defense&security (chemical/biological protection and sensor) [3], biomedical applications (tissue scaffolds, wound healing materials and delivery of bioactive molecules) [17-18] and immobilization of catalysts/enzymes [5] (Figure 3).

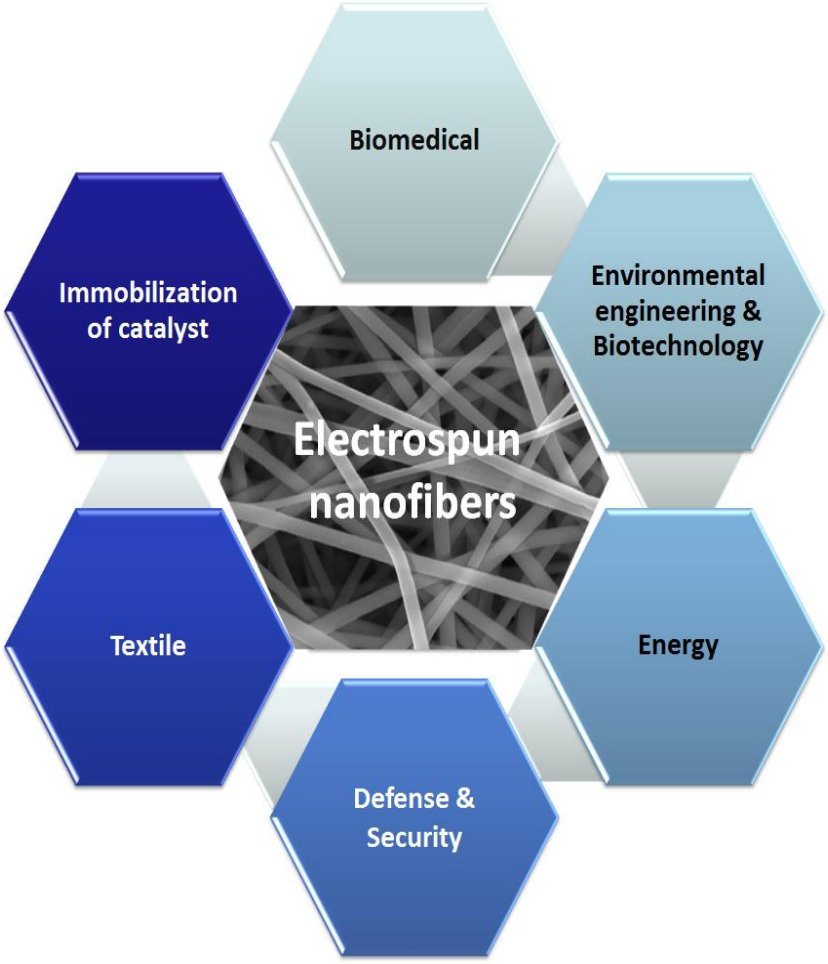

Figure 3. Applications of electrospun nanofibers.

Electrospun nanofibers in biomedical applications include tissue scaffolds, wound healing materials and delivery of bioactive molecules [5,17-18]. Initially, in order for a material to be used in biomedical applications; it should have high porosity that makes it to be physically similar with extracellular matrix found in native tissues and as low as possible fiber diameter (nanoscale range). Therefore electrospun nanofibers have ability to fulfill the requirements of biomedical materials thanks to its high surface to volume ratio and highly porous structure. In addition, above-mentioned unique properties of electrospun nanofibers enhance cell attachment, drug loading, and mass transfer properties as well [17]. There exist many biocompatible and biodegradable polymers that can be electrospun, this variety in polymer types make electrospun nanofibers quite applicable for biomedical applications [17]. Moreover, electrospun nanofibers

could be used as wound healing materials especially for burns and abrasions [5]. The large surface area to volume ratio and porous structure provide absorption of liquid and gases; releasing of the drugs at the same time; whereas protecting wounds from bacterial penetration [5,18].

1.2. Electrospinning of biopolymers and biodegradable polymers

In general, polymers are produced from non-renewable materials and not biodegradable. This situation has caused environmental problems. In order to overcome these problems, there is a gradually increasing interest in biopolymers and synthetic biodegradable polymers. Biopolymers are produced by microorganisms, plants and animals or synthesized from biological materials like amino acids, sugars etc. [19]. They have properties such as biodegradability, biocompatibility and sustainability. On the other hand, biopolymers might have different molecular weight, degree of substitution, crystallinity etc. In addition, it is very difficult to control the properties of them during processing, since different conditions should be applied even for different batches of the same polymer.

In principle, biopolymers are divided into three groups: polynucleotides (DNA, RNA), polypeptides and polysaccharides (starch, chitin, chitosan, cellulose and its derivatives; hyaluronic acid, glycogen, alginate etc.) [20]. Polysaccharides consist of several monosaccharide molecules and are linked by glycosidic bonds [19]. Cellulose is a kind of polysaccharide that can be produced by plant tissues or certain bacteria [19]. It composes of D-anhydro-glucose repeating units and linked by 1, 4-β-D-glycosidic bridges. It is the most common polymer with properties like biodegradability and renewability [20-21]. The presence of many hydroxyl groups in the structure leads to formation of inter- and intra-hydrogen bonds. Thereby cellulose does not dissolve in common solvents [20]. Cellulose has many derivatives like cellulose acetate (CA), ethyl cellulose (EC), hydroxypropyl cellulose (HPC), hydroxypropyl methylcellulose (HPMC), carboxymethyl cellulose (CMC) etc. These are synthesized by substitution of some of the hydroxyl groups of cellulose with another functional

group. In general, cellulose derivatives overcome the problem of cellulose regarding solubility in common solvents [20].

Through electrospinning method, various polymers can be used to obtain nanofibers. However, usually electrospinning of polysaccharides into nanofibers is problematic [22]. The formation of nanofibers from polysaccharides might be related with shear thinning property of the polymer and lack of sufficient chain entanglement. Initially, in order for a solution to be electrospun into nanofibers chain entanglements must be formed before the evaporation of solvent during electrospinning process. The formation of entanglement is related with chain conformation of polysaccharide. Hence, as compactness of the structure increases, fewer entanglements are formed [23]. Secondly, especially anionic polysaccharides exhibit shear thinning behavior which results in breaking of the polymer jet during electrospinning process and hinders the formation of nanofibers [23].

Biodegradation is the decomposition of a material by environmental means such as sunlight, temperature or biological means like bacteria and microorganisms [24]. The synthetic polymers like poly (ε-caprolactone) (PCL), polyvinyl alcohol (PVA), poly (acrylic acid) (PAA) are classified as biodegradable polymers [25]. For instance, PCL is degraded by enzymes or lipases of microorganisms [24]. It is linear polyester synthesized from Ɛ-caprolactone by ring-opening polymerization and it is a hydrophobic polymer. It finds application in pharmacy and agriculture areas [25]. On the other side, PVA is a hydrophilic polymer and synthesized by hydrolysis acetate groups of poly (vinyl acetate). It is widely used polymer in paper processing, textile sizing, finishing adhesives and binders [25]. PAA is a hydrophilic polymer and synthesized from acrylic acid.

Many groups have produced PCL nanofibers by electrospinning. In these studies various solvent systems were used such as: chloroform, chloroform/methanol, chloroform /acetone, chloroform/ethanol, chloroform/ dimethylformamide (DMF), dichloromethane (DCM), DCM/DMF,

DCM/methanol, acetone, trifluoroethanol (TFE) , TFE/water, DMF/ tetrahydrofuran (THF), glacial acetic acid, 90% acetic acid, glacial formic acid, formic acid/acetone [26-27]. There are drug delivery studies of electrospun PCL nanofibers in the literature [28-31]. PVA is commonly used polymer in electrospinning method and it is generally dissolved in water to be electrospun. In the literature, there exist studies regarding drug delivery applications of electrospun PVA nanofibers [32-35]. Electrospinning of PAA was also studied for drug delivery applications [36-37].

1.3. Cyclodextrins

Cyclodextrins (CDs) are cyclic oligosaccharides and linked by α-(1,4) glucopyranose units [38-39]. The native CDs are (alpha-cyclodextrin) (α-CD), beta-cyclodextrin (β-CD), gamma-cyclodextrin (γ-CD) with 6, 7, 8 glucopyranose units, respectively. The height of cavity in three native CDs is the same but cavity volume; outer diameter and cavity diameter gradually increases from α-CD to γ-CD [38] (Figure 4). The main properties of α-CD, β-CD, and γ-CD are shown in Table 1. The solubility of native CDs differs from each other due to the hydrogen bond formation between C-2-OH groups and C-3-OH groups of neighboring glucopyranose units. Thus, complete secondary belt is formed by these hydrogen bonds. As α-CD is only able to form four hydrogen bonds instead of six and γ-CD has a non-coplanar and flexible structure; these two CDs are much more soluble in water as compared to β-CD [39]. β-CD is the least water soluble among three native CDs because of its rigid structure. Moreover, several CD derivatives such as methyl-β-CD, hydroxypropyl β-CD, hydroxypropyl γ-CD, sulfobutylated β-CD were synthesized by substitution of primary and secondary hydroxyl groups of the cyclodextrins to improve the safety and solubility of CDs. CD derivatives might have different cavity volume, solubility, stability against light or oxygen than their parent CDs [38]. CDs are synthesized by degradation of starch with the help of glucosyl transferase enzyme (CGTase) produced by several microorganisms such as bacillus macerans, klebsiella oxytoca, bacillus circulans and alkalophylic bacillus [39].

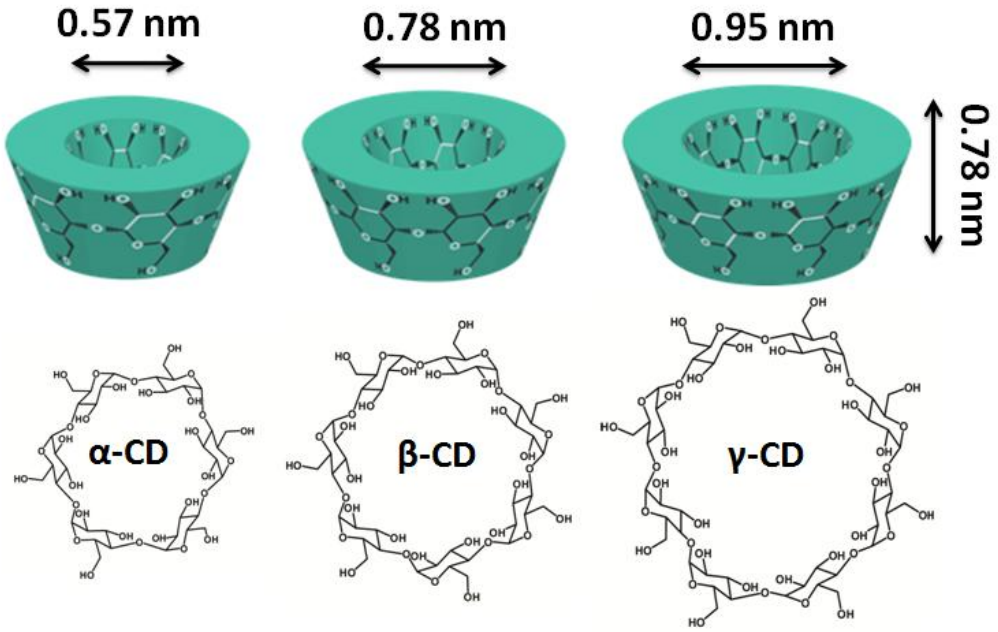

Figure 4. Schematic views and chemical structures of α-CD, β-CD, γ-CD.

Table 1. General properties of cyclodextrins [39].

Properties	***α-cyclodextrin***	***β-cyclodextrin***	***γ-cyclodextrin***
Number of glucopyranose units	6	7	8
Molecular weight (g/mol)	972	1135	1297
Solubility in water at 25 ^{o}C (g/100 mL)	14.5	1.85	23.2
Outer diameter (Å)	14.6	15.4	17.5
Cavity diameter (Å)	5.7	7.8	9.5
Height of torus (Å)	7.9	7.9	7.9
Approximate cavity volume (Å^3)	174	262	427

The secondary hydroxyl groups of CDs are located in one edge of the ring; whereas primary hydroxyl groups are in the other edge. As the free rotation ability of primary hydroxyl groups lead to smaller diameter of the cavity in that edge; the diameter of the two edges of the ring is not same. So, CDs have truncated cone shape structure [39]. In addition, apolar hydrogens and ether-like

oxygens are situated inside the truncated cone shape molecule. Therefore, CDs have relatively hydrophobic cavity [38]. Owing to this cavity, CDs are able to form host-guest interactions, that is inclusion complexes with various solid, liquid, gaseous molecules [38].

CDs (host) form inclusion complexes with guest molecules in appropriate polarity and dimension (Figure 5). The main driving force of the inclusion complexation is substitution of water molecules inside the cavity by hydrophobic guest molecule. Since in the apolar cavity of CDs there are slightly apolar water molecules with high entalpy; so the addition of apolar (hydrophobic) guest molecule gave rise to the replacement of high entalpy water molecules with the guest molecule [38]. Thereby, apolar-apolar association is formed and more stable energy state is achieved with the decrease of CD ring strain [68]. The inclusion complex is a dynamic process and neither covalent bonds are broken nor new covalent bonds are formed [38]. There are many advantages that inclusion complex have over the pure guest molecule for instance, higher solubility of hydrophobic guests, higher thermal stability, control of volatility and sublimation, masking off unpleasant odors, and controlled release of drugs and flavors [38].

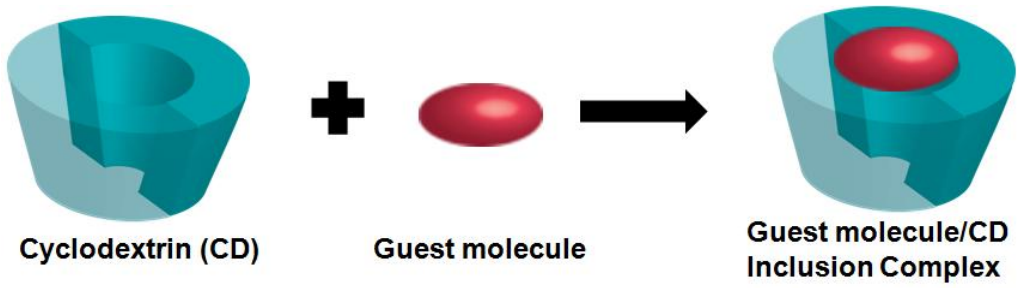

Figure 5. Schematic view of inclusion complex formation between CD and guest molecule.

CDs are widely used in analytical chemistry; food, cosmetic, pharmaceutical, chemical, textile and paper industries; also in pesticides, flavors, adhesives and coatings [38-40]. In pharmaceutical industry in which drugs are sparingly soluble in water, CDs are of vital importance. The conventional drug formulation systems are not enough to attain drug

formulations without adverse effects and irritation. However, CDs increase solubility, enhance stability, improve bioavailability, reduce dose and volatility of the so-called drugs and masking the unpleasant odors and bitter tastes [38,40].

PART II.

CHAPTER I. ELECTROSPINNING of POLYSACCHARIDES FUNCTIONALIZED with CYCLODEXTRINS

2.1. General Information

Polysaccharides are one of the main groups of biopolymers [19-20]. Several monosaccharide molecules linked by glycosidic bonds and form polysaccharides [19]. Electrospinning is a cost-effective, simple and versatile technique to produce nanofibers [20]. But electrospinning of polysaccharides is difficult. Because they are not able to form sufficient chain entanglement which is of great importance in the formation of nanofibers and they show shear thinning behavior which is not favorable for formation of nanofibers [23]. Cellulose is a kind of polysaccharide and produced by plant tissues or certain bacteria [19]. Each glucose unit in the structure has three hydroxyl groups. Due to the presence of these hydroxyl groups, cellulose forms inter- and intra-hydrogen bonds that restricts its solubility in common solvents [20-21]. Cellulose derivatives which can be dissolved in common solvents are produced by substitution of certain hydroxyl groups of cellulose with another functional group [20].

Hydroxypropyl cellulose (HPC) is a non-ionic cellulose derivative. It is obtained by substitution of some hydroxyl groups of cellulose to hydroxypropyl groups [22] (Figure 6). It is water soluble, biodegradable polymer and widely used in food, pharmaceutical industries; and tissue engineering [41-43]. Electrospun HPC nanofibers could be quite applicable owing to the unique properties of electrospun nanofibers like high surface area and nanoporous structure. However, there are a few studies concerning electrospinning of HPC [44-45]. One of them was carried out by Shukla et al. They have produced HPC nanofibers in ethanol and 2-propanol [44]. In another study, Francis et al. obtained HPC nanofibers in aqueous solution with the help of polyethylene oxide (PEO) [45].

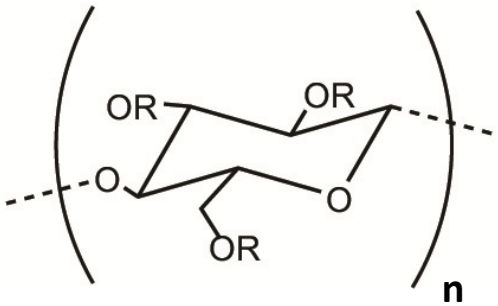

R=H or R=$CH_2CH(OH)CH_3$

Figure 6. Chemical structure of HPC.

Carboxymethyl cellulose (CMC) is anionic cellulose derivative and synthesized by replacing certain amount of hydroxyl groups with carboxymetyl groups (Figure 7) [22]. CMC is used in pharmaceutical applications; textile, paper, food and cosmetic industries [19]. It is very difficult for CMC to be produced as nanofibers due to its inability to form a jet in aqueous solution [23]. That's why there are a few studies in the literature on electrospinning of CMC [46-48]. In previous studies concerning electrospinning of CMC, Frenot et al. investigated the effect of molecular weight (Mw), degree of substitution, and substitution pattern of CMC on electrospinning of CMC/PEO blend in aqueous solution. They deduced that substitution pattern of CMC is of vital importance on the morphology of electrospun nanofibers [46]. Aluminum nanoparticles containing carboxymethyl cellulose nitrate composite nanofibers were produced via electrospinning by Long et al. [47]. In another study, silver nanoparticles were deposited on electrospun cellulosic (cellulose, cellulose acetate, carboxymethyl cellulose) nanofibers [48].

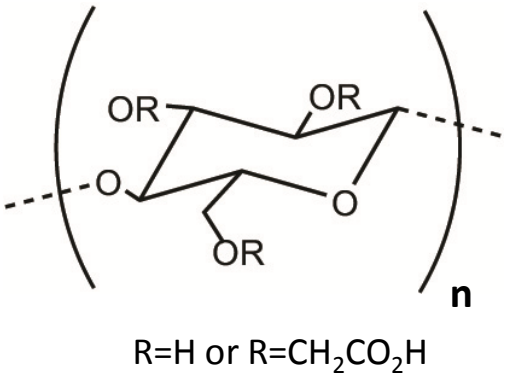

Figure 7. Chemical structure of CMC.

Alginate is an anionic polysaccharide that is obtained from marine brown algae. It is a copolymer composed of β-1, 4-D-mannuronic acid (M) and α-1, 4-L-glucuronic acid (G) units (Figure 8). The repeating units (M and G) are arranged in different proportions and sequences of homopolymer blocks (MM or GG) and alternating blocks (MG) [49]. Alginate is widely used polymer in cosmetic industry, food industry as additive and in biomedical applications such as wound dressing, tissue engineering scaffold, and drug delivery carrier [49]. On the other hand, electrospinning of alginate from its aqueous solution is still a challenge. Because of its rigid conformation that does not allow chain entanglement formation [50]. In order to overcome this problem, alginate was used in mixture with polymers like polyethylene oxide (PEO) [51-64], polyvinyl alcohol (PVA) [53, 65-68] except two studies [50, 69]. Nie et al. attained to produce sodium alginate nanofibers in aqueous solution with the help of glycerol [50]. Sodium alginate nanofibers were obtained in N, N-dimethylformamide (DMF) with the addition of Ca^{2+} cations by Fang et al [69].

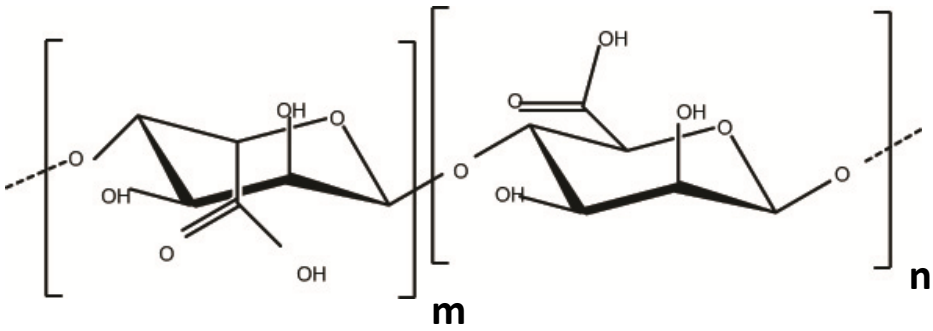

Figure 8. Chemical structure of alginate.

Cyclodextrins (CDs) are cyclic oligosaccharides and linked by α-(1,4) glucopyranose units. They have truncated-cone shape structure. Owing to their hydrophobic cavity, they are able to form host-guest interactions (inclusion complex) with a variety of solid, liquid, gaseous molecule in appropriate polarity and dimension [39]. They might be used in functionalization of nanofibers for different applications like filtration [70-74] and active food packaging [75-76].

In this study, electrospinning of HPC- CMC- and alginate-based nanofibers were successfully produced. Then these nanofibers were functionalized with modified CDs (hydroxypropyl-beta-cyclodextrin (HPβ-CD), methyl-beta-cyclodextrin (Mβ-CD), hydroxypropyl-gamma-cyclodextrin (HPγ-CD). Moreover, improvement was observed in the electrospinnability of CD functionalized nanofibers with the addition of CDs. The morphology of electrospun nanofibers were examined by scanning electron microscopy (SEM); whereas viscosity and conductivity of prepared solutions were measured by viscometer and conductivity meter.

2.2. Materials

Hydroxypropyl cellulose (HPC, Mw ~300.000 g/mol, Scientific polymer products), cellulose carboxyl methyl sodium salt (400-800 cp, Scientific polymer products), alginic acid sodium salt (30cp, Scientific polymer products), polyethylene oxide (PEO, Mv ~ 900.000 g/mol, Sigma aldrich); hydroxypropyl-beta-cyclodextrin (HPβ-CD), methyl-beta-cyclodextrin (Mβ-CD), hydroxypropyl-gamma-cyclodextrin (HPγ-CD) (Wacker chemie AG, Germany), ethanol (Sigma aldrich, ≥99.8%), 2-propanol (Sigma aldrich, ≥99.5%), Triton X-100 (Sigma aldrich) were purchased and used without any purification. The water was distilled from a Millipore Milli-Q Ultrapure Water System.

2.3. Electrospinning unit at UNAM

Electrospinning unit at UNAM is composed of syringe pump (Model: SP 101IZ, WPI), high voltage power supply (Matsusada Precision, AU Series, Japan), and grounded collector and these are located in Plexiglas box (Figure 9).

The syringe is placed horizontally on syringe pump and electric field is supplied from high voltage power supply. Electrospun nanofibers are collected on a grounded cylindrical metal collector that is covered by aluminum foil. Temperature and relative humidity inside the Plexiglas box are measured by thermo-hygrometer (Honeywell, TM0005-X).

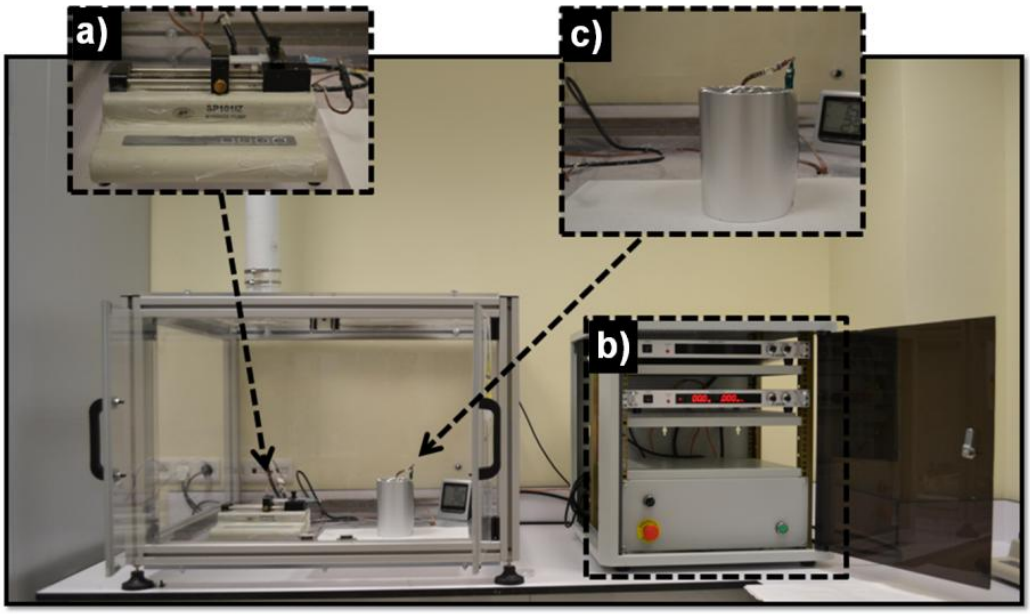

Figure 9. Electrospinning unit at UNAM: a) syringe pump, b) high voltage supply, and c) collector.

2.4. Production of electrospun nanofibers

HPC was dissolved in various solvent systems (water, ethanol/water, ethanol, ethanol/ 2-propanol) and solutions were stirred overnight at room temperature. While preparing solutions containing Triton X-100 (1% (w/v)), HPC was dissolved in water and then Triton X-100 was added immediately after the addition of solvent and stirred overnight at room temperature. With respect to CD including solutions, CDs (HPβ-CD, Mβ-CD, and HPγ-CD) was put in polymer solution after 12 hours stirring of HPC dissolved in ethanol and the solution was stirred 6 hours more. Finally, HPC solutions was loaded into 3 ml plastic syringe with a needle inner diameter of 0,7 mm or 0,8 mm placed horizontally on the pump and was sent towards to collector at a rate varies

between 0.5ml/h to1ml/h. A voltage ranging from 15-19 kV was obtained from a high voltage power supply. Cylindrical metal covered by aluminum foil was used as a collector. Distance between needle tip and collector is between 7 cm to 15 cm. Experiments were performed at 22-24°C, 20-32 % humidity.

CMC was dissolved in water and stirred at room temperature overnight. For Triton X-100 containing solutions, Triton X-100 (1% (w/v)) was added immediately after the addition of solvent and solutions stirred at room temperature overnight. For CMC/PEO blend solutions; firstly, CMC was dissolved in water. After solvation of CMC, PEO was put in and solution was stirred at room temperature overnight. As regards to CD including solutions, CMC and PEO was dissolved in water and the solution was stirred at room temperature overnight. Then CDs (HPβ-CD, Mβ-CD, and HPγ-CD) was put in polymer solution and stirred 6 hours more. Lastly, CMC solutions was loaded into a 3 ml plastic syringe with a needle inner diameter of 0,8 mm placed horizontally on the pump and was sent towards to collector at a rate 1ml/h. A voltage ranging from 15-17 kV was obtained from a high voltage power supply. Cylindrical metal covered by aluminum foil was used as a collector. Distance between needle tip and collector is 10 cm. Experiments were performed at 21-25°C, 25-41% humidity.

Alginate was dissolved in water and stirred at room temperature overnight. While preparing blend solutions with alginate and PEO; initially, alginate was dissolved in water. Afterwards PEO and Triton X-100 (1% (w/v)) was added and stirred at room temperature overnight. For CD including solutions, alginate, PEO and Triton X-100 (1% (w/v)) was dissolved in water and stirred at room temperature overnight. Then CDs (HPβ-CD, Mβ-CD) were put in polymer solution and the solution was stirred 6 hours more. In the end, alginate solutions was loaded into a 3 ml plastic syringe with a needle inner diameter of 0,7 or 0,8 mm placed horizontally on the pump and was sent towards to collector at a rate 1ml/h. A voltage ranging from 15-17.5 kV was obtained from a high voltage power supply. Cylindrical metal covered by aluminum foil was used as a

collector. Distance between needle tip and collector is between 10 cm to 12 cm. Experiments were performed at 21-22°C, 22-44% humidity.

2.5. Measurements and characterization techniques

The viscosity of HPC solutions were determined by Brookfield Viscometer DV-II+ Pro; whereas those of CMC solutions were investigated at a constant shear rate of a 100 1/sec at 22°C by Anton Paar Physica MCR 301 rheometer equipped with a spindle CP 40-2°C. The conductivity of both HPC and CMC solutions were measured with Multiparameter meter InoLab® Multi 720 (WTW) at room temperature.

The morphologies and average fiber diameter (AFD) of electrospun nanofibers were examined by SEM (FEI – Quanta 200 FEG). Samples were coated 6 nm Au/Pd before taking SEM images. In order to calculate AFD, around 100 fibers were analyzed.

2.6. Results and discussion

2.6.1. Electrospinning of CD functionalized HPC nanofibers

Electrospinning of HPC is quite difficult in aqueous solution because of its rigid structure that prevents formation of chain entanglement [23]. Nevertheless, we initially dissolved HPC polymer in aqueous solution at different concentrations (1%, 2%, 3%, 4%, 5%, 7%, 9% (w/v)) and tried to electrospin these solutions. But we observed splashes rather than nanofibers. SEM image of 3% (w/v) HPC solution was shown in Figure 10a. The formation of beads may be due to the capillary breakup of the spinning jet by high surface tension [1]. So, we thought that reducing the surface tension of the solution may support the formation of fibers without beads. Therefore, we added a nonionic surfactant (Triton X-100) to polymer solution. Surfactants make easier the spinning of a polymer solution by reducing the surface tension; and more uniform nanofibers are obtained [1]. However, in this study we did not observe nanofiber formation from HPC solutions with the addition of Triton X-100 (Figure 10b, 10c, 10d).

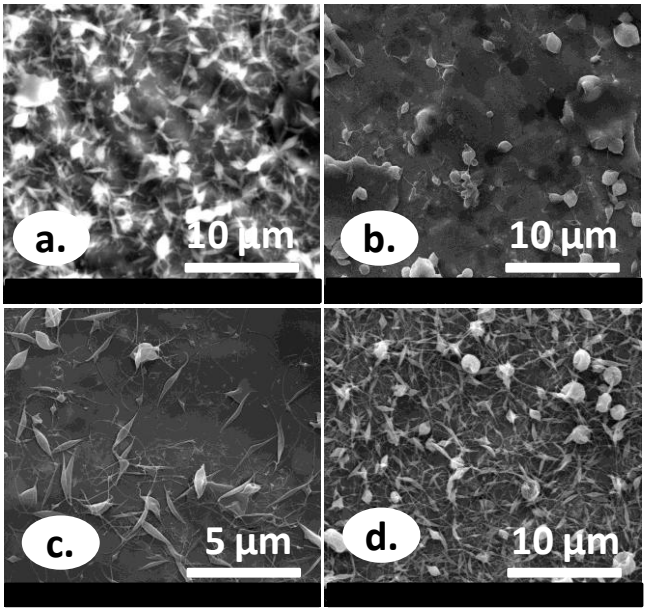

Figure 10. SEM images of electrospun (a) 3% (w/v) HPC; (b) 3% (w/v) HPC and 1% (w/v) Triton X-100, (c) 3.5% (w/v) HPC and 1% (w/v) Triton X-100, (d) 4% (w/v) HPC and 1% (w/v) Triton X-100 solutions in aqueous solution.

Moreover, we changed the solvent system to have bead-free HPC nanofibers. As seen in Figure 11a, the morphology has changed from completely beaded structure to beaded nanofibers by adding ethanol to solvent system. We also dissolved HPC polymer in ethanol (100%) and ethanol:2-propanol (1:1). As a result, we attained to produce bead-free nanofibers (Figure 11b, 11c). This might be related with lower surface tension of ethanol and 2-propanol compared to water [1]. This result was consistent with the study of Shukla et al. in the literature [44].

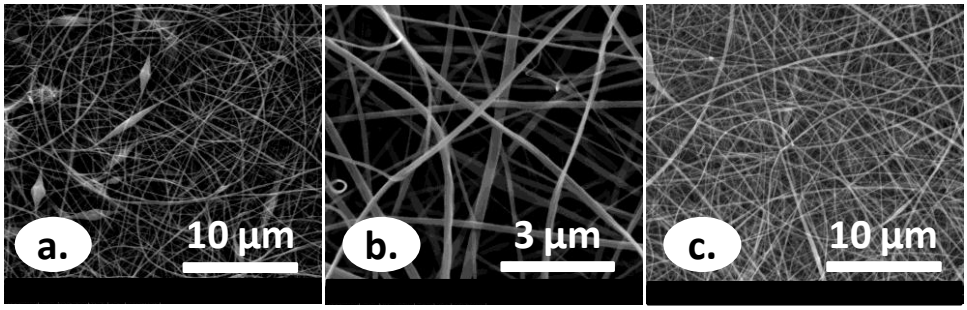

Figure 11. SEM images of electrospun HPC (3% (w/v)) nanofibers: (a) in ethanol/water (1:1), (b) in ethanol, (c) in ethanol/2-propanol (1:1).

We functionalized electrospun HPC nanofibers with CDs. Therefore, we may increase the application of HPC for drug delivery and biomedical applications. Because we have combined high surface area and nanoporous structure of electrospun nanofibers, and inclusion complexation ability of CDs with various molecules such as unpleasant odors and organic wastes. Three different modified CD types (HPβ-CD, Mβ-CD, and HPγ-CD) with three different 25%, 50%, 100 % (w/w) proportions were used to produce functional electrospun HPC nanofibers. According to SEM images displayed in Figure 12a-i, all fibers were bead-free and uniform.

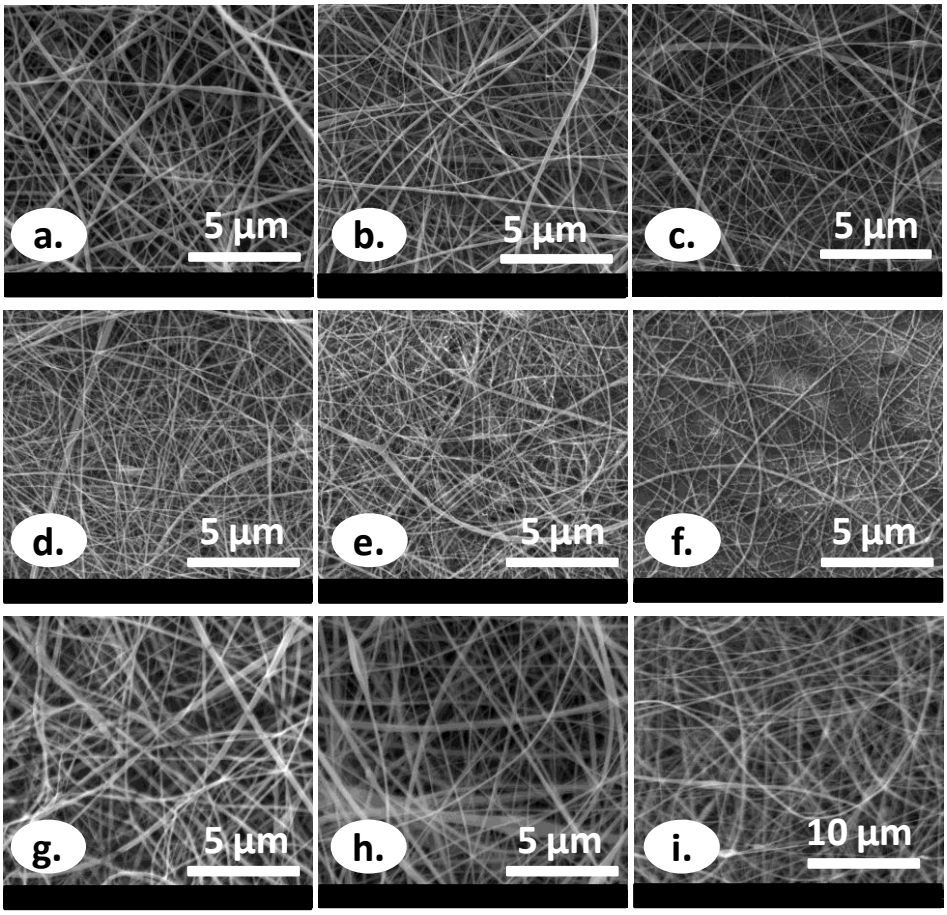

Figure 12. SEM images of electrospun HPC (3% (w/v)) nanofibers incorporated (a) 25% (w/w) HPβ-CD, (b) 50% (w/w) HPβ-CD, (c) 100% (w/w) HPβ-CD; (d) 25% (w/w) Mβ-CD, (e) 50% (w/w) Mβ-CD, (f) 100% (w/w) Mβ-CD; (g) 25% (w/w) HPγ-CD, (h) 50% (w/w) HPγ-CD, (i) 100% (w/w)HPγ-CD in ethanol.

Viscosity and conductivity measurements were also performed for HPC solutions to investigate their effect on AFD (Table 2). We successfully produced HPC nanofibers which have 150±65 nm diameter. On the other side, AFD of HPβ-CD functionalized HPC nanofibers are lower than electrospun HPC nanofibers. Thus, 25%, 50%, 100 % (w/w) HPβ-CD including HPC nanofibers have 115±40 nm, 100±40 nm and 70±35 nm, respectively. This might be due to much higher conductivity and lower viscosity of these solutions. Moreover; as the amount of HPβ-CD increases, the AFD is getting lower. The higher conductivity was the main reason for this situation. AFD of 25%, 50%, 100 % (w/w) Mβ-CD containing HPC nanofibers are 65±25 nm, 65±30 nm and 55±25 nm respectively. This is also related with extremely higher conductivity and lower viscosity than that of electrospun HPC nanofibers. Lastly, HPγ-CD functionalized HPC nanofibers with 25% (w/w) and have 50% (w/w) HPγ-CD have a little bit higher conductivity and lower viscosity as compared to electrospun HPC nanofibers. That's why they were only about 30 nm smaller in diameter than electrospun HPC nanofibers. On the other hand, as 100% (w/w) HPγ-CD containing HPC nanofibers has a little bit lower conductivity than electrospun HPC nanofibers, average fiber diameter is higher than electrospun HPC nanofibers.

Table 2. The characteristics of HPC solution and CD incorporated HPC solutions and the resulting electrospun fibers.

Solutions	***Conductivity (μS/cm)***	***Viscosity (Pa.s)***	***Diameter (nm)***	***Fiber morphology***
HPC3	4.35	0.207	150±65	beaded nanofibers
HPC3/HPβ-CD25	13.90	0.068	115±40	bead-free nanofibers
HPC3/HPβ-CD50	23.60	0.104	100±40	bead-free nanofibers
HPC3/HPβ-CD100	37.70	0.133	70±35	bead-free nanofibers
HPC3/MβCD25	34.00	0.084	65±25	bead-free nanofibers
HPC3/MβCD50	63.40	0.088	65±30	bead-free nanofibers
HPC3/MβCD100	110.00	0.123	55±25	bead-free nanofibers
HPC3/HPγCD25	4.71	0.096	120±50	bead-free nanofibers

HPC3/HPγCD50	4.65	0.084	120±55	bead-free nanofibers
HPC3/HPγCD100	4.16	0.131	205±80	bead-free nanofibers

2.6.2. Electrospinning of CD functionalized CMC nanofibers

CMC has rigid structure and high surface tension that prevent chain entanglement among the chains. Therefore electrospinning of CMC is still challenging [23]. Nonetheless, we prepared 1% (w/v) CMC solution in aqueous solution and observed only splashes on collector. Since higher viscosity favors formation of nanofibers without beads, concentration of the solution was increased up to 7% (w/v) in order to obtain bead-free nanofibers. But we could not obtain bead-free nanofibers. The solution with 7% (w/v) CMC was not possible to pass through the needle. This probably related with high viscosity of the solution. On the other hand, formation of splashes may due to the capillary breakup of the spinning jet by high surface tension. So, we thought that reducing the surface tension of the solution may support the formation of fibers without beads [1]. That's why, a nonionic surfactant (1% (w/v) Triton X-100) was added into CMC solutions, but again splashes were seen on the collector**.** We inferred from these results that reducing surface tension of solution is not adequate to electrospin CMC solution into nanofibers.

Another way to electrospin CMC could be blending it with other polymers such as PEO and PVA that enable CMC to be electrospun. CMC is a rigid structure with its compact chain conformation [3]. On the other side, with the addition of PEO; it breaks the hydrogen bonds among CMC chains and form new hydrogen bonds. So viscosity was getting higher due to the newly created hydrogen bonds as shown in Table 3. In general, electrospinnability of CMC is increasing with the increasing ratio of PEO [11]. We combined CMC with PEO at different ratios (1:1, 3:1) and total concentrations (2%, 3%, 4% (w/v)) (Figure 13, Figure 14). Figure 13 showed SEM images of CMC/PEO blended at a ratio of 1:1 at different total concentrations (2%, 3%, 4% (w/v)). When total polymer concentration was 2% (w/v), only beads were observed (Figure 13a). As we increased total polymer concentration to 3% (w/v), we obtained beaded

nanofibers (Figure 13b). Finally, if we electrospin the solution having 4% (w/v) total polymer concentration, we successfully electrospun bead-free nanofibers (Figure 13c).

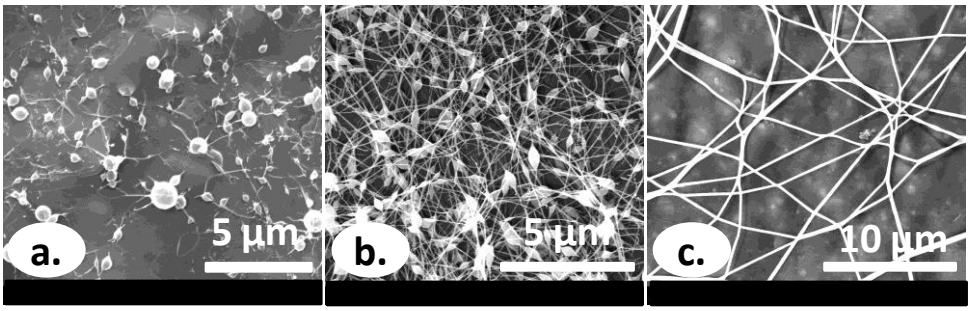

Figure 13. SEM images of electrospun CMC/PEO solutions at 1:1 ratio with different total polymer concentrations: (a) 2%, (b) 3%, (c) 4% (w/v).

Then, we increased the proportion of CMC in the mixture. Figure 14 showed SEM images of CMC/PEO blended at a ratio of 3:1 at different total concentrations (2%, 3%, 4% (w/v)). Similarly, we could not achieve to produce bead-free nanofibers with 2% (w/v) (Figure 14a) and 3% (w/v) (Figure 14b) total polymer concentrations. Lastly, we electrospun CMC/PEO with 4% (w/v) total polymer concentration and only few beads were observed in SEM images (Figure 14c).

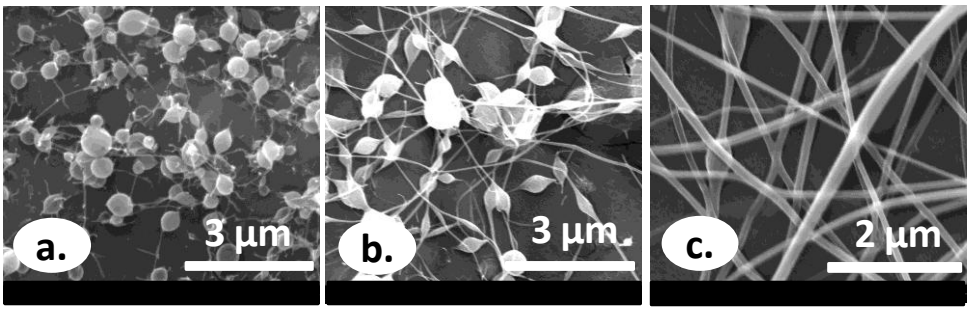

Figure 14. SEM images of electrospun CMC/PEO solutions at 3:1 ratio with different total polymer concentrations: (a) 2%, (b) 3%, (c) 4% (w/v).

On the other hand, CMC based nanofibers were functionalized with modified (HPβ-CD, Mβ-CD, HPγ-CD) CDs in various proportions (25%, 50%, 100% (w/w)). These nanofibers could be used for biomedical applications. Since they have both unique properties of electrospun nanofibers and inclusion

complex formation capability of CDs. SEM images of above mentioned nanofibers were shown in Figure 15a-i. As it is seen, there was no bead on CD functionalized CMC nanofibers. Therefore, we can easily conclude that the addition of CD eliminates formation of the beads in the structure.

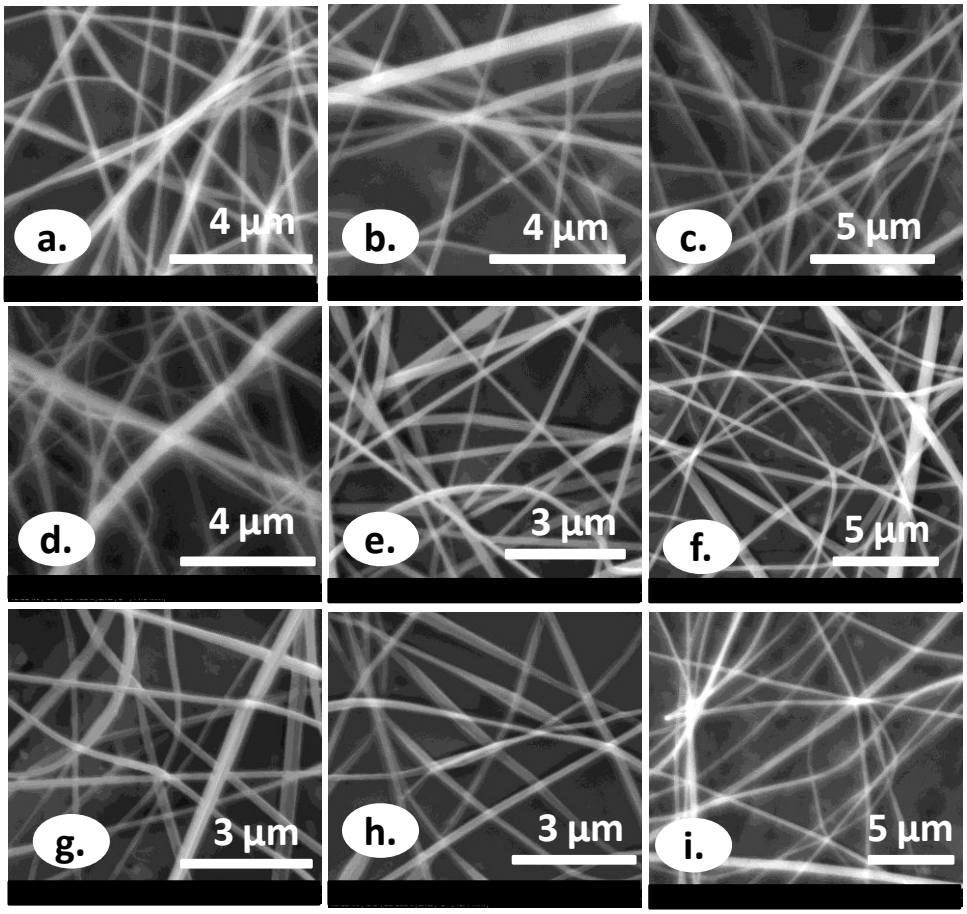

Figure 15. SEM images of electrospun CMC/PEO (3:1) nanofibers incorporated (a) 25% (w/w) HPβ-CD, (b) 50% (w/w) HPβ-CD, (c) 100% (w/w) HPβ-CD; (d) 25% (w/w) Mβ-CD, (e) 50% (w/w) Mβ-CD, (f) 100% (w/w) Mβ-CD; (g) 25% (w/w) HPγ-CD, (h) 50% (w/w) HPγ-CD, (i) 100% (w/w) HPγ-CD in aqueous solution.

The effect of viscosity and conductivity on the morphology and AFD of CD functionalized CMC nanofibers were investigated as well (Table 3). The addition of CD caused viscosity of all of the CMC/PEO/CD solutions to increase compared with solution without CD. Increasing viscosity might be due to the chain entanglement formation among the CMC chains. That's why electrospinnability of almost bead-free CMC/PEO nanofibers with a high ratio

of CMC is possible with the addition of CDs. The other property affecting the morphology of electrospun nanofibers is the conductivity of the solutions. Higher conductivity facilitates the production of bead-free fibers owing to the higher stretching of solution under high electrical field [1]. The conductivity of solutions containing CD was higher than solutions without CD, thus the beads were eliminated in the structure. Therefore the viscosity and conductivity are of crucial importance for the production of bead-free electrospun nanofibers. Moreover, we calculated AFDs of nanofibers functionalized with CDs. During electrospinning more viscous solutions exhibit greater resistance to stretching, so thicker fibers are formed when the viscosity of solution is higher [1]. In general, the AFD was higher in nanofibers functionalized with CDs due to the higher viscosity of solutions than solutions without CD. Also increasing amount of CD usually resulted in thicker fibers. On the other hand, the conductivity values of CD containing solutions were slightly higher than CMC/PEO solution. That's why we did not observe the decreasing effect of higher conductivity in diameter for CD containing nanofibers.

If we evaluate AFD results in detail; when we functionalized CMC nanofibers with 25%, 50%, 100% (w/w) HPβ-CD, we obtained functional CMC nanofibers which have 165±85, 160±40, 195±75 nm, respectively. As the amount of HPβ-CD increased, the viscosity of the solution also increased but the conductivity did not change much. That's why increment in AFD is an expected result for HPβ-CD functionalized CMC nanofibers due to the increasing viscosity. Secondly, AFD of functional CMC nanofibers containing 25%, 50%, 100% (w/w) Mβ-CD are 150±50, 185±80, 240±105 nm, respectively. The increase of AFD from 25% (w/w) to 50% Mβ-CD (w/w) and from 50% (w/w) to 100% (w/w) Mβ-CD might be due to the little decrease in conductivity. Thirdly, 25%, 50%, 100% (w/w) HPγ-CD including CMC nanofibers are 170±65, 200±65, 295±100 nm, respectively. This increment is related with gradually decreasing conductivity.

Table 3. The characteristics of CMC, CMC/PEO and CD incorporated CMC solutions and the resulting electrospun fibers.

Solutions	*Conductivity (μS/cm)*	*Viscosity (Pa.s)*	*Diameter (nm)*	*Fiber morphology*
CMC3	5.16	0.182	-	
CMC3/PEO1	4.34	0.258	100±35	bead-free nanofibers
CMC3/PEO1/HPβ-CD25	6.33	0.355	165±85	bead-free nanofibers
CMC3/PEO1/HPβ-CD50	5.64	0.617	160±60	bead-free nanofibers
CMC3/PEO1/HPβ-CD100	5.96	0.683	195±75	bead-free nanofibers
CMC3/PEO1/MβCD25	6.72	0.819	150±50	bead-free nanofibers
CMC3/PEO1/MβCD50	6.26	0.325	185±80	bead-free nanofibers
CMC3/PEO1/MβCD100	6.24	0.452	240±105	bead-free nanofibers
CMC3/PEO1/HPγCD25	5.76	0.514	170±65	bead-free nanofibers
CMC3/PEO1/HPγCD50	5.52	0.311	200±65	bead-free nanofibers
CMC3/PEO1/HPγCD100	5.16	0.314	295±100	bead-free nanofibers

2.6.3. Electrospinning of CD functionalized alginate nanofibers

It is a known fact that electrospinning of pure alginate is not easy in aqueous solutions. This might be related with absence of chain entanglement in aqueous solutions due to the rigid and extended chain conformation of alginate [57]. Nevertheless, we firstly prepared pure alginate solutions which have total polymer concentrations ranging from 1.5% (w/v) to 4.5% (w/v) in aqueous solution. As a result, we only observed splashes on the collector, due to discontinuous jet formation. This result was consistent with the literature [57].

Secondly, PEO was added into alginate solutions to improve the electrospinnability and uniformity of alginate-based nanofibers. PEO is known to form hydrogen bond interaction between its ether oxygen groups and hydroxyl groups of alginate. By this way it breaks the rigid structure of alginate [57]. For this purpose, alginate solution including alginate:PEO (1:1) was prepared in two different total concentrations (4%, 5% (w/v)). As seen from SEM images in Figure 16a, we were able to achieve bead-on-string structure

with 4% (w/v) polymer concentration. However, almost bead-free nanofibers were obtained from 5% (w/v) total polymer concentration (Figure 16b).

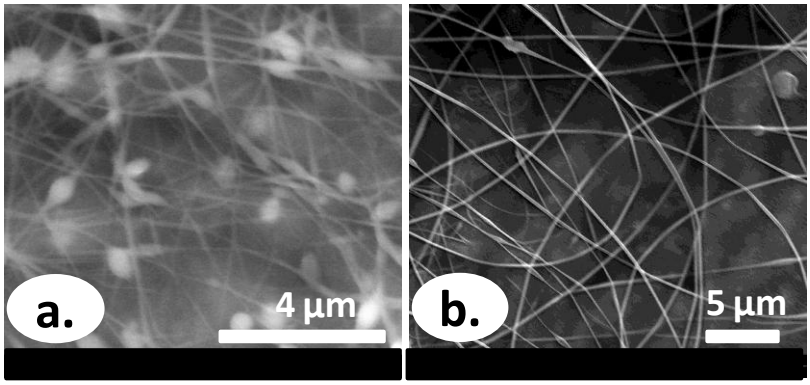

Figure 16. SEM images of electrospun alginate/PEO solutions at 1:1 ratio with different total polymer concentrations (a) 4% (w/v), (b) 5% (w/v) in aqueous solution.

Then we tried to increase percentage of alginate and solutions having 3% (w/v) total concentration including 62% and 75% alginate were prepared (Figure 17a, 17b). But we could not achieve to produce bead-free nanofibers from these solutions. Thus, Figure 17a exhibited bead-on-string structure; whereas only beads were observed in Figure 17b. On the other hand, 4% (w/v) total concentration including 62% and 75% alginate was also prepared (Figure 17c, 17d). In Figure 17c, we observed beads and fibers at the same time; while in Figure 17d, beads were seen rather than bead-free nanofibers.

Formation of beads may be the consequence of breaking up of spinning jet due to the high surface tension of the solution [1]. Therefore, we tried to reduce surface tension of the solution. So we added a nonionic surfactant called Triton X-100 into these solutions to improve the electrospinnability of the so-called solutions. In principle, surfactants reduce surface tension of polymer solution. Therefore, it is getting easier to overcome surface tension of polymer solution and indirectly electrospinning is facilitated [1]. But bead-on-string structure observed in Figure 17a did not change much (Figure 18a). On the other side, beaded structure in Figure 17b has changed to bead-on-string with the addition of surfactant (Figure 18b). Addition of Triton X-100 improved the spinnability

of both of the solutions prepared from 4% (w/v) total concentration (Figure 18c, 18d). But the effect of Triton X-100 was best seen in Figure 18c.

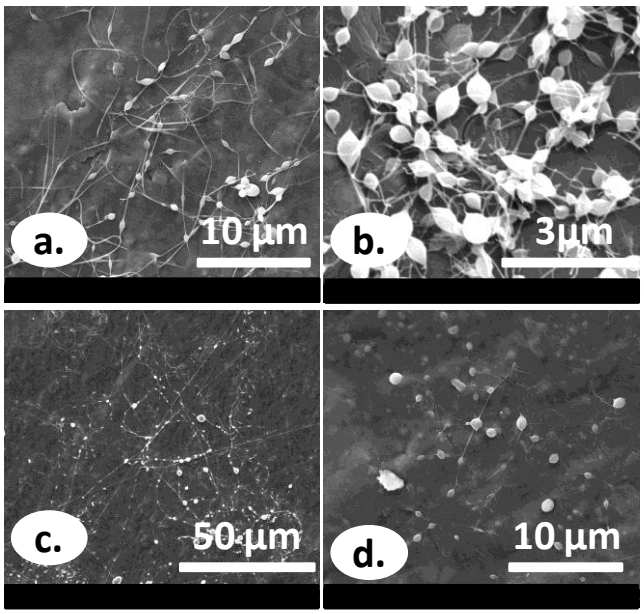

Figure 17. SEM images of electrospun alginate/PEO solutions with 3% (w/v) total polymer concentrations and different ratios (a) 62:28 (b) 75:25; 4% (w/v) total polymer concentrations and different ratios (c) 62:28 (d) 75:25 in aqueous solution.

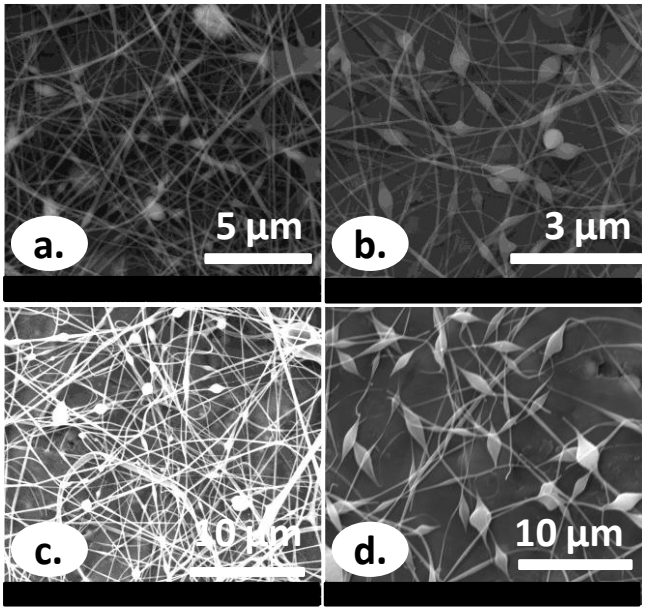

Figure 18. SEM images of electrospun alginate/PEO solutions with 3% (w/v) total polymer concentrations and different ratios (a) 62:28 (b) 75:25; 4% (w/v)

total polymer concentrations and different ratios (c) 62:28 (d) 75:25 in aqueous solution including 1% (w/v) Triton X-100.

Finally, we put in two types of modified CD in two different ratios (HPβ-CD and HPγ-CD; 25% (w/w) and 50% (w/w)) into the solution that includes 4% (w/v) total polymer concentration with 62% alginate to functionalize alginate based nanofibers. These nanofibers could be find application for drug delivery and biomedical applications. The alginate based nanofibers including 25% (w/w) HPβ-CD was almost bead-free but it seems that CD facilitated spinnability of nanofibers and as a result much more nanofibers were collected compared to sample without CD (Figure 19a). When we increase the amount of HPβ-CD to 50% (w/w), we attained to produce bead-free nanofibers (Figure 19b). In addition, amount of collected nanofibers has increased compared to nanofibers without CD due to the facilitating effect of CDs in nanofiber formation. Finally, the AFD of HPβ-CD functionalized alginate nanofibers comprising 25% and 50% HPβ-CD (w/w) are 100±30 nm and 140±35 nm, respectively. On the other hand, 25% (w/w) and 50% (w/w) HPγ-CD containing alginate based nanofibers were also produced (Figure 19c, 19d). As shown in SEM images of both of the samples, almost bead-free nanofibers were obtained. However, more nanofibers were collected on nanofibers including 50% (w/w) HPγ-CD as compared to 25% (w/w) HPγ-CD. In addition, the amount of nanofibers collected was not more than 50% (w/w) HPβ-CD containing nanofibers. Lastly, the AFD of HPγ-CD functionalized alginate nanofibers comprising 25% and 50% HPγ-CD (w/w) are 205±60 nm and 265±110 nm, respectively. As a conclusion, we thought that facilitating effect of both of the CDs (HPβ-CD and HPγ-CD) in spinnability of alginate based nanofibers might be related with viscosity of CD containing solutions.

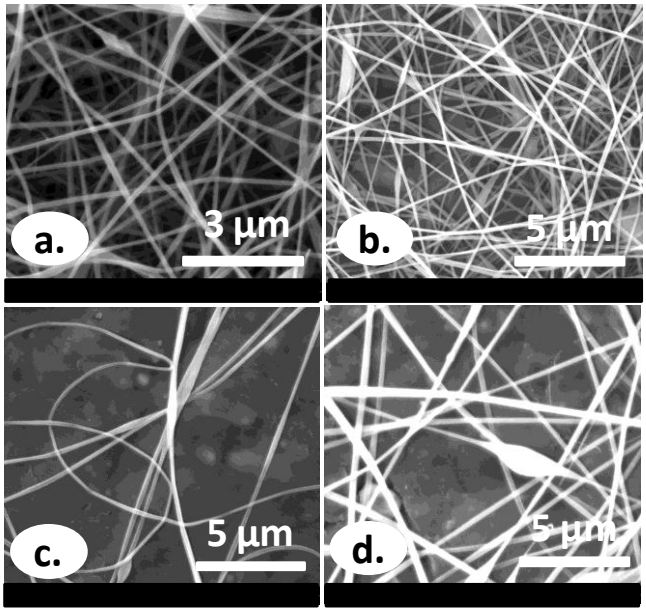

Figure 19. SEM images of electrospun alginate/PEO (62:28) nanofibers incorporated (a) 25% (w/w) HPβ-CD, (b) 50% (w/w) HPβ-CD; (c) 25% (w/w) HPγ-CD, (d) 50% (w/w) HPγ-CD in aqueous solution including 1% (w/v) Triton X-100.

2.7. Conclusion

Polysaccharides are difficult polymers to be electrospun due to shear thinning property and lack of chain entanglement. However, we successfully achieved to electrospin nanofibers from three different polysaccharides (HPC, CMC, and alginate) with the addition of CDs. Here, CDs not only improve the electrospinnability but also functionalized the nanofibers which might be used in drug delivery, wound healing, tissue engineering applications. Since CD functionalized electrospun nanofibers have both high surface area to volume ratio and nanoporous structure of electrospun nanofibers; and inclusion complex formation ability of CDs with various molecules like unpleasant odors and organic wastes.

CHAPTER II. RELEASE of SULFISOXAZOLE from ELECTROSPUN HYDROXYPROPYL CELLULOSE NANOFIBERS INCORPORATING CYCLODEXTRIN INCLUSION COMPLEX

3.1. General Information

The drug delivery systems are used to reduce adverse side effects and improve bioavailability and therapeutic efficacy of drugs [77]. Polymeric drug delivery systems have various advantages like reduced toxicity, improved therapeutic effect, and convenience. On the other hand, they have disadvantages such as low efficiency and burst release at the initial stage compared to conventional dosage forms [78]. Polymeric nanofibers are used as drug carriers owing to their nanoporous structure and high surface area to volume ratio [79-80]. The releasing behavior of a drug from a polymer matrix depends on many factors like loading capacity; drug/matrix interaction; the solubility of the drug in the polymer matrix and testing medium; the diffusion of the drug from the polymer matrix; the swelling ability and the solubility of the polymer matrix in the testing medium etc. [79-80].

Electrospinning is one of the most extensively used techniques to produce polymeric nanofibers due to its simplicity and versatility [5]. Electrospun nanofibers have shown potentials to be used in biotechnology applications, particularly for the development of functional biomaterials for wound healing, drug delivery systems and scaffolds for tissue engineering [5]. Moreover, biomaterials for wound healing, drug delivery systems and scaffolds for tissue engineering are widely manufactured through the use of electrospinning [17-18]. Electrospinning of biopolymers functionalized with various molecule such as drug, antibacterial, protein, gene is of increasing interest [81-84].

Cyclodextrins (CDs) are cyclic oligosaccharides consisting of α-(1,4)-linked glucopyranose units with a toroid-shaped molecular structure. It is a known fact that CDs form inclusion complexes (IC) with variety of molecules that have suitable characteristics in terms of polarity and dimension [39]. In

pharmaceutical industry, CDs are commonly used compounds. IC of CDs with hydrophobic drugs has many advantages like increasing solubility, enhancing stability; improving bioavailability, reducing dose and volatility of the hydrophobic drugs [40]. The hydroxyalkylated CDs like hydroxypropyl-beta-cyclodextrin (HPβ-CD) is more suitable for the solubilization of drugs than the natural CDs, because of their greater aqueous solubility and lack of toxicity [85].

In this study, IC of sulfisoxazole (SFS) which is a hydrophobic drug (Figure 1a) with HPβ-CD (Figure 1b, 1c) (SFS/HPβ-CD-IC) was prepared at 1:1 molar ratio. The schematic representation of SFS/HPβ-CD-IC was shown in Figure 1d. Then SFS/HPβ-CD-IC incorporating hydroxypropyl cellulose (HPC) nanofibers (SFS/HPβ-CD-IC-HPC-NFs) were produced through electrospinning method. SFS without HPβ-CD incorporated in HPC nanofibers (SFS-HPC-NFs) was also electrospun as control sample. The characterization of electrospun nanofibers were carried out by scanning electron microscopy (SEM), X-ray diffraction (XRD), differential scanning calorimetry (DSC) and thermogravimetric analysis (TGA). The release of SFS from SFS-HPC-NFs and SFS/HPβ-CD-IC-HPC-NFs were tested at 37°C in phosphate buffer solution (PBS) and the amount of released SFS was measured through the use of liquid chromatography-mass spectroscopy (LC-MS).

3.2. Materials

Hydroxypropyl cellulose (HPC, M_w ~ 300.000 g/mol, Scientific polymer products), polycaprolactone (PCL, M_n ~ 70.000-90.000 g/mol, Sigma aldrich), hydroxypropyl-beta-cyclodextrin (HPβ-CD, Wacker chemie AG, Germany), sulfisoxazole (SFS, Sigma aldrich, min. 99%), ethanol (Sigma aldrich, 99.8%), dichloromethane (DCM, Sigma aldrich, extra pure), acetonitrile chromasolv (Sigma aldrich), N,N-dimethylformamide (DMF, Riedel, pestanal), potassium phosphate monobasic (Riedel de haen), disodium hydrogen phosphate 12-hydrate (Riedel de haen) and sodium chloride (Sigma-aldrich) were purchased and used as-received without any further purification.

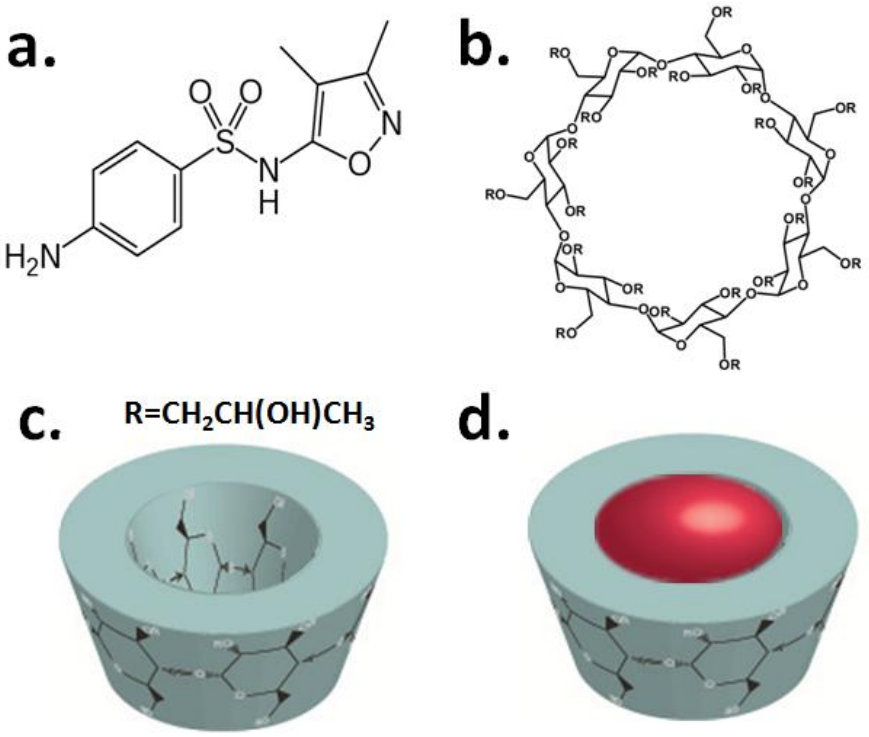

Figure 20. Chemical structure of (a) SFS, (b) HPβ-CD; schematic representation of (c) HPβ-CD, and (d) SFS/HPβ-CD-IC.

3.3. Production of electrospun nanofibers

3% (w/v) HPC solution was prepared by dissolving HPC in ethanol and this solution was electrospun. Two types of drug delivery systems were prepared by incorporating SFS without HPβ-CD and SFS/HPβ-CD-IC into HPC nanofibers. The amount of SFS was determined as 1:1 molar ratio (SFS:HPβ-CD), and for both of the samples same amount of SFS was used. In order to prepare SFS-HPC-NFs, SFS and 3% (w/v) HPC was dissolved in ethanol; and stirred overnight at room temperature. Afterwards this solution was electrospun into nanofibers. With regard to SFS/HPβ-CD-IC-HPC-NFs, SFS was dissolved in ethanol at room temperature. Then HPβ-CD were added into the solution; and stirred overnight at room temperature. Finally, 3% (w/v) HPC was added into the solution and the solution was stirred 6 hours more. Resultant solution was electrospun into nanofibers. HPC solution, SFS-HPC solution and SFS/HPβ-CD-IC-HPC solution were loaded into a 3 ml plastic syringe with a needle inner diameter of 0.8 mm placed horizontally on the pump and were sent towards to

the collector at 1 ml/h rate. 16-18 kV was obtained from a high voltage power supply. Cylindrical metal covered with aluminum foil was used as a collector. Distance between needle tip and collector was 11 cm. Experiments were performed at 20-22°C, 21-22% humidity.

On the other side, 10% (w/v) polycaprolactone (PCL) was dissolved in the binary solvent system containing 3:1 (DMF:DCM) and electrospun into nanofibers. PCL solution was loaded into a 3 ml plastic syringe with a needle inner diameter of 0.8 mm placed horizontally on the pump and was sent towards to the collector at 1 ml/h rate. Distance between needle tip and collector was 12 cm and applied voltage was 15 kV. Experiments were performed at 20-21°C, 21-22% humidity.

3.4. Preparation of phosphate buffer

PBS was chosen as a releasing medium for drug release tests. In order to prepare the buffer solution, 1.44 g of potassium phosphate monobasic, 10.74 g of disodium hydrogen phosphate 12-hydrate and 90 g of sodium chloride were dissolved in 1000 ml of distilled water. Finally, this solution was diluted with distilled water at the rate of 1:9. The pH of the prepared solution was determined around 7.

3.5. Drug release assay

PCL is a semi crystalline and hydrophobic polymer that is widely employed in electrospinning method. It is commonly used for biomedical applications as tissue engineering scaffold, drug delivery system and wound dressing material, due to its biocompatibility and biodegradability [29, 86-87]. For release experiments we prepared three layered composite nanofibers composed of nanofiber structures. As shown in Figure 2, there were SFS-HPC-NFs or SFS/HPβ-CD-IC-HPC-NFs between two electrospun PCL nanofiber layers.

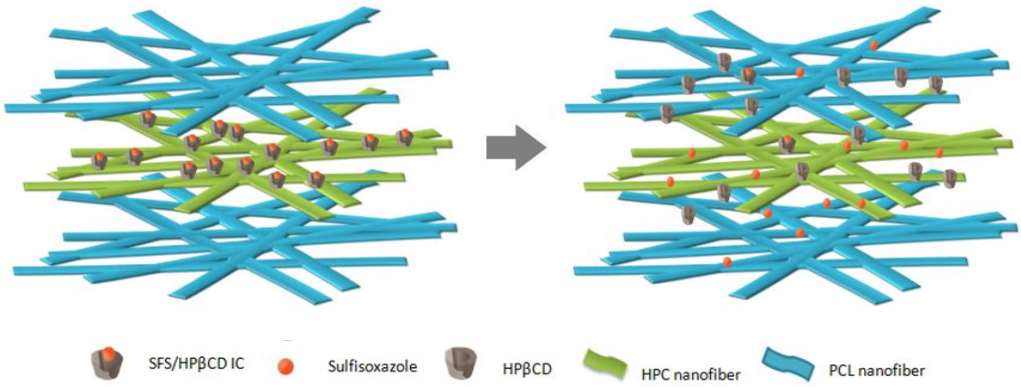

Figure 21. Schematic representation of release of SFS from SFS/HPβ-CD-IC-HPC-NFs.

Total immersion method was used to study the cumulative release profiles of drugs from SFS-HPC-NFs and SFS/HPβ-CD-IC-HPC-NFs containing composite nanofibers. Based on this technique, each of the SFS including composite nanofibers was immersed in 30 ml of PBS releasing medium at 37°C. At a predetermined time intervals between 0 and 720 minutes, 0.5 ml of the test medium was withdrawn (i.e., sample solution) and an equal amount of the fresh medium was refilled. The amount of the SFS in the sample solution was determined using LC-MS equipped with VWD UV detector against the predetermined calibration curve for SFS. The calibration samples were prepared in methanol. The data were carefully calculated to determine the cumulative amount of SFS released from the samples at each specified immersion period. The experiments were carried out in triplicate and the results were reported as the average±standard deviation.

3.6. Measurements and characterization techniques

The viscosity and conductivity of HPC solution, SFS-HPC solution and SFS/HPβ-CD-IC-HPC solution were determined by Brookfield Viscometer DV-II+ Pro and Inolab pH/Cond 720-WTW, respectively.

The morphologies and average fiber diameters (AFDs) of electrospun PCL nanofibers, electrospun HPC nanofibers, SFS-HPC-NFs and SFS/HPβ-CD-IC-HPC-NFs were examined by SEM (FEI – Quanta 200 FEG). Before taking SEM

images, samples were coated 6 nm Au/Pd. So as to calculate AFDs, around 100 fibers were analyzed.

XRD data for SFS, electrospun HPC nanofibers, HPβ-CD, SFS-HPC-NFs and SFS/HPβ-CD-IC-HPC-NFs were recorded using a PANalytical X'Pert powder diffractometer applying Cu Kα radiation in a 2θ range 5°–30°.

In order to investigate the thermal behavior of the drug in the electrospun nanofibers; SFS, SFS-HPC-NFs and SFS/HPβ-CD-IC-HPC-NFs were assessed via DSC (Q 2000, TA Instruments, USA); and SFS, electrospun HPC nanofibers, HPβ-CD, SFS-HPC-NFs and SFS/HPβ-CD-IC-HPC-NFs was tested through TGA (Q 500, TA Instruments, USA). For DSC measurement, the samples were prepared in an aluminum pan and were heated from 25°C to 250°C at a rate of 20°C/min under nitrogen purge. TGA measurements were carried out under nitrogen atmosphere, the samples were heated up to 450°C at a constant heating rate of 20°C/min.

The released amount of SFS from SFS-HPC-NFs and SFS/HPβ-CD-IC-HPC-NFs was determined through LC-MS (Agilient, 1200 series) equipped with VWD UV detector. The column (Agilient C18) was 4.6 mmx50 mm that contains 1.8 µm packing and the detection was accomplished at 270 nm. Mobile phase, flow rate, injection volume, total run time were 100% acetonitrile, 0.7 ml/min, 20 µl and 3 minutes, respectively.

3.7. Results and discussion

HPC is a hydrophilic polymer and synthesized by substitution some hydroxyl groups of cellulose with hydroxypropyl groups. It is generally used in food, pharmaceutical and tissue engineering applications due to its biodegradability and hydrophilicity [41-43]. In the literature, there are various polymer types that are used to produce nanofibers by electrospinning method for various applications, but studies on electrospinning of HPC is limited [44-45]. This is related with shear thinning property and lack of chain entanglement in polysaccharides. Due to the compact structures, polysaccharides are not able to form sufficient chain entanglements. So their electrospinning is quite difficult

[23,88]. Moreover, there is somehow limited study regarding biomedical applications of HPC nanofibers in the literature.

The sulfonamide drugs have a basic chemical structure comprising a sulfanilamide group and five or six-member heterocyclic ring. SFS is a sulfonamide drug with an oxazole substituent. It is a weak acidic antibacterial and poorly soluble in water [89]. In the literature, there are studies regarding IC of SFS with β-CD and HPβ-CD in order to increase its solubility [89-90]. Here we incorporated SFS/HPβ-CD-IC in HPC nanofibers to benefit high surface area to volume ratio and highly porous structure of electrospun nanofibers; and high solubility of SFS/ HPβ-CD-IC at the same time.

Figure 22 showed the SEM images and AFDs of electrospun HPC nanofibers; SFS-HPC-NFs and SFS/HPβ-CD-IC-HPC-NFs. First of all, bead-free HPC nanofibers were produced from 3% (w/v) polymer concentration. Secondly, incorporation of SFS into HPC nanofibers did not change the morphology of nanofibers. In addition, it was obviously seen that both of the electrospun HPC nanofibers incorporating SFS have smooth surface and neither drug crystals nor aggregates was observed on the surfaces of these nanofibers. It indicated that SFS was not on the surface of nanofibers. Similar results were reported for another type of drugs incorporated into electrospun nanofibers [79].

AFD of electrospun HPC nanofibers was 150±65 nm; whereas those of SFS-HPC-NFs and SFS/HPβ-CD-IC-HPC-NFs were 95±50 nm and 70±40 nm, respectively. This situation was explained by higher conductivity and lower viscosity of HPC solutions containing SFS compared to HPC solution as shown in Table 4. In addition, SFS/HPβ-CD-IC-HPC solution has higher conductivity and lower viscosity than SFS-HPC solution. That's why AFD of SFS/HPβ-CD-IC-HPC-NFs was lower than SFS-HPC-NFs. Taepaiboon et al. also showed the effect of conductivity and viscosity in the AFD of polyvinyl alcohol (PVA) nanofibers with the addition of four different drugs [33]. Moreover, the concentration of HPC polymer in the solution was reduced when polymer matrixes were loaded with SFS, so interaction of polymer with solvent

weakened and the evaporation of solvent became easier [91]. Therefore, the addition of SFS may decrease the concentration of polymer in the solution. In other words, the decrease in the viscosity of the solution led to the formation of thinner fibers.

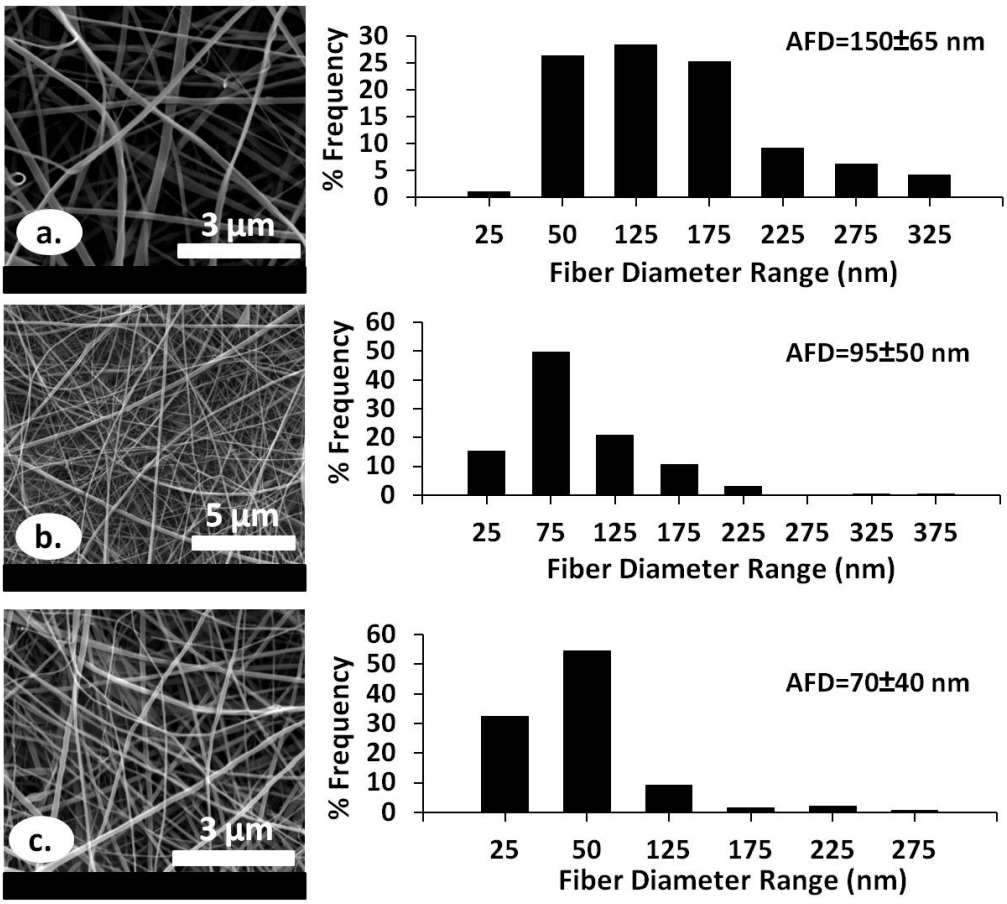

Figure 22. SEM images and AFD distributions of (a) electrospun HPC nanofibers, (b) SFS-HPC-NFs, (c) SFS/HPβ-CD-IC-HPC-NFs.

Table 4. The characteristics of HPC solution, SFS-HPC solution and SFS/HPβ-CD-IC- HPC solutions and the resulting electrospun fibers.

Solutions	*% HPC[a] (w/v)*	*% HPβ-CD[b] (w/w)*	*SFS[b] (w/w)*	*Conductivity (µS/cm)*	*Viscosity (cP)*	*Diameter (nm)*	*Fiber morphology*
HPC	3	-	-	2.52	1355	150±65	bead-free nanofibers
SFS-HPC	3	-	9.11	4.13	975.2	95±50	bead-free nanofiber
SFS/HPβ-CD-IC-HPC	3	50	9.11	13.04	785.3	70±40	bead-free nanofiber

[a] with respect to solvent.

[b] with respect to polymer.

As mentioned before, three layered composite nanofibers were prepared from electrospun PCL nanofibers and SFS-HPC-NFs or SFS/HPβ-CD-IC-HPC-NFs for release experiments. SEM image of bead-free PCL nanofibers was shown in Figure 23 and AFD was calculated as 260±110 nm.

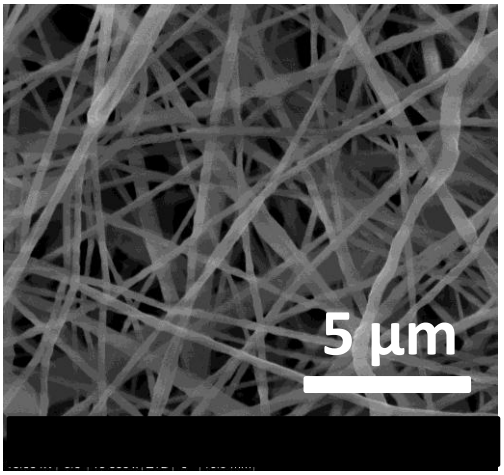

Figure 23. SEM image of electrospun PCL nanofibers.

Figure 24 represents the XRD patterns of SFS, electrospun HPC nanofibers, HPβ-CD, SFS-HPC-NFs and SFS/HPβ-CD-IC-HPC-NFs. XRD diffractogram of SFS clearly confirmed the crystalline nature of SFS with sharp diffraction peaks. The diffractogram of the electrospun HPC nanofibers with broad diffraction peaks exhibited amorphous nature of the HPC polymer. This result was consistent with the literature which stated that characteristic diffraction peaks of cellulose are at around 2Θ=6-8° and 2Θ=15-20° [92]. XRD pattern of SFS-HPC-NFs was very similar to that of electrospun HPC nanofibers. In addition, the diffraction peaks of SFS were completely disappeared. This result supported the formation of an amorphous state of the drug in SFS-HPC-NFs. This situation was also observed in the study of Li et al. Thus, crystalline peaks of borneol were disappeared and amorphous state of borneol was observed inside the nanofibers [93]. As regards to HPβ-CD, there was no crystalline peak in its XRD pattern. Therefore, we may conclude that HPβ-CD has an amorphous structure. Celebioglu et al. has also shown the

amorphous structure of HPβ-CD nanofibers [94]. On the other hand, XRD graph of SFS/HPβ-CD-IC-HPC-NFs was similar to electrospun HPC nanofibers and the diffraction peaks of crystalline SFS were completely disappeared. As is known, when a molecule forms IC with CDs, its interaction with other molecules and the formation of crystalline aggregates is restricted [94]. Therefore, absence of crystalline peaks of SFS may indicate formation of IC between HPβ-CD and SFS. In the literature, the inclusion complexation between a guest molecule and CD was confirmed with disappearance of crystalline diffraction peaks of the guest molecule [95].

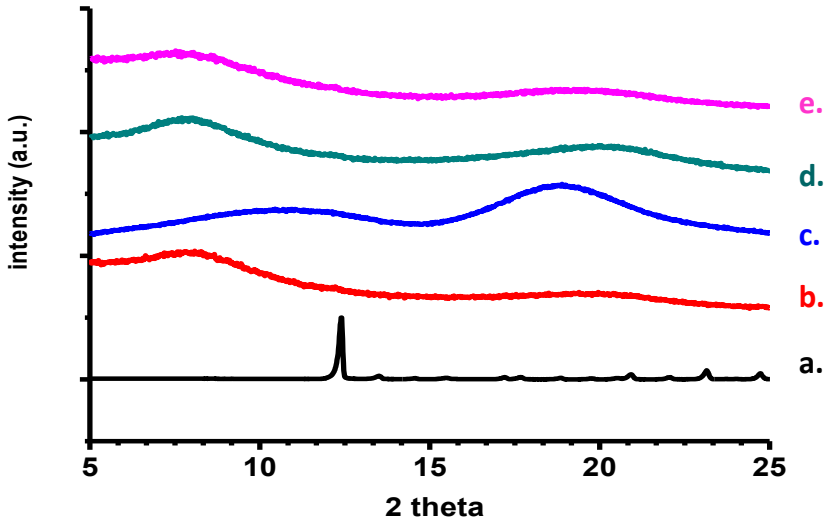

Figure 24. XRD patterns of (a) SFS, (b) electrospun HPC nanofibers, (c) HPβ-CD, (d) SFS-HPC-NFs, (e) SFS/HPβ-CD-IC-HPC-NFs.

Thermal properties of the SFS, SFS-HPC-NFs and SFS/HPβ-CD-IC-HPC-NFs were investigated by means of DSC (Figure 25). The sharp endothermic peak observed at 198°C in the thermogram of SFS corresponded to the melting temperature of SFS [90]. However, this peak did not exist in DSC thermogram of SFS-HPC-NFs. This might be due to the inability of SFS to form crystalline aggregates inside the electrospun nanofibers. Therefore, the high surface area of electrospun nanofibers might cause solvent to evaporate rapidly; the mobility of SFS inside the fiber was restricted and there might be no time for SFS to recrystallize inside the matrix. So it was dispersed in amorphous state in the

electrospun HPC nanofibers. This similar result was observed about dexamethasone loaded PCL nanofibers in the study of Martins et al. in the literature [80]. As regards to DSC pattern of SFS/HPβ-CD-IC-HPC-NFs, the sharp endothermic peak of SFS at 198°C was not observed in these nanofibers as well. The disappearance of melting peak of SFS might show that SFS molecules were distributed inside the nanofibers without crystalline aggregates and it may also confirm the complexation of HPβ-CD with SFS [90].

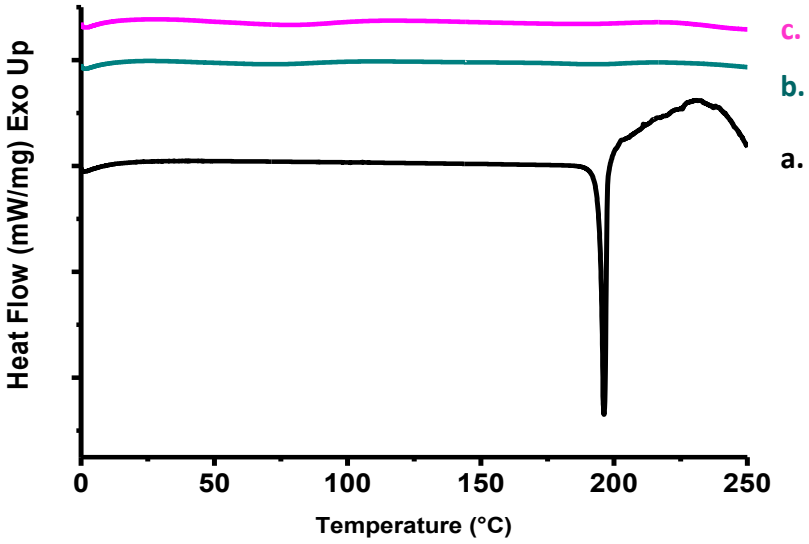

Figure 25. DSC thermograms of (a) SFS, (b) SFS-HPC-NFs, (c) SFS/HPβ-CD-IC-HPC-NFs.

To determine thermal stability of electrospun HPC nanofibers; TGA measurements of SFS, electrospun HPC nanofibers , HPβ-CD, SFS-HPC-NFs and SFS/HPβ-CD-IC-HPC-NFs were carried out and curves were depicted in Figure 26. Thermal degradation of SFS started at about 190°C [90]. For as-spun HPC nanofibers, the weight loss beginning from 300°C represents the thermal degradation of HPC polymer. In the case of SFS-HPC-NFs, weight loss started at around 275°C which was due to the degradation of SFS and HPC. Therefore thermal stability of SFS has increased to higher temperature by encapsulation of free SFS in electrospun HPC nanofibers thanks to the interaction between SFS and HPC. Similar results were obtained for another drugs and polymer in the literature [33]. On the other hand, TGA curve of HPβ-CD exhibited two weight

loss stages: the initial weight loss below 100°C might be attributed to removal of water, while the major weight loss above 290°C corresponded to the main thermal degradation of HPβ-CD [90]. With respect to SFS/HPβ-CD-IC-HPC-NFs; first of all, initial weight loss that is observed below 100°C might be due to the removal of water. Secondly, the main weight loss of SFS/HPβ-CD-IC-HPC-NFs started approximately at 275°C, corresponding to the thermal degradation of SFS, HPC and HPβ-CD. So, the thermal stability of SFS did not improve by encapsulation of SFS/HPβ-CD-IC in electrospun HPC nanofibers. As a result we cannot draw conclusion whether IC exist or not between SFS and HPβ-CD from TGA results.

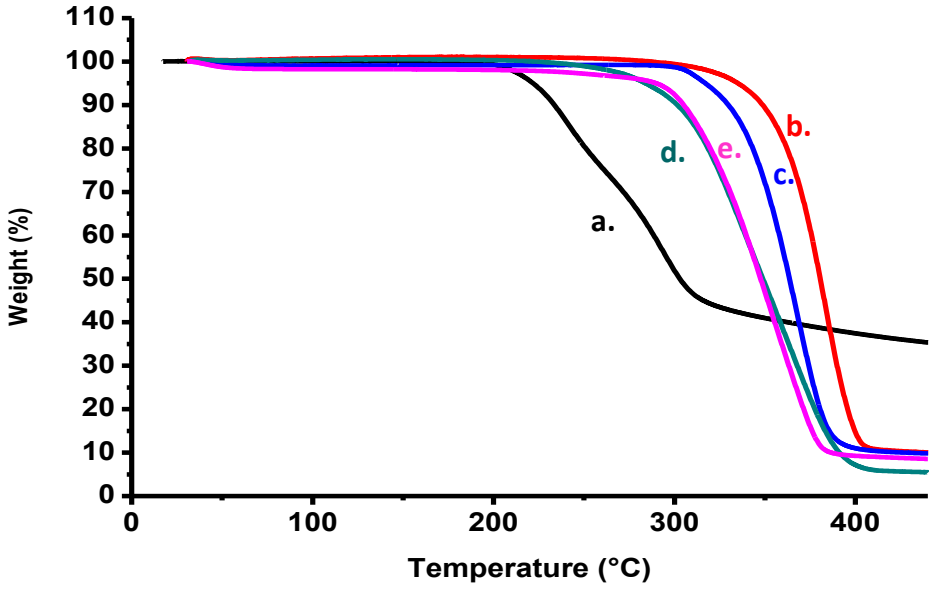

Figure 26. TGA thermograms of (a) SFS, (b) electrospun HPC nanofibers, (c) HPβ-CD, (d) SFS-HPC-NFs, (e) SFS/HPβ-CD-IC-HPC-NFs.

Releasing of a drug from nanofibers is rapid in the first stage due to the high surface area to volume ratio and nanoporous structure enabling much more drug to diffuse into the releasing medium, and this is called burst effect [96]. Burst effect is primarily controlled by the solubility of the drug in the releasing medium, the drug diffusion coefficient and initial drug distributions within the polymer carrier [97, 98]. Rapid swelling or dissolution of polymer matrix will also give rise to burst release [80, 97, 98]. On the other hand, the sustained release from a polymer matrix is mainly controlled by not only the drug

diffusion through the matrix but also the dissolution of matrix [99-100]. So, as a consequence of initial surface erosion arising from the water penetrating into the nanofibers' surface and high surface area, drug is released faster from the nanofibers at the initial stage as we mentioned before. Then water reaches inside the nanofibers; as a result swelled polymer and interconnected pores within the nanofibers released the remaining drug slowly, this situation is called sustained release [80].

The release profiles of SFS from composite nanofibers containing SFS-HPC-NFs and SFS/HPβ-CD-IC-HPC-NFs were shown in Figure 27 as a function of submersion time. The experiments were carried out by total immersion method in PBS at the physiological temperature of 37°C for 720 minutes. The release mechanism of SFS from both of the samples might include dissolution through polymer matrix, diffusion through water-filled pores in the matrix; and would be followed with complete drug liberation as a result of dissolution of matrix if only HPC nanofibers were used instead of composite nanofibers. Based on the results given in Figure 27, the shape of the release profiles for SFS-HPC-NFs and SFS/HPβ-CD-IC-HPC-NFs containing composite nanofibers was essentially similar and can be divided into three stages: In the initial stage (up to 180 minutes) near linear release kinetics was observed; thereafter release rate increased slightly until 600 minutes of immersion time for both of the nanofibers and finally followed by a steady release of up to 720 minutes in where the curve was a plateau. As a consequence, composite nanofibers including SFS-HPC-NFs and SFS/HPβ-CD-IC-HPC-NFs exhibited rapid enough release at the first and second stage; and then sustained release for the third stage.

In composite nanofibers containing SFS-HPC-NFs, about 67±30 ppm SFS was released within the first 180 minutes; and at the end of the 720 minutes, 121±15 ppm SFS had been released from SFS-HPC-NFs. As is known, the solubility of drug in polymer solution is of great importance in the release behavior of drug. Although SFS is a hydrophobic drug, it is quite soluble in polymer solution; thus it was less likely to form a phase separation with HPC

polymer during the rapid elongation of the jet and evaporation of the solvent because of the large surface area of the as-spun nanofibers. As a result, when fiber completely dried during electrospinning, it was more likely to be inside the HPC nanofibers rather than the surface. This idea was supported by a study in the literature [78]. Secondly, SFS is hydrophobic molecule which means it is not soluble in the releasing medium. If it was hydrophilic, physical interaction between polymer and drug would be limited, it would be most likely to locate at the surface [98]. Thirdly, wetting and swelling of hydrophilic HPC nanofibers was slowed down; owing to higher thickness of the composite nanofibers. In this case, the higher thickness of the matrix, the lower drug release rate was observed as in the study of Wang et al. [99]. Otherwise water could easily penetrate through the matrix, HPC nanofibers would wet, swell and dissolve rapidly and releasing rate of SFS would increase and moving of SFS through the pores would quickly lead to all SFS to release in the initial stage. So, we would observe only burst release; rather than the controlled release [99].

In regard to composite nanofibers containing SFS/HPβ-CD-IC, the release increased up to 105±37 ppm in 180 minutes; and at the end of the 720 minutes, 152±20 ppm SFS was released. In addition to the reasons for SFS-HPC-NFs containing composite nanofibers to exhibit sustained release, SFS/HPβ-CD-IC containing composite nanofibers has more reasons for showing sustained release behavior. Unlike the composite nanofibers containing SFS-HPC-NFs at the same load, nanofibers having SFS/HPβ-CD-IC released much more SFS in each time given on graph and the maximum amount of released SFS is almost 30 ppm more in total than other sample. This situation might be related with the existence of HPβ-CD in the matrix. Thus, CDs have ability to enhance drug release from polymeric systems by increasing the concentration of diffusible species within the matrix [97]. When a hydrophobic drug makes complex with CDs; its solubility, dissolution rate and stability increases considerably. Because CD complex of a drug is usually much more hydrophilic than the free drug, nanofibers including IC wets easier, the crystalline structure disintegrates and the substance quickly dissolves. So CD complex increase the drug solubility,

[100]. This result complies with the literature. Panichpakdee et al. stated that solubility of asiaticoside was increased via inclusion complexation of asiaticoside with HPβ-CD [95]. Consequently, presence of CDs may lower the required dose of an active molecule by improving its solubility. SFS/HPβ-CD-IC-HPC-NFs containing composite nanofibers were superior to SFS-HPC-NFs containing composite nanofibers. That's why; it could be used as an efficient drug carrier system for hydrophobic drugs.

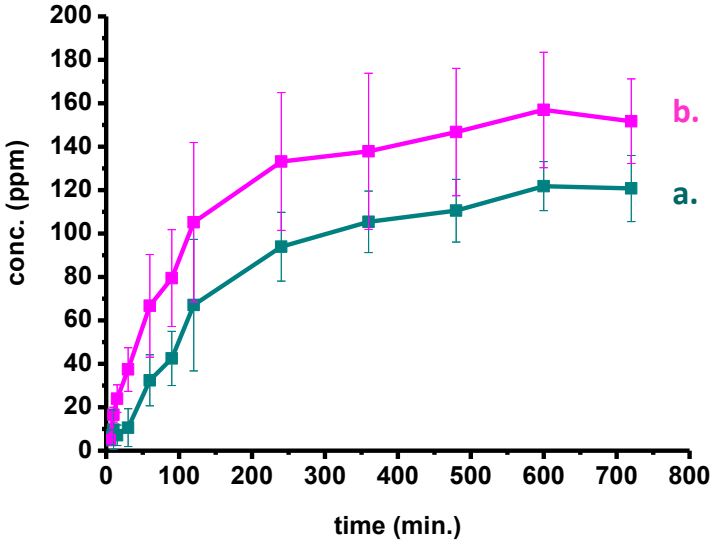

Figure 27. Cumulative release profiles of (a) SFS-HPC-NFs, (b) SFS/HPβ-CD-IC-HPC-NFs.

3.8. Conclusion

SFS/HPβ-CD-IC-HPC-NFs were successfully produced via electrospinning. SEM, XRD, DSC and TGA were used to investigate the structural and thermal characterizations of nanofibers. SEM images exhibited that incorporation of SFS inside HPC nanofibers did not affect the morphology of electrospun HPC nanofibers. Higher drug release was achieved owing to the property of CDs to enhance the solubility of hydrophobic drugs. As a conclusion, composite nanofibers allowed us to obtain an excellent drug delivery system for controlled release of hydrophobic drugs.

CHAPTER III. RELEASE of α-TOCOPHEROL (VITAMIN E) from ELECTROSPUN POLYCAPROLACTONE NANOFIBERS INCORPORATING CYCLODEXTRIN INCLUSION COMPLEX

4.1. General Information

Polymeric drug delivery systems are superior to other drug delivery systems in terms of therapeutic effect, toxicity and convenience. However, they have also disadvantages like low efficiency in drug delivery and burst release of drugs [78]. On the other hand, due to the unique properties such as porous structure at nanoscale and high surface area to volume ratio, nanofibers are of outstanding importance in delivery of drugs [101].

Electrospinning is a simple, versatile and cost-effective method to produce nanofibers. Electrospun nanofibers are used in many areas including tissue scaffolds, wound healing, drug delivery systems owing to their high surface to volume ratio and nanoporous structure [2].

Cyclodextrins (CDs) are cyclic oligosaccharides and have truncated-cone shaped structure [39]. They form host-guest complexes with several kinds of compounds depending on the polarity and size of the compound according to cavity of CD [39]. Owing to the inclusion complex (IC) between CD and guest molecule, many improvements might be achieved such as enhancing solubility, bioavailability and the chemical stability of poorly soluble drugs; increasing thermal stability of volatile substances [102].

In this study, IC of α-Tocopherol (α-TC) (Vitamin E) (Figure 1a) with beta-cyclodextrin (β-CD) (Figure 1b, 1c) was prepared (α-TC/β-CD-IC) an then incorporated in poly caprolactone (PCL) including solution and electrospinning was performed. The schematic representation of α-TC/β-CD-IC was shown in Figure 1d. α-TC/β-CD-IC incorporated PCL nanofibers (α-TC/β-CD-IC-PCL-NFs) were characterized via scanning electron microscopy (SEM), X-ray

diffraction (XRD), differential scanning calorimetry (DSC), thermogravimetric analysis (TGA). The release of α-TC into phosphate buffer saline (PBS) including methanol and tween 20 (PBMT) from untreated and UV-treated nanofibers was measured via high performance liquid chromatography (HPLC). Moreover, antioxidant activity was determined by UV-Vis NIR spectroscopy. α-TC without β-CD incorporated in PCL nanofibers (α-TC-PCL-NFs) was used as a control sample for above-mentioned experiments.

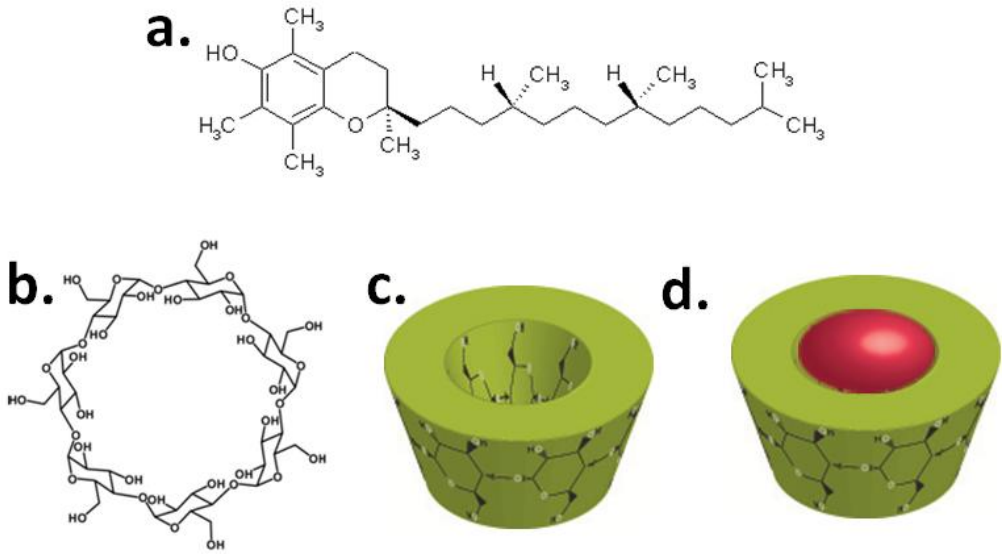

Figure 28. Chemical structure of (a) α-TC, (b) β-CD; schematic representation of (c) β-CD, and (d) α-TC/β-CD-IC.

4.2. Materials

Polycaprolactone (PCL, M_n ~ 70.000-90.000 g/mol, Sigma aldrich), beta-cyclodextrin (β-CD, Wacker chemie AG, Germany), α-Tocopherol (α-TC, Sigma aldrich), formic acid (FA, Sigma aldrich, extra pure 98-100%), acetic acid (AA, Sigma aldrich, extra pure 100%), methanol (Sigma Aldrich, extra pure), methanol chromasolv (Sigma aldrich), potassium phosphate monobasic (Riedel de haen), disodium hydrogen phosphate 12-hydrate (Riedel de haen), sodium chloride (Sigma aldrich), tween 20 (Sigma aldrich), 2,2-diphenyl-1-

picrylhydrazyl (DPPH, Sigma aldrich) were used as purchased without any purification.

4.3. Production of electrospun nanofibers

PCL solution was prepared by dissolving PCL in FA/AA (1:3) and this solution was electrospun. Drug delivery systems were prepared by electrospinning of α-TC-PCL or α-TC/β-CD-IC-PCL solutions. The molar ratio of α-TC to β-CD was 2:1 in α-TC/β-CD-IC-PCL solution, and for both of the samples the same amount of α-TC was used. Firstly, α-TC-PCL solution was prepared. α-TC was dissolved in FA/AA (1:3) and PCL was added to this solution; then the solution was stirred at room temperature overnight. Vials were covered with aluminum foil during the stirring to protect α-TC from light-induced degradation. As for α-TC/β-CD-IC-PCL solution, α-TC was dissolved in FA/AA (1:3) solution, then β-CD was added and this mixture was stirred overnight at room temperature. Vials were covered with aluminum foil during stirring period to protect α-TC from light-induced degradation. After stirring overnight, PCL was added; the solution stirred 6 hours more. PCL solution, α-TC-PCL solution and α-TC/β-CD-IC-PCL solution loaded into 3 ml plastic syringe with a needle inner diameter of 0.8 mm were placed horizontally on the pump and sent towards to the collector at 0.5 ml/h rate. 15 kV was obtained from a high voltage power supply. Cylindrical metal covered with aluminum foil was used as a collector. Distance between needle tip and collector was 8 cm. Experiments were performed at 22°C-26°C, 17%-20% humidity.

4.4. Preparation of phosphate buffer

In order to prepare the PBS, 1.44 g potassium phosphate monobasic, 10.74 g disodium hydrogen phosphate 12-hydrate and 90 g sodium chloride were dissolved in 1000 ml of distilled water. Then, this solution was diluted with distilled water at the rate of 1:9. In order to increase the solubility of α-TC in the releasing medium 10% methanol and 0.5% tween 20 were added into PBS and PBMT was obtained. pH of the releasing media was measured as about 7.

4.5. Drug release assay

Total immersion method was used to study the cumulative release profiles of α-TC from α-TC-PCL-NFs and α-TC/β-CD-IC-PCL-NFs. Based on this technique, each of α-TC including (both in free form and IC) electrospun PCL nanofiber taken from the aluminum foil was immersed in 30 ml of PBMT at 37°C, stirred at 50 rpm. At a specified immersion period between 0 and 1440 minutes, 0.5 ml of the test medium was withdrawn and an equal amount of the fresh medium was refilled. The amount of α-TC in the sample solution was determined using HPLC equipped with VWD UV detector against the predetermined calibration curve for α-TC. The calibration samples were prepared in PBMT. The data were carefully calculated to determine the cumulative amount of α-TC released from the samples at each specified immersion period. The experiments were carried out in triplicate and the results were reported as average values±standard deviation.

4.6. Measurements and characterization techniques

The viscosity and conductivity of PCL, α-TC-PCL and α-TC/β-CD-IC-PCL solutions were determined by Brookfield Viscometer DV-II+ Pro and Inolab pH/Cond 720-WTW, respectively.

The morphologies and average fiber diameters (AFDs) of electrospun PCL nanofibers, α-TC-PCL-NFs and α-TC/β-CD-IC-PCL-NFs were examined by SEM (FEI – Quanta 200 FEG). SEM images of α -TC-PCL-NFs and α-TC/β-CD-IC-PCL-NFs were also taken after HPLC measurement and UV treatment. Samples were coated 5 nm Au/Pd before taking SEM images. So as to calculate AFD, around 100 fibers were analyzed.

XRD data for electrospun PCL nanofibers, β-CD, α-TC-PCL-NFs and A-TC/β-CD-IC-PCL-NFs were recorded using a PANalytical X'Pert powder diffractometer applying Cu Kα radiation in a 2θ range 5°–30°.

In order to investigate the thermal behavior of α-TC in electrospun nanofibers; α-TC, electrospun PCL nanofibers, β-CD, α-TC-PCL-NFs and α -TC/β-CD-IC-PCL-NFs were assessed via DSC (Q 2000, TA Instruments, USA)

and TGA (Q 500, TA Instruments, USA). For DSC measurement, the samples were prepared in an aluminum pan and were heated from -90°C to 150°C at a rate of 20°C/min under nitrogen purge. TGA measurements were carried out under nitrogen atmosphere, the samples were heated up to 500°C at a constant heating rate of 20°C/min.

Amount of released α-TC from α-TC-PCL-NFs and α -TC/β-CD-IC-PCL-NFs were measured using HPLC (Agilient, 1200 series) equipped with VWD UV detector. The column was Agilient C18, 150 mm x 4.6 mm (5 µm pores) and the detection was accomplished at 292 nm. Mobile phase, flow rate, injection volume and total run time were 98:2 methanol:water, 1 ml/min, 10 µl and 12 minutes, respectively.

α-TC-PCL-NFs and α-TC/β-CD-IC-PCL-NFs were tested for their photostability as well. Nanofibers were cut into square shaped samples and exposed to UV light a distance of 10 cm from the UV source (8W, UVLMS-38 EL) at 365 nm for 45 minutes. Then each sample was submerged into 30 ml of PBMT at 37°C, stirred at 50 rpm for 1440 minutes; and 0.5 ml solution was withdrawn at certain time intervals and fresh PBMT was added instead. The released α-TC was measured by means of HPLC method as mentioned in release assay. These experiments were done triplicate and the results were reported as average values±standard deviation.

Antioxidant tests for α-TC-PCL-NFs and α-TC/β-CD-IC-PCL-NFs were done via DPPH radical scavenging assay. PCL nanofibers were also used as a control sample for this assay. 10^{-4} M DPPH solution was prepared in methanol; meanwhile 2 mg nanofibers sample was dissolved in methanol. Then, 2.9 ml of DPPH solution was mixed with 0.1 ml of nanofibers solution. The mixture was remained in the dark for 30 minutes at room temperature. At the end of the 30 minutes, the absorbance of the solution was measured with UV-Vis NIR Spectroscopy (Varian Cary 5000) at 517 nm during 5 minutes in every 1 minute.

4.7. Results and discussion

PCL, a semi-crystalline polymer, is widely used in the field of biotechnology due to slow biodegradability, high biocompatibility, good drug permeability, mechanical properties and comparatively lower cost [29]. Electrospinning of PCL was studied by several groups in the literature. But generally organic solvents are used rather than acids [26]. Kanani et al. acquired to produce electrospun PCL nanofibers by using glacial acetic acid, 90% acetic acid, glacial formic acid, and formic acid / acetone [27].

α-TC is the main component of Vitamin E and used in food and cosmetic industries. It is a natural antioxidant and poorly soluble compound [103]. In the literature, there are studies concerning IC preparation between α-TC with CDs [104-105] and loading of α-TC/CD-IC into polymeric films [106-108]. In these studies as prepared α-TC/β-CD-IC was acted as protective agent for α-TC or controlled release were achieved for α-TC. Here, we prepared α-TC/β-CD-IC-PCL-NFs were obtained via electrospinning.

SEM was used to characterize the morphology of the electrospun PCL nanofibers. SEM images and AFD distributions of electrospun PCL nanofibers, α-TC-PCL-NFs and α-TC/β-CD-IC-PCL-NFs were presented in Figure 29. As it is seen from Figure 29a, bead-free nanofibers of PCL were obtained from 15% (w/v) polymer concentration in FA/AA (1:3) solution. After the addition of α-TC both free α-TC (Figure 29b) or α-TC/β-CD-IC (Figure 29c), the morphology of PCL nanofibers did not change.

As shown in Table 5, the average diameters of electrospun PCL nanofibers was 285±105 nm; whereas α-TC-PCL-NFs was 345±270 nm and α-TC/β-CD-IC-PCL-NFs was 495±350 nm. So, higher AFD of α-TC-PCL-NFs may be due to the lower conductivity compared to PCL solution; however, lower viscosity might suppress the increase in AFD. As regards to α-TC/β-CD-IC-PCL-NFs, its AFD was also higher than PCL nanofibers. This is related with lower conductivity of α-TC/β-CD-IC-PCL solution than PCL solution.

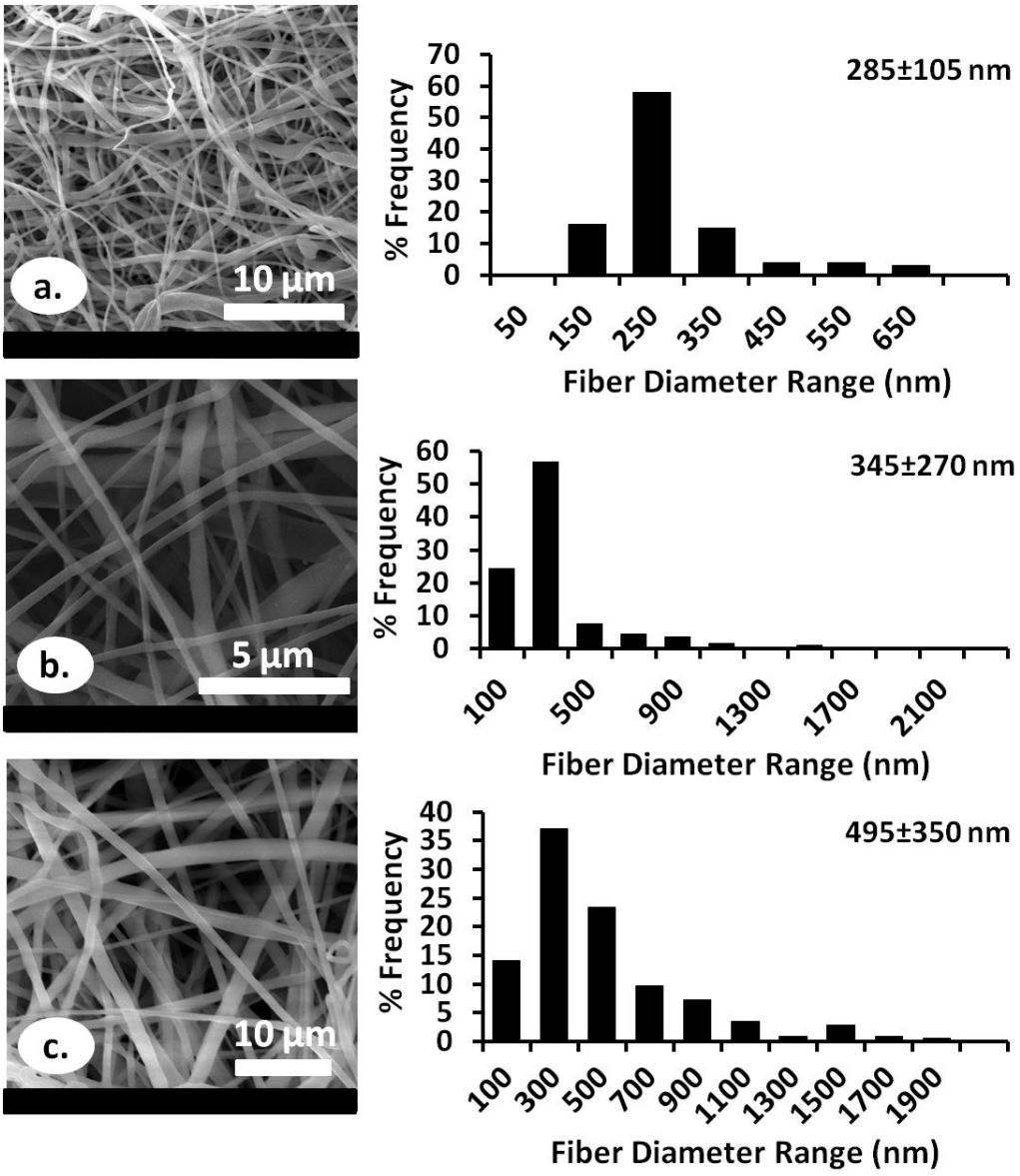

Figure 29. SEM images and AFD distributions of (a) electrospun PCL nanofibers, (b) α-TC-PCL-NFs, (c) α-TC/β-CD-IC-PCL-NFs.

Table 5. The characteristics of PCL, α-TC-PCL and α-TC/βCD-IC- PCL solutions and the resulting electrospun fibers.

Solutions	***% PCL[a] (w/v)***	***% βCD[b] (w/w)***	***α-TC[b] (w/w)***	***Conductivity (µS/cm)***	***Viscosity (cP)***	***Diameter (nm)***	***Fiber morphology***
PCL	15	-	-	4.7	1795	285±105	bead-free nanofibers
α-TC-PCL	15	-	10	4.0	1156	345±270	bead-free nanofiber

α-TC /βCD-IC-PCL	15	13.33	10	4.3	1631	495±350	bead-free nanofiber

[a] with respect to solvent.

[b] with respect to polymer

XRD patterns of electrospun PCL nanofibers, β-CD, α-TC-PCL-NFs and α-TC/β-CD-IC-PCL-NFs were displayed in Figure 30. α-TC is a liquid compound at room temperature, so it has no diffraction peak. Electrospun PCL nanofibers exhibited characteristic peaks of semi-crystalline PCL at 2θ=21.7◦ and 24.0◦. α-TC-PCL-NFs showed very similar XRD pattern with PCL nanofibers. Similarly, α-TC/β-CD-IC-PCL-NFs showed only characteristic peaks of PCL. β-CD exhibits channel type packing when it forms IC with a guest molecule and has its own characteristic diffraction peaks [109]. But characteristic channel type packing peaks of β-CD (2θ=12◦, 18◦) was not observed in α-TC/β-CD-IC-PCL-NFs. Therefore, XRD results did not draw a clear conclusion that α-TC molecules formed IC with β-CD or not.

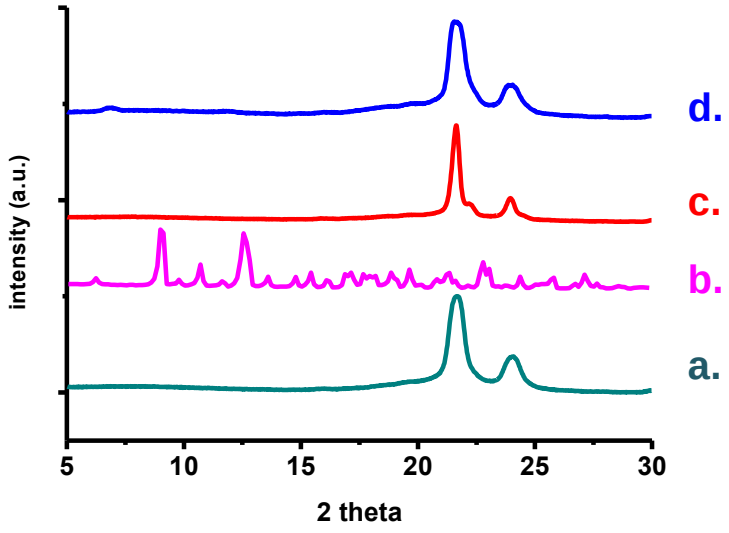

Figure 30. XRD patterns of (a) electrospun PCL nanofibers, (b) β-CD, (c) α-TC-PCL-NFs, (d) α-TC/β-CD-IC-PCL-NFs.

Differential scanning calorimetry was performed for α-TC, electrospun PCL nanofibers, β-CD, α-TC-PCL-NFs and α-TC/β-CD-IC-PCL-NFs (Figure 31). α-TC had a glass transition at around -40°C which was confirmed by

literature as well [105]. PCL is a semi-crystalline polymer with a sharp peak at 58°C that corresponds to the melting temperature of polymer. α-TC-PCL-NFs had very similar thermal degradation profile to PCL nanofibers. Thus, it shows sharp endothermic peak at around 57°C, whereas it does not exhibit glass transition of α-TC. Thereby, we might deduce that α-TC molecules were well dispersed in PCL nanofibers.

The disappearance of thermal transitions of guest molecule clearly indicates that guest molecule is in the cavity of CD; therefore the formation of IC between CD and guest molecule is proved as well [105]. So, disappearance the peaks of both α-TC and β-CD for α-TC/β-CD-IC-PCL-NFs showed that there is an interaction between α-TC and β-CD. Moreover, we might conclude that IC formation was successfully achieved in α-TC/β-CD-IC-PCL-NFs.

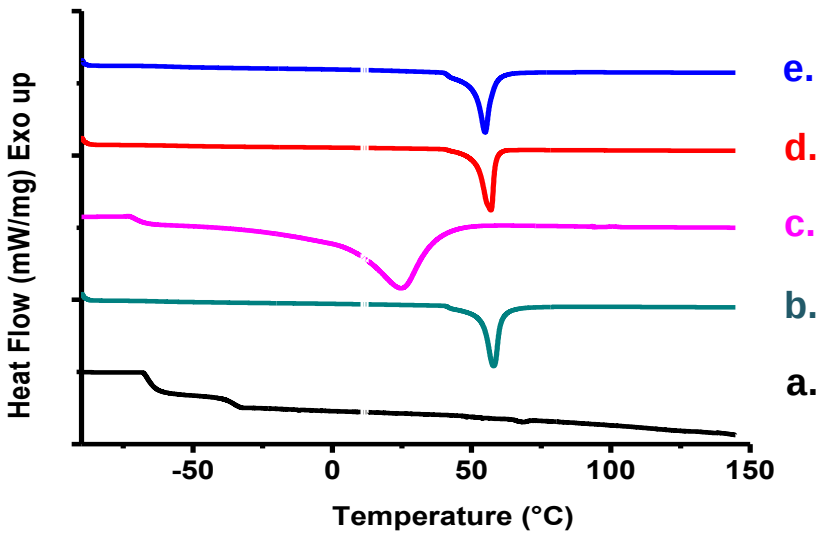

Figure 31. DSC thermogram of (a) α-TC, (b) electrospun PCL nanofibers (c) β-CD, (d) α-TC-PCL-NFs, (e) α-TC/β-CD-IC-PCL-NFs.

TGA is used to determine thermal stability of nanofibers. Figure 32 displayed the TGA measurements for α-TC, electrospun PCL nanofibers, β-CD, α-TC-PCL-NFs and α-TC/β-CD-IC-PCL-NFs. The thermal degradation of α-TC began at around 230°C and this result was correlated with the literature [110]. The onset temperature for degradation of PCL is 360°C and its degradation

finished at about 450°C similar with literature [111]. α-TC-PCL-NFs exhibited two weight losses: In the first weight loss that might corresponds to the degradation of α-TC, the degradation started at around 230°C. So, the onset of degradation temperature of α-TC did not change. Whereas in the second weight loss the degradation began about 360°C and it may attributed to the degradation of PCL. With regard to α-TC/β-CD-IC-PCL-NFs, there existed two degradation points in the curve. The first one ascribed to the decomposition of α-TC and started at 230°C, thus the thermal stability of α-TC was not improved. The second weight loss of α-TC/β-CD-IC-PCL-NFs beginning at around 350°C and finished at around 440°C may belong to the decomposition of β-CD and PCL. Typically, β-CD represents water loss below 100°C and weight loss above 275°C corresponded to the main thermal degradation of β-CD [112]. Finally, as there was no increase in the thermal stability of α-TC, we cannot conclude that there was an IC between α-TC and β-CD or not [105].

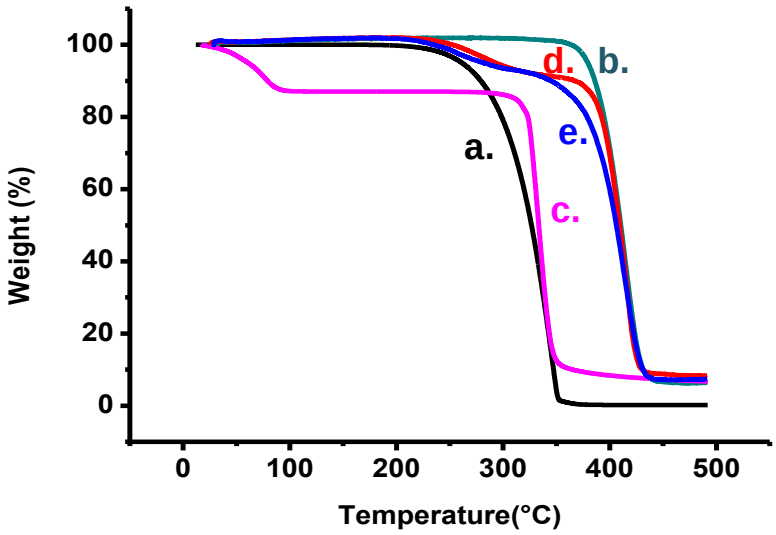

Figure 32. TGA thermograms of (a) α-TC, (b) electrospun PCL nanofibers (c) β-CD, (d) α-TC-PCL-NFs, (e) α-TC/β-CD-IC-PCL-NFs.

The release experiments were done in PBMT according to total immersion method at the physiological temperature of 37°C and 50 rpm for 1440 minutes. Percent of released α-TC in PBMT from α-TC-PCL-NFs and α-TC/β-CD-IC-PCL-NFs were presented in Figure 33 as versus of time. SEM images of

nanofibers were also taken after HPLC measurement; and as seen from Figure 34, the samples kept their fiber structure after immersion into PBTM.

As shown, zero-order release kinetic was observed for both α-TC-PCL-NFs and α-TC/β-CD-IC-PCL-NFs. We can analyze the release of α-TC from both of the nanofibers basically in 3 stages. In the first stage that is up to 60 minutes, α-TC exhibited relatively quick release. Afterwards release of α-TC continued with lower rate compared to first stage until 240 minutes of immersion time. During this stage, water molecules penetrated inside PCL nanofibers deeply, PCL swelled and bulk erosion occurred. Lastly, the drug was released at a constant rate from interconnected pores in the third stage [80, 106].

α-TC is hydrophobic molecule, it is not soluble in PBS; however we added methanol and tween 20 to buffer solution in order to help dissolution of α-TC and detection of α-TC in HPLC. Additionally, α-TC was not soluble in polymer solution; therefore, its interaction with polymer was weak and partition of α-TC from polymer matrix occurred rapidly [113]. As nanofibers have unique properties like high surface area to volume ratio and nanoporous structure; diffusion rate of a molecule from nanofibers was rapid in the first stage [114]. α-TC-PCL-NFs released 11±3 ppm α-TC; whereas α-TC/β-CD-IC-PCL-NFs released 9±6 ppm α-TC within the first 60 minutes. The initial release of α-TC was slower in α-TC/β-CD-IC-PCL-NFs compared with α-TC-PCL-NFs; because α-TC molecules were in the cavity. The difference is basically related with lower diffusion coefficient of α-TC/β-CD-IC-PCL-NFs and higher molecular weight of α-TC/β-CD-IC. This became clear after 30 minutes of immersion. It is known that presence of another compound in a solution reduces the diffusion rate [108]. In our case, IC between α-TC and β-CD might reduce the diffusion rate of α-TC. Finally, α-TC-PCL-NFs released more α-TC than α-TC/β-CD-IC-PCL-NFs in total. So; at the end of 1440 minutes, 21±2 ppm α-TC was released from α-TC-PCL-NFs; while 17±3 ppm α-TC was released from α-TC/β-CD-IC-PCL-NFs. Consequently; the release rate gradually decreased and sustained release of α-TC was achieved with α-TC/β-CD-IC-PCL-NFs [106,108]. In fact, this is very applicable for most of the drugs.

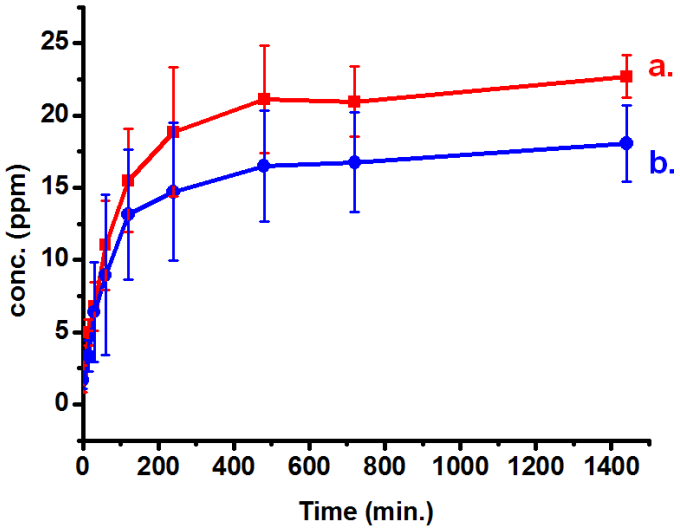

Figure 33. Cumulative release profiles of (a) α-TC-PCL-NFs, (b) α-TC/β-CD-IC-PCL-NFs.

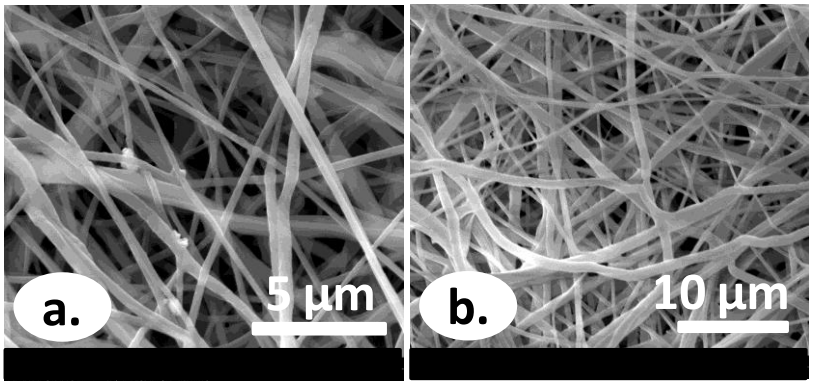

Figure 34. SEM images of (a) α-TC-PCL-NFs, (b) α-TC/β-CD-IC-PCL-NFs after HPLC.

It is known fact that α-TC degrades when exposed to UV light [103]. That's why; the percent of released α-TC from α-TC-PCL-NFs and α-TC/β-CD-IC-PCL-NFs samples after UV treatment for 45 minutes were investigated and shown in Figure 35. We calculated percent of released α-TC at the end of 1440 minutes, with the assumption of that the amount of α-TC released from untreated nanofibers at the end of 1440 minutes as 100% for each sample. Therefore, α-TC-PCL-NFs released 75% of α-TC; whereas, α-TC/β-CD-IC-PCL-NFs released 84% of α-TC after UV treatment for 45 minutes. So, the

protection of α-TC from UV light was more effective in α-TC/β-CD-IC-PCL-NFs. This situation is related with inclusion complexation between α-TC and β-CD [115]. The SEM images were taken after UV treatment as well (Figure 36). However, nanofibers kept their fiber structure after UV treatment for 45 minutes.

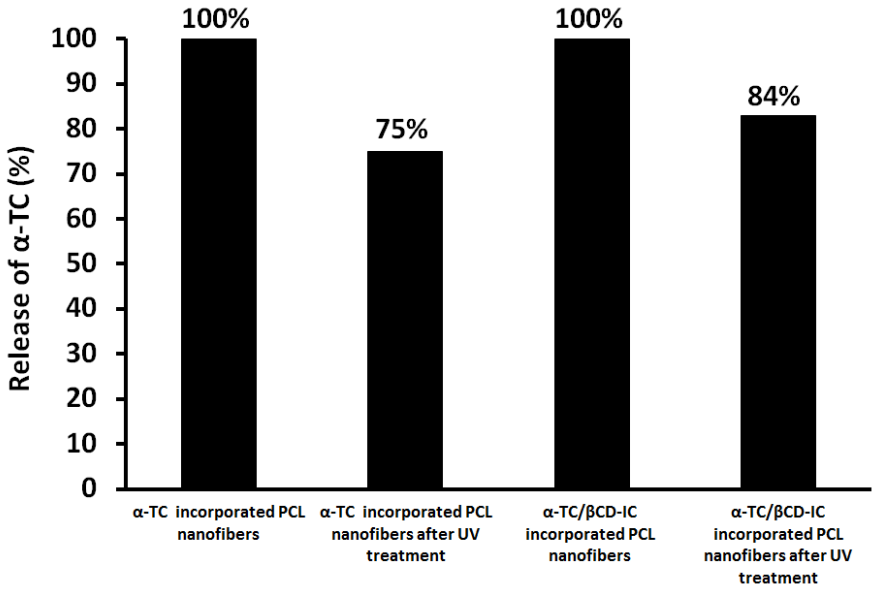

Figure 35. Percent of released α-TC from α-TC-PCL-NFs and α-TC/β-CD-IC-PCL-NFs after UV treatment for 45 minutes.

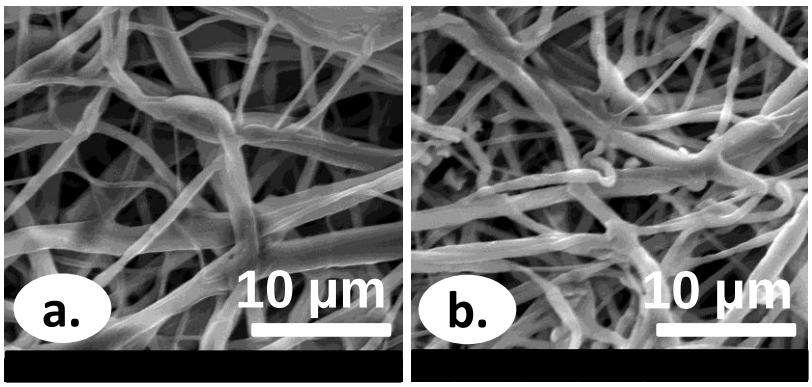

Figure 36. SEM images of (a) α-TC-PCL-NFs, (b) α-TC/β-CD-IC-PCL-NFs after UV treatment for 45 minutes.

The antioxidant activity of α-TC within α-TC/β-CD-IC-PCL-NFs was determined via DPPH radical scavenging assay. Electrospun PCL nanofibers and α-TC-PCL-NFs were used as control samples. The results were obtained

after 30 minutes of reaction in the dark between α-TC and DPPH and the graph was plotted absorbance (%) versus time in Figure 37. When α-TC encounter with an oxidant compound it loses its phenolic hydrogen and α-tocopheroxyl radical is formed. The abovementioned radical is highly stable and bind another radical by forming non-radical products or α-TC [116]. DPPH with a violet color is a stable free radical which can readily be scavenged by an antioxidant substance and that's why it is widely used compound to test the antioxidant activity of various molecules. The antioxidant activity of an antioxidant substance can be measured spectrophotometrically at 517 nm by the loss of absorbance as the pale yellow non-radical form (DPPH-H) is produced. In scavenging mechanism, antioxidant molecule acting as a donor of a hydrogen atom transform a DPPH radical into its reduced form DPPH; thus free radical character of DPPH is neutralized [117].

Initially, the violet color of solution in the beginning of the experiment turned to pale yellow at the end of 35 minutes. At the initial stage of UV measurement absorbance at 517 nm reduced, and then reached a plateau in 5 minutes, so there existed no more DPPH to deactivate in the solution [118].

From the reduction of the DPPH solution's absorbance at 517 nm, the antioxidant activity was calculated with the help of following formula:

$$\%\ \text{of DPPH scavenging} = \frac{(A_B - A_S)}{A_B} \times 100$$

where A_B is the absorption of the blank and A_S is the absorption of the sample [118]. Therefore, the antioxidant activity of electrospun PCL nanofibers, α-TC-PCL-NFs and α-TC/β-CD-IC-PCL-NFs were calculated as 19%, 43% and 63%, respectively. Firstly, high surface area to volume ratio of electrospun nanofibers might lead to absorption certain amount of DPPH and as a result electrospun PCL nanofibers exhibited 19% antioxidant activity. This situation was reported in the literature [118]. Secondly, antioxidant activity of α-TC/β-CD-IC-PCL-NFs was almost 20% more than α-TC-PCL-NFs. In addition, it is a known fact that CDs have no ability to degrade DPPH from the literature [119]. Owing to

the inclusion complexation between α-TC and β-CD, the solubility of α-TC might have increased; so enhanced solubility of α-TC may be the main reason of higher antioxidant activity of α-TC/β-CD-IC-PCL-NFs. This result was consistent with literature as well [120-121]. Finally, we can conclude that after electrospinning α-TC including (both in free form and IC) PCL nanofibers still maintained their antioxidant property in spite of high electrical potential applied during electrospinning onto α-TC (both in free form and IC) containing PCL solutions [114].

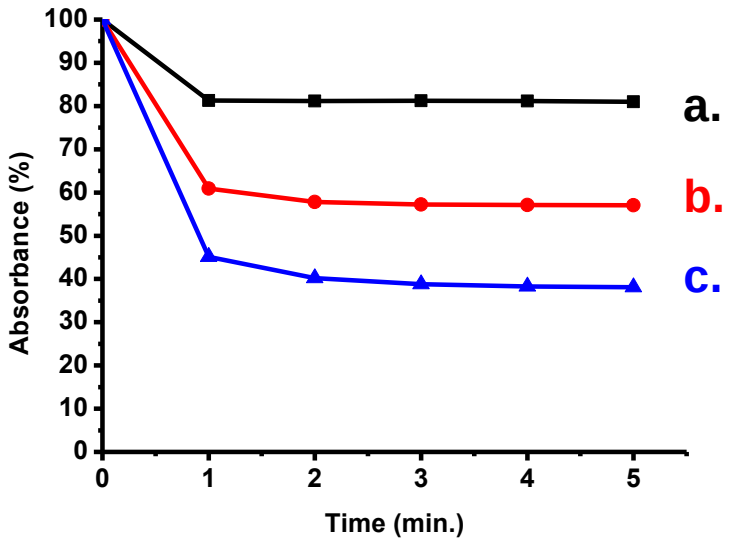

Figure 37. Antioxidant activity of (a) electrospun PCL nanofibers, (b) α-TC-PCL-NFs, (c) α-TC/β-CD-IC-PCL-NFs.

4.8. Conclusion

α-TC/β-CD-IC was prepared, incorporated into PCL and nanofibers were produced via electrospinning technique. The characterization of nanofibers was done by SEM, XRD, DSC, and TGA. As observed in SEM images incorporating α-TC into nanofibers, immersing these nanofibers in PBTM and exposing them to UV light did not result in any deformation in the morphology of nanofibers. α-TC/β-CD-IC-PCL-NFs showed controlled release and better photostability than α-TC-PCL-NFs. Moreover, α-TC/β-CD-IC-PCL-NFs displayed much

higher antioxidant activity as compared to α-TC-PCL-NFs, due to the higher solubility of α-TC.

CHAPTER IV. RELEASE of ALLYL ISOTHIOCYANATE from ELECTROSPUN POLYVINYL ALCOHOL NANOFIBERS INCORPORATING CYCLODEXTRIN INCLUSION COMPLEX

5.1. General Information

The drug delivery systems are designed to reduce side effects, and improve bioavailability and therapeutic efficacy of drugs. Polymeric drug delivery systems have higher therapeutic effect, convenience, and lower toxicity than conventional drug delivery systems. However, burst release at the initial stage and low efficiency in drug delivery are the main problems of polymeric drug delivery systems [78]. Electrospinning is a widely used method to produce nanofibers with unique properties like high surface area to volume ratio and nanoporous structure [5]. These unique properties enable them to be used in wound dressing, tissue scaffold and drug delivery applications [101].

Cyclodextrins (CDs) are cyclic oligosaccharides and they have a hydrophobic cavity. Owing to this cavity, CDs are able to form host-guest complexes with molecules in appropriate polarity and dimension. Inclusion complex (IC) of CDs with a guest molecule has advantages like higher solubility of hydrophobic guests, higher thermal stability and bioavailability, control of volatility, masking off unpleasant odors, and controlled release of drugs and flavors [38].

In this study, allyl isothiocyanate (AITC) (Figure 38a) encapsulated electrospun polyvinyl alcohol (PVA) nanofibers were generated. IC of AITC and beta-cyclodextrin (β-CD) (Figure 38b, 38c) (AITC/β-CD-IC) was prepared in aqueous solution and then incorporated in PVA solution; lastly AITC/β-CD-IC including PVA nanofibers (AITC/β-CD-IC-PVA-NFs) was produced via electrospinning. The schematic representation of AITC/β-CD-IC was shown in Figure 38d. The resulting AITC/β-CD-IC-PVA-NFs were characterized by scanning electron microscope (SEM), X-ray diffraction (XRD), thermogravimetric analysis (TGA), and gas chromatography-mass spectrometry

(GC-MS). The antibacterial activity of AITC/β-CD-IC-PVA-NFs was tested against Escherichia coli (E.coli) and Staphylococcus aureus (S.aureus) according to colony counting method. The sustained released behavior and quite high antibacterial activity of AITC/β-CD-IC-PVA-NFs enable these nanofibers to be used in wound healing applications.

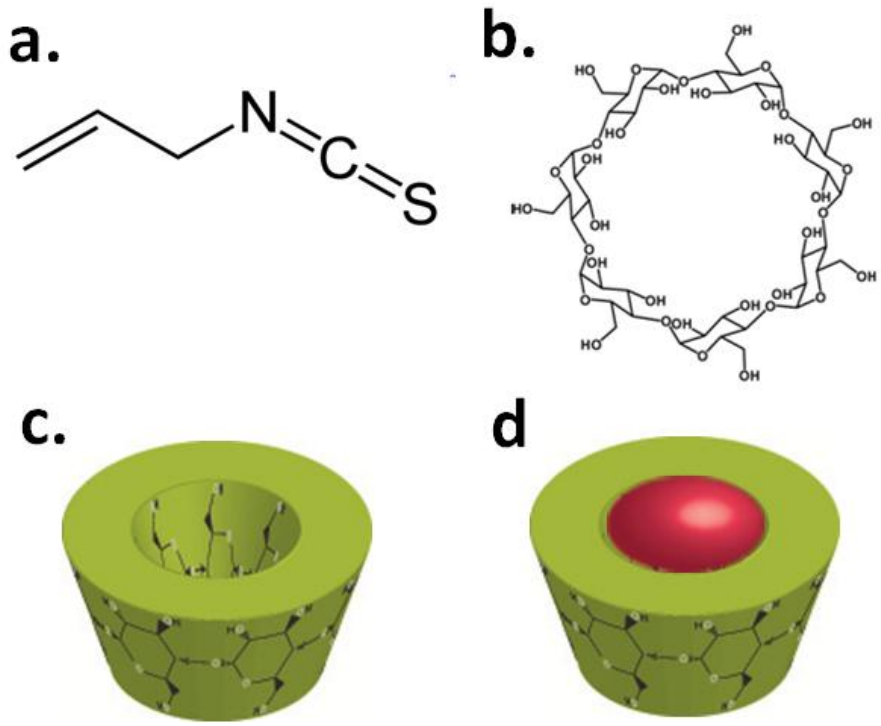

Figure 38. Chemical structure of (a) AITC, (b) β-CD; schematic representation of (c) β-CD, and (d) AITC/ β-CD-IC.

5.2. Materials

Polyvinyl alcohol (PVA, M_w ~ 85.000-146.000 g/mol, Sigma aldrich, 87-89% hydrolyzed), allyl isothiocyanate (AITC, Sigma aldrich, 95%), beta-cyclodextrin (β-CD, Wacker chemie AG, Germany) were purchased and used as-received without any further purification. Distilled water was supplied from Millipore Milli-Q Ultrapure Water System.

5.3. Production of electrospun nanofibers

PVA solution was prepared by dissolving PVA (7.5% (w/v)) in aqueous solution and this solution was electrospun. Drug delivery systems were prepared

by electrospinning of AITC without β-CD including PVA (AITC-PVA) solution or AITC/β-CD-IC including PVA (AITC/β-CD-IC-PVA) solution. AITC/β-CD-IC was prepared at 2:1 molar ratio (AITC:β-CD). The same amount of AITC was used for both of the samples. Initially, AITC-PVA solution was prepared. AITC was dissolved in aqueous solution and PVA (7.5% (w/v)) was put in this solution; then the solution was stirred at room temperature overnight. With regard to, AITC was dispersed in water for 0.5 hour and clear solution was obtained. Then β-CD was added and resulting solution was stirred overnight at room temperature and white, turbid solution was obtained. This turbidity might be due to aggregation of AITC/β-CD-IC. Then, PVA (7.5% (w/v)) was put in and stirred 6 hours more at room temperature. Lastly, PVA solution, AITC-PVA solution and AITC/β-CD-IC-PVA solution were loaded into a 3 ml plastic syringe with a needle inner diameter of 0.8 mm placed horizontally on the pump and was sent towards to the collector at 1 ml/h rate. 15 kV was obtained from a high voltage power supply. Cylindrical metal covered with aluminum foil was used as a collector. Distance between needle tip and collector was 10 cm. Experiments were performed at 24-25°C, 17-20% humidity.

5.4. Measurements and characterization techniques

The morphologies and average fiber diameters (AFDs) of PVA nanofibers and AITC/β-CD-IC-PVA-NFs were examined by SEM (FEI – Quanta 200 FEG). Before taking SEM images, samples were coated 5 nm Au/Pd. In order to calculate AFDs, around 100 fibers were analyzed.

XRD data for PVA nanofibers, β-CD and AITC/β-CD-IC-PVA-NFs were recorded using a PANalytical X'Pert powder diffractometer applying Cu Kα radiation in a 2θ range 5°–30°.

In order to investigate the thermal stability of AITC in the electrospun nanofibers; AITC/β-CD-IC-PVA-NFs were assessed via TGA (Q 500, TA Instruments, USA). AITC, electrospun PVA nanofibers and β-CD were also tested for comparison. The measurements were carried out under nitrogen

atmosphere, the samples were heated up to 500°C at a constant heating rate of 20°C/min.

The amount of released AITC from AITC without β-CD including PVA nanofibers (AITC-PVA-NFs) and AITC/β-CD-IC-PVA-NFs were determined by headspace GC-MS of Agilent Technologies 7890A gas chromatograph coupled to an Agilent Technologies 5975C inert MSD with a triple-axis detector for 300 minutes. AITC-PVA-NFs were used as control sample. The used capillary column was HP-5MS (Hewlett-Packard, Avondale, PA) (30ml X 0.25mm i.d., 0.25μm film thickness). 20 mg of AITC-PVA-NFs and AITC/β-CD-IC-PVA-NFs were placed in 20 mL headspace glass vials. The vials were agitated at 500 rpm at 37°C of incubation temperature. Helium was used as carrier gas was at a flow rate of 1.2 mL/min. Five hundred microliters of vapor was injected to the GC-MS by using a headspace injector (MSH 02-00B, volume = 2.5 mL, scale = 60 mm). The syringe temperature was 50°C. Oven temperature was held at 50°C for 1 min and increased to 200°C at the rate of 20°C/min and held at this temperature for 3 min. Thermal desorption was conducted in the split mode (20:1). GC-MS analyses were carried out in the complete selected ion monitoring mode (SIM). Flavor 2 and NIST 0.5 libraries were used to decide AITC peak. The retention time of AITC was 11.5 minutes. For calibration samples were put in vials and analyzed with same parameters as nanofibers samples. Two samples were tested and results were given as average.

The antibacterial activity of AITC/β-CD-IC-PVA-NFs was tested against both gram-negative bacterium and gram-positive bacterium which are E.coli and S. aureus, respectively. This test was assessed by colony counting method. 400μL of the overnight grown E. coli and S. aureus were inoculated into 40 mL of Luria-Bertani (LB) broth (in 100 mL-flask) and AITC/β-CD-IC-PVA-NFs was sterilized by UV irradiation and put into the flasks. The mediums with bacteria and nanofibers were incubated at 37^0C and 125 rpm for 24 hours. Controls were E. coli and S. aureus grown at 37^0C and 125 rpm for 24 hours without fibers. Samples from each flask and controls were serially diluted, 100μL of each was spread onto LB agar and colonies were counted. All samples

and controls were performed in triplicate and reported as average. The colony forming units (cfu) of bacteria with fibers were compared to controls.

5.5. Results and discussion

PVA is a polymer that is widely used in biomedical applications owing to its biocompatibility and biodegradability. Electrospun PVA nanofibers found application in drug delivery, tissue engineering and wound healing [33, 122-123]. AITC is an antimicrobial compound found in horseradish, mustard, and wasabia [124-125]. It could be used in wound dressing applications [126-127] as well as food packaging [128-129]. IC of AITC with CDs was investigated as well [125, 130]. In a study, Ohta et al. prepared IC of AITC with alpha-cyclodextrin (α-CD) and beta-cyclodextrin (β-CD); and deduced that decomposition of AITC was reduced by inclusion complexation [130]. In another study, Li et al. investigated controlled release property of AITC/α-CD-IC and AITC/β-CD-IC. They concluded that the release of AITC increased as relative humidity increases, and the release rate of AITC was slower in AITC/α-CD-IC compared to AITC/β-CD-IC [125]. Here, we produced AITC/β-CD-IC-PVA-NFs via electrospinning. Therefore, we combined high surface area and nanoporous structure of electrospun nanofibers with high solubility of AITC/β-CD-IC.

Figure 39 showed the SEM images and AFD distributions of electrospun PVA nanofibers and AITC/β-CD-IC-PVA-NFs. Initially, we produced bead-free PVA nanofibers (7.5% (w/v)) in aqueous solution through electrospinning and AFD was calculated as 290±65 nm. Then we incorporated AITC/β-CD-IC into PVA solution and electrospinning was performed. As seen in SEM images, incorporation of AITC/β-CD-IC into PVA nanofibers did not change the morphology of nanofibers. On the other hand, the AFD of AITC/β-CD-IC-PVA-NFs was 235±90 nm. The slightly thinner nanofiber formation was likely due to the lower viscosity and/or higher conductivity of AITC/β-CD-IC-PVA solution than PVA solution [1].

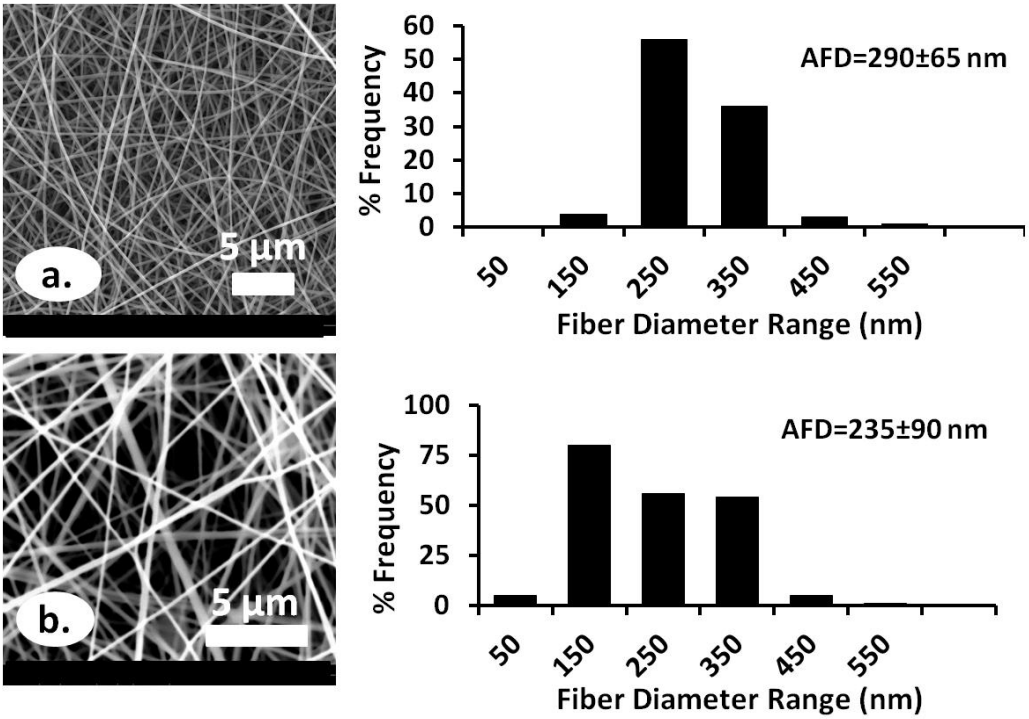

Figure 39. SEM images and AFD distributions of (a) electrospun PVA nanofibers, (b) AITC/β-CD-IC-PVA-NFs.

The XRD patterns of electrospun PVA nanofibers, β-CD and AITC/β-CD-IC-PVA-NFs were depicted in Figure 40. Since AITC is liquid at room temperature, it has no crystalline diffractions. PVA is an amorphous polymer with a broad diffraction at around 2θ~19.6. Our data were supported by the literature [131]. On the other hand, once β-CD forms IC with a guest molecule; the cage type packing turns into channel type packing. The channel type packing of β-CD has two characteristic peaks at 2θ~12◦ and 18◦. The observation of characteristic peaks of channel type packing on XRD pattern indicates IC formation between CD and guest molecule [132]. Therefore; as we observed peak at 2θ~12◦, we concluded that there might be IC formation between AITC and β-CD in AITC/β-CD-IC-PVA-NFs. In addition; the difference from cage type packing of β-CD curve supported IC formation.

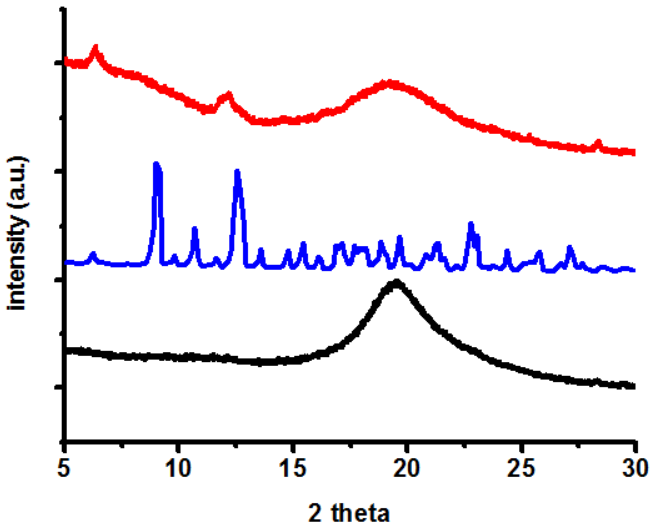

Figure 40. XRD patterns of (a) electrospun PVA nanofibers, (b) β-CD, (c) AITC/β-CD-IC-PVA-NFs.

TGA was performed to investigate thermal stability of AITC/β-CD-IC-PVA-NFs (Figure 41). AITC, electrospun PVA nanofibers, β-CD were also tested by TGA for comparison. AITC is known to be a volatile compound, that's why its decomposition was below 100°C. This result was consistent with the literature [128]. Electrospun PVA nanofibers exhibited weight loss starting ~250°C that corresponds to the main thermal degradation of PVA [133]. On other side, thermal degradation of β-CD occurs in two steps. One of them was water loss which continues up to 100°C; whereas the second was main thermal degradation of β-CD which was above ~275°C [128]. With respect to TGA thermogram of AITC/β-CD-IC-PVA-NFs, the first weight loss below 100°C might be attributed to the water loss; the second weight loss which was between ~200°C and ~375°C was likely due to the AITC, β-CD and PVA loss. As a result, incorporation of AITC/β-CD-IC in PVA nanofibers has greatly improved the thermal stability of AITC. Therefore, it was concluded AITC might form IC with β-CD. This was also observed in the literature [128].

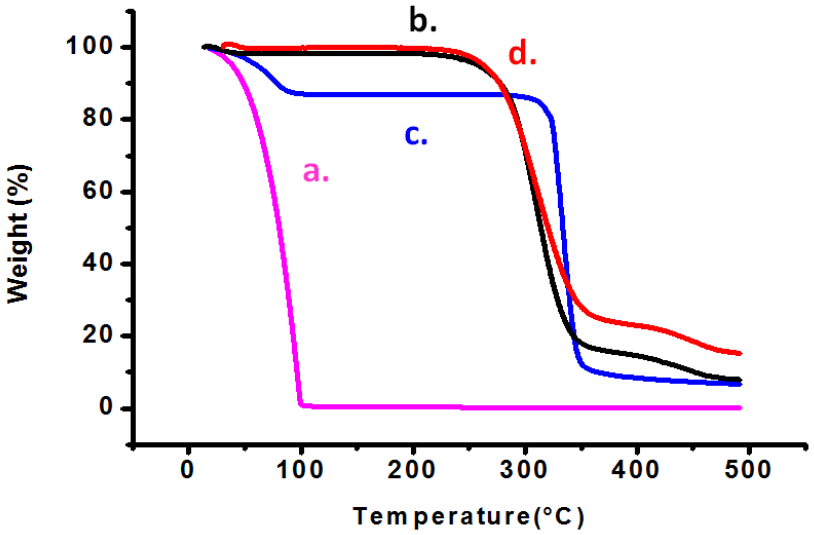

Figure 41. TGA thermograms of (a) AITC, (b) electrospun PVA nanofiber, (c) βCD, (d) AITC/βCD inclusion complex incorporated electrospun PVA nanofibers.

The release behavior of AITC from AITC/β-CD-IC-PVA-NFs was evaluated by GC-MS for 300 minutes (Figure 42). 20 mg of AITC/β-CD-IC-PVA-NFs were placed in headspace glass vials and stirred at 37°C during the experiment. According to the calibration curve the results were converted to concentration versus time. AITC-PVA-NFs were also tested as a control sample. The release of AITC was relatively quick in the initial stage, then release rate of AITC reduced and finally constant release was observed [125]. Therefore, we successfully achieved to produce AITC/β-CD-IC-PVA-NFs with a sustained release behavior. On the other hand, the release values of AITC-PVA-NFs were only 1.6% of AITC/β-CD-IC-PVA-NFs. However, at the end of 300 minutes AITC/β-CD-IC-PVA-NFs released almost 67% of AITC that we theoretically put in the solution. This result showed that β-CD prevented AITC to evaporate during preparation of solution or electrospinning process. This result was in consistence with the literature [129].

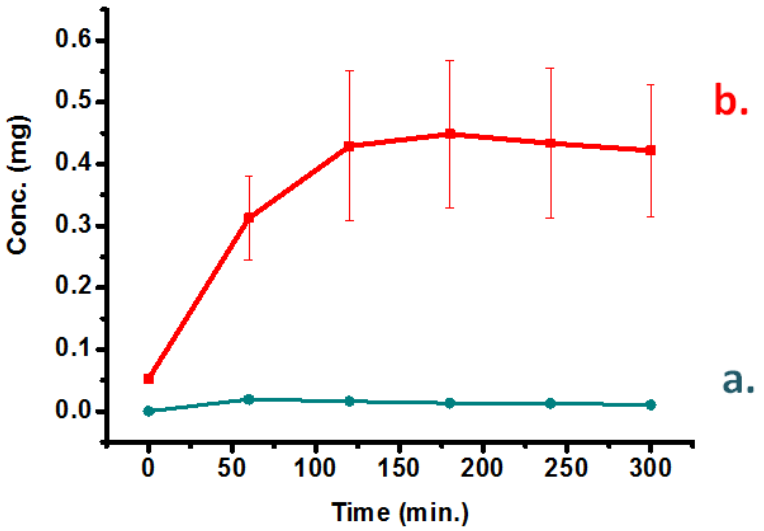

Figure 42. Cumulative release of (a) AITC-PVA-NFs, (b) AITC/β-CD-IC-PVA-NFs.

Antibacterial activity of AITC/β-CD-IC-PVA-NFs was tested by colony counting method against E.coli and S. aureus for 24 hours. Figure 43 presented exemplary images of bacteria, bacteria colonies treated by AITC/β-CD-IC-PVA-NFs and the growth inhibition rate (%) of AITC/β-CD-IC-PVA-NFs for both E.coli and S. aureus. It was calculated by assuming plates without nanofibers as 100%. AITC/β-CD-IC-PVA-NFs exhibited 97.62% antibacterial activity against E.coli; whereas antibacterial activity against S.aureus was 99.19%. The difference in the antibacterial activity against E.coli and S.aureus is likely related with difference between cell wall composition of two bacteria which are gram negative and gram positive, respectively. Thus gram negative bacteria have a semi-permeable barrier that decelerates passing of macromolecules and hydrophobic compounds [133]. Moreover, electrospinning in which we applied high voltage has no negative effect on the antibacterial property of AITC/β-CD-IC-PVA-NFs.

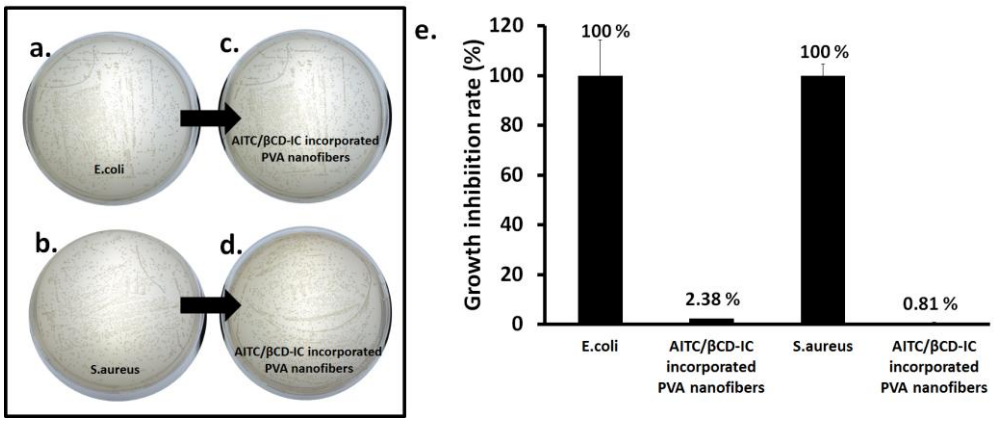

Figure 43. Exemplary images of (a) control sample - colonies of E.coli and (b) S.aureus; c) E.coli colonies and (d) S.aureus colonies treated by AITC/β-CD-IC-PVA-NFs; (e) antibacterial activity of AITC/β-CD-IC-PVA-NFs against E.coli and S.aureus.

5.6. Conclusion

AITC/β-CD-IC-PVA-NFs were produced via electrospinning. The characterizations were performed by SEM, XRD, and TGA. SEM images demonstrated that the morphology of PVA nanofibers did not change after the incorporation of AITC/β-CD-IC. In addition; owing to IC between AITC and β-CD, the release of AITC from AITC/β-CD-IC-PVA-NFs was significantly higher than AITC-PVA-NFs. The antibacterial activity of AITC/β-CD-IC-PVA-NFs against E.coli and S.aureus was 97.62% and 99.19%, respectively. Finally, both sustained release and quite high antibacterial activity of AITC/β-CD-IC-PVA-NFs enable it to be used in wound dressing applications.

CHAPTER V. RELEASE of QUERCETIN from ELECTROSPUN POLYACRYLIC ACID NANOFIBERS INCORPORATING CYCLODEXTRIN INCLUSION COMPLEX

6.1. General Information

The polymeric drug delivery systems have advantages such as improving therapeutic effect and convenience, and reducing toxicity; while they might cause burst release of drugs and low efficiency in drug delivery [78]. Electrospinning is a simple and cost-effective method for producing nanofibers with high surface area to volume ratio and nanoporous structure [5]. Owing to these unique properties electrospun nanofibers is of importance in wound dressing, drug delivery systems and tissue engineering scaffolds [101].

Cyclodextrins (CDs) are cyclic oligosaccharides with truncated cone shape structure. They have relatively hydrophobic cavity that allows formation of inclusion complex (IC) with a variety of molecules in appropriate polarity and dimension. ICs of CDs are favorable because they might exhibit higher solubility and thermal stability of hydrophobic guests; controlling volatility, masking off unpleasant odors, and controlled release of drugs and flavors [38].

In this study, IC of quercetin (QU) (Figure 44a) and beta-cyclodextrin (β-CD) (Figure 44b, 44c) was formed (QU/β-CD-IC) at 1:1 molar ratio. The schematic representation of QU/β-CD-IC was shown in Figure 44d. Then QU/β-CD-IC incorporating polyacrylic acid (PAA) nanofibers (QU/β-CD-IC-PAA-NFs) were produced via electrospinning. QU/β-CD-IC including PAA films (QU/β-CD-IC-PAA films) was also produced as control. Obtained films and nanofibers were thermally crosslinked at 140°C for 40 minutes, and insoluble films and nanofibers were obtained. The characterizations were performed by scanning electron microscopy (SEM), X-ray diffraction (XRD) and thermogravimetric analysis (TGA). The release of QU into phosphate buffer saline (PBS) including methanol and tween 20 (PBMT) from QU/β-CD-IC-PAA-films and QU/β-CD-IC-PAA-NFs were determined via high performance

liquid chromatography (HPLC). In addition, the antioxidant activity was investigated through UV-Vis NIR spectroscopy.

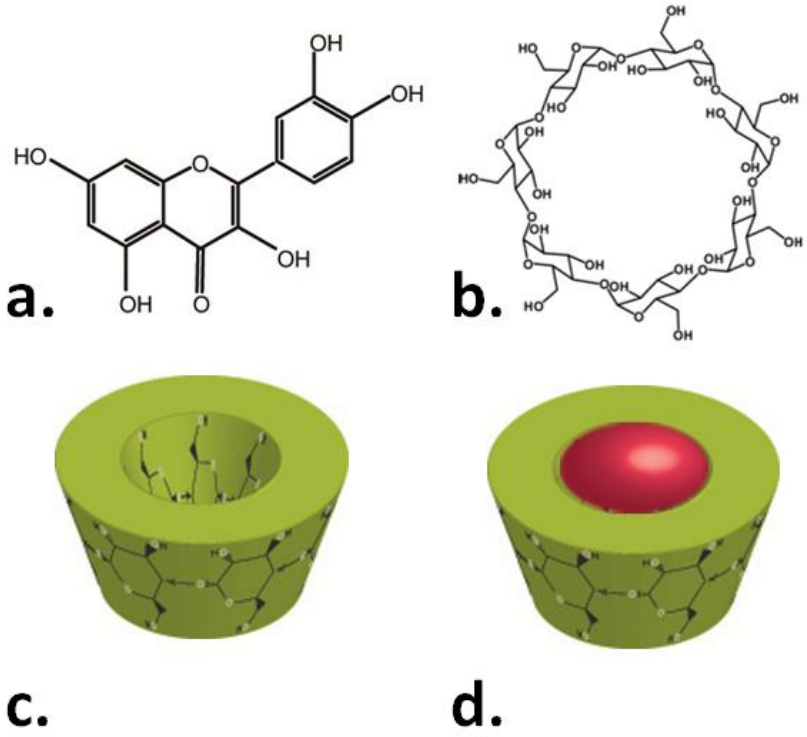

Figure 44. Chemical structure of (a) QU, (b) β-CD; schematic representation of (c) β-CD, and (d) QU/β-CD-IC.

6.2. Materials

Polyacrylic acid (PAA, M_w ~ 450.000 g/mol, Sigma aldrich), beta-cyclodextrin (β-CD) (Wacker chemie AG, Germany), quercetin (QU, Sigma aldrich, ≥98%), methanol (Sigma aldrich, extra pure), ethanol (Sigma aldrich, 99.8%), methanol chromasolv (Sigma aldrich), potassium phosphate monobasic (Riedel de haen), disodium hydrogen phosphate 12-hydrate (Riedel de haen), sodium chloride (Sigma aldrich), tween 20 (Sigma aldrich), 2,2-diphenyl-1-picrylhydrazyl (DPPH, Sigma aldrich) were purchased and used as-received without any further purification. Distilled water was supplied from Millipore Milli-Q Ultrapure Water System.

6.3. Production of films and electrospun nanofibers

QU/β-CD-IC-PAA-films and QU/β-CD-IC-PAA-NFs were produced via solvent casting method and electrospinning, respectively. The molar ratio of QU:β-CD was 1:1 for both of the samples. For preparation of QU/β-CD-IC-PAA-films, QU was dissolved in aqueous solution. Then, β-CD was added and the solution was stirred for 12 hours at room temperature. Finally, PAA (7.5% (w/v)) was added and the solution was stirred 4 hours more. Films were prepared from as-prepared solutions by casting them onto glass petri dish; as the solvent evaporates, films were formed in petri dish. In order to produce QU/β-CD-IC-PAA-NFs; initially, QU was dissolved in aqueous solution for 0.5 hours; after the addition of β-CD, the solution was stirred for 12 hours at room temperature. Lastly, PAA (7.5% (w/v)) was added and stirred 4 hours more. The resulting solution loaded into 3 ml plastic syringe with a needle inner diameter of 0.8 mm were placed horizontally on the pump and sent towards to the collector at 1 ml/h rate. 15 kV was obtained from a high voltage power supply. Cylindrical metal covered with aluminum foil was used as a collector. Distance between needle tip and collector was 15 cm. Experiments were performed at 23°C-26°C, 17%-18% humidity. Finally, QU/β-CD-IC-PAA-films and QU/β-CD-IC-PAA-NFs were thermally crosslinked at 140°C for 40 minutes in vacuum drying oven. Here, we think that hydroxyl groups of β-CD and carboxyl groups of PAA was crosslinked and insoluble QU/β-CD-IC-PAA-films and QU/β-CD-IC-PAA-NFs were obtained.

6.4. Preparation of phosphate buffer

For the preparation of PBS, 1.44 g potassium phosphate monobasic, 10.74 g disodium hydrogen phosphate 12-hydrate and 90 g sodium chloride were dissolved in 1000 ml of distilled water. Then, this solution was diluted with distilled water at the rate of 1:9. 10% methanol and 0.5% tween 20 were added into PBS to increase the solubility of α-TC in the releasing medium and lastly PBMT was obtained. pH of the releasing media was measured as about 7.

6.5. Drug release assay

Total immersion method was used to investigate the cumulative release profiles of QU from QU/β-CD-IC-PAA-films and QU/β-CD-IC-PAA-NFs. The films and nanofibers were immersed in 30 ml of PBMT at 37°C, stirred at 50 rpm for 360 minutes. 0.5 ml of the test medium was withdrawn and an equal amount of the fresh medium was refilled. The amount of released QU was measured via HPLC equipped with VWD UV detector. The calibration samples were prepared by dissolving QU in PBMT. The concentration of QU was calculated to determine the cumulative amount of QU released from the samples at each specified immersion period. The experiments were performed in triplicate and the results were reported as average values±standard deviation.

6.6. Measurements and characterization techniques

The morphologies and average fiber diameters (AFDs) of QU/β-CD-IC-PAA-NFs before and after crosslink were examined by SEM (FEI – Quanta 200 FEG). Before taking SEM images, samples were coated 5 nm Au/Pd. In order to calculate AFDs, around 100 fibers were analyzed.

XRD data for QU, PAA, β-CD, QU/β-CD-IC-PAA-films and QU/β-CD-IC-PAA-NFs were recorded using a PANalytical X'Pert powder diffractometer applying Cu Kα radiation in a 2θ range 5°–30°.

In order to investigate the thermal stability of QU in the electrospun nanofibers; QU/β-CD-IC-PAA-NFs were assessed via TGA (Q 500, TA Instruments, USA). QU, PAA, β-CD and QU/β-CD-IC-PAA-films were also tested for comparison. The measurements were carried out under nitrogen atmosphere, the samples were heated up to 600°C at a constant heating rate of 20°C/min.

Amount of released QU from QU/β-CD-IC-PAA-films and QU/β-CD-IC-PAA-NFs were measured using HPLC (Agilient, 1200 series) equipped with VWD UV detector. The column used was a 250 mm×4.6 mm i.d., 5μm, Inertisil GL Sciences Inc. diol column and the detection was accomplished at 375 nm.

Mobile phase, flow rate, injection volume and total run time were 100% methanol, 1 ml/min, 20 µl and 7 minutes, respectively.

Antioxidant tests for QU/β-CD-IC-PAA-films and QU/β-CD-IC-PAA-NFs were performed via DPPH radical scavenging assay. 10^{-4} M DPPH solution was prepared in ethanol/water (50:50); and 2 mg nanofibers were dissolved in ethanol. Then, 0.5 ml of nanofibers solution was added on 2.5 ml of DPPH solution. The resulting mixture was remained in the dark for 15 minutes at room temperature. At the end of the 15 minutes, the absorbance of the solutions was measured with UV-Vis NIR Spectroscopy (Varian Cary 5000) at 517 nm.

6.7. Results and discussion

PAA is an anionic polyelectrolyte and amorphous polymer [134]. Electrospinning of PAA was studied by many groups [37, 135-136]. In addition, there are also studies on bioapplications of PAA [36, 137]. On the other hand, QU is an antioxidant flavonoid and a hydrophobic compound. It is a widely used substance especially for bioapplications [138]. There exist many studies in the literature about IC of QU with CDs [105, 139-141]. Furthermore, IC of QU and CDs were incorporated in polymeric films. In these studies CDs used for controlled release or acted as protective compound against oxidation of QU [107-108]. Here, we produced QU/β-CD-IC-PAA-NFs through electrospinning in order to combine high surface area to volume ratio and nanoporous structure of electrospun nanofibers with high solubility of QU/β-CD-IC.

The SEM images and AFD distributions of QU/β-CD-IC-PAA-NFs before crosslink were shown in Figure 45. We observed that uniform nanofibers were obtained from 7.5% (w/v) polymer concentration in aqueous solution (Figure 45). In addition, QU molecules were dispersed homogenously inside the nanofiber. Therefore, we might deduce that QU molecules were inside the nanofibers due to the rapid evaporation of solvent molecules during electrospinning. Similar results were observed in a study in which four different kinds of drugs were encapsulated in electrospun cellulose acetate nanofibers [79]. We calculated AFD of QU/β-CD-IC-PAA-NFs as 805±185 nm.

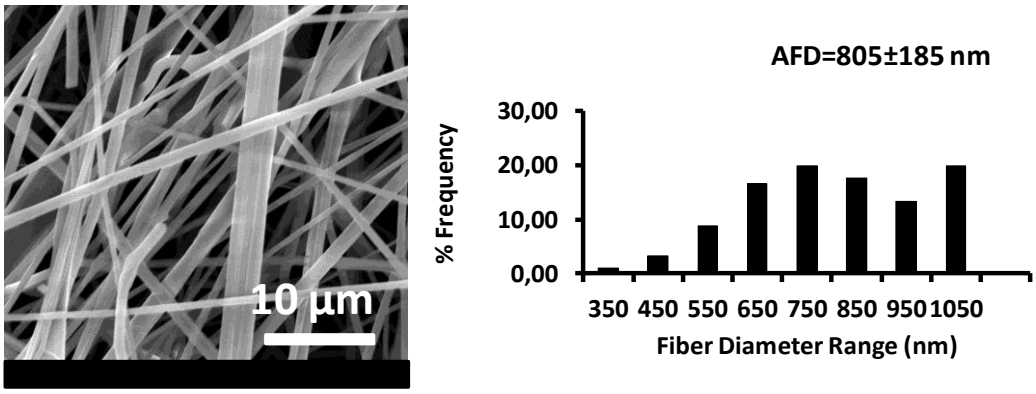

Figure 45. SEM images and AFD distributions of QU/β-CD-IC-PAA-NFs before crosslink.

Moreover, SEM image of QU/β-CD-IC-PAA-NFs after crosslink was shown in Figure 46. As seen from the SEM image nanofibers kept their fiber structure after crosslink.

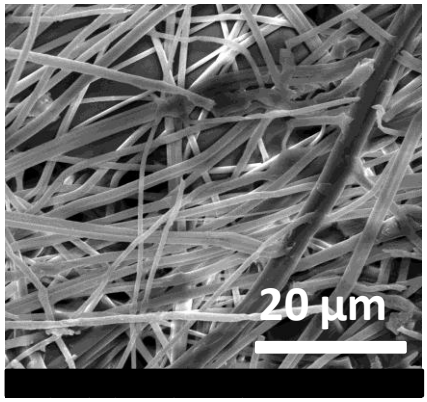

Figure 46. SEM images of QU/β-CD-IC-PAA-NFs after crosslink.

The XRD patterns of QU, PAA, β-CD, QU/β-CD-IC-PAA-films and QU/β-CD-IC-PAA-NFs were displayed in Figure 47. QU is a highly crystalline compound with sharp diffraction peaks. This result was supported by a study about QU loaded nanoparticles from the literature [142]. On the other side, PAA has an amorphous nature with broad diffraction peak as stated in a study that is on synthesizing PAA-metal nanocomposites [143]. In the XRD pattern of QU/β-CD-IC-PAA-films, we observed some of the diffraction peaks (2θ=5.56°, 10.98°, 13.58°, 16.53°) those belong to QU. This might show that there existed

uncomplexed QU molecules inside the films. The XRD pattern of QU/β-CD-IC-PAA-NFs showed broad halo diffraction pattern with a distinct diffraction peak at 2θ=13.58°. This result showed that QU/β-CD-IC-PAA-NFs were mostly amorphous. In addition, the diffraction peak at 2θ=13.58° showed the presence of some uncomplexed free QU inside the nanofibers. On the other hand; when β-CD forms IC with a guest molecule, the cage type packing of β-CD turns into channel type packing (2θ=12° and 18°) [132]. We could not observe channel type packing of β-CD in XRD pattern of QU/β-CD-IC-PAA-NFs, so we could not deduce that there was IC formation between QU and β-CD or not.

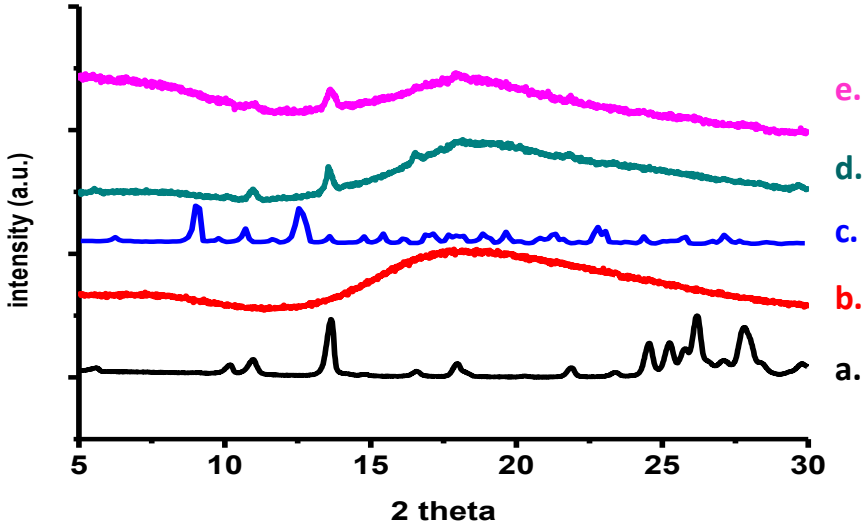

Figure 47. XRD patterns of (a) QU, (b) PAA, (c) βCD, (d) QU/β-CD-IC-PAA films, (e) QU/β-CD-IC-PAA-NFs.

The thermal stability of QU, PAA, β-CD, QU/β-CD-IC-PAA-films, and QU/β-CD-IC-PAA-NFs were investigated by TGA (Figure 48). The thermal degradation of QU started at around 280°C and this was consistent with the literature investigating solid dispersions of QU and a polymer [144]. The thermal degradation of PAA occurred in three steps. The first degradation was between 190-290°C, second degradation was between 290-350°C; whereas the third degradation which was the main thermal degradation started at around 420°C. This was also observed in the literature concerning PAA doped polyaniline [145]. β-CD had two steps of thermal degradation. The first one is

water loss that is up to 100°C and the second one is its main thermal degradation and above 275°C [112]. QU/β-CD-IC-PAA-films exhibited three stages during its thermal degradation. The first degradation which started at around 200°C ascribed to the first thermal degradation of PAA, the second one attributed to thermal degradation of β-CD, QU and PAA and started at about 250°C; finally, the last one started at about 360°C and belonged to the main thermal degradation of PAA. Similarly, QU/β-CD-IC-PAA-NFs had three steps of thermal degradation. These degradation points started at around 220°C, 280°C, 360°C and attributed to thermal degradations of PAA; β-CD, QU and PAA; and PAA respectively. In brief, we could not observe any improvement in the thermal stability of QU; therefore we cannot state that there is an IC formation between QU and β-CD or not. Similarly, in the study of Koontz et al. the improvement could not be achieved for QU/gamma-cyclodextrin (γ-CD)-IC as well [105].

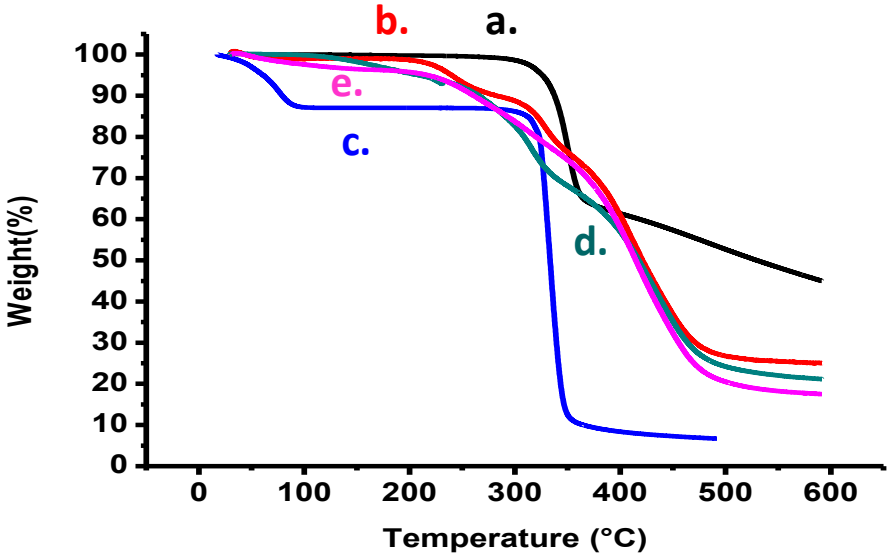

Figure 48. TGA thermograms of (a) QU, (b) PAA, (c) βCD, (d) QU/β-CD-IC-PAA films, (e) QU/β-CD-IC-PAA-NFs.

The release experiments for QU/β-CD-IC-PAA-films and QU/β-CD-IC-PAA-NFs were performed in PBMT at 37°C for 360 minutes. The concentration of released QU versus time was shown in Figure 49. Zero-order release kinetic was observed for QU/β-CD-IC-PAA-films and QU/β-CD-IC-PAA-NFs. We can

divide into two stages the release behavior of QU from both of the samples. QU released relatively quickly in the first stage; then the release rate became constant.

QU is a hydrophobic compound, so it is not soluble in PBS. That's why we added methanol and tween 20 into PBS in order to increase dissolution and facilitate detection of QU. It is not soluble in polymer solution as well. Therefore, its interaction with polymer was not strong. This was also observed between another drug molecule and polymer in the literature [113]. Briefly, we expected QU to release rapidly in the first stage. On the other hand, we know that presence of another molecule in the solution reduces the diffusion rate [108]. So, the existence of QU/β-CD-IC reduced the diffusion coefficient and release rate of QU from QU/β-CD-IC-PAA-films and QU/β-CD-IC-PAA-NFs. QU/β-CD-IC-PAA-films released 24±3 ppm QU; while QU/β-CD-IC-PAA-NFs released 21±6 ppm in the initial stage. In general nanofibers exhibit higher release rate than films due to their high surface area to volume ratio and porous structure at nanoscale as reported in the literature [146]. In our case, uncomplexed QU molecules might be responsible from relatively higher release rate of films compared with nanofibers at the initial stage. Lastly, the released amount of QU was almost same for QU/β-CD-IC-PAA films and QU/β-CD-IC-PAA-NFs. As a result, we successfully achieved to produce controlled release of QU from QU/β-CD-IC-PAA-NFs.

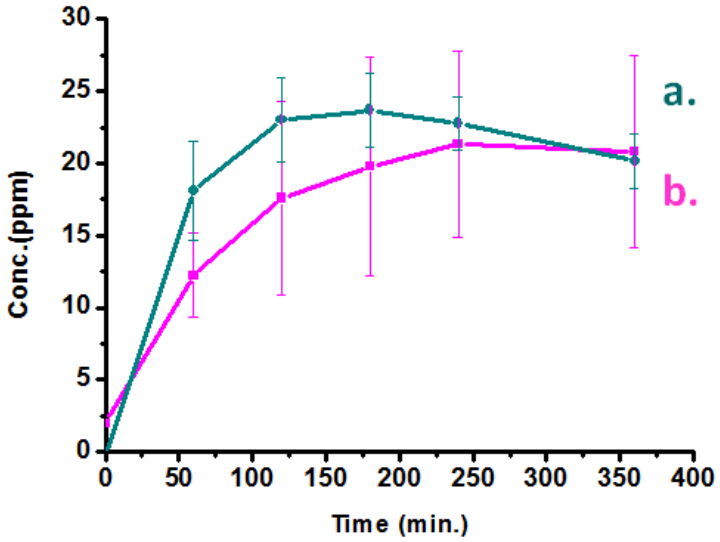

Figure 49. Cumulative release profiles of (a) QU/β-CD-IC-PAA-films, (b) QU/β-CD-IC-PAA-NFs.

The antioxidant activity of QU in QU/β-CD-IC-PAA-films and QU/β-CD-IC-PAA-NFs were examined through DPPH radical scavenging assay. The results were shown in Figure 50. DPPH is a stable free radical in violet color. It is commonly used for testing antioxidant activity of antioxidant molecules. In radical scavenging mechanism, antioxidant molecule is a hydrogen donor that transforms DPPH radical into its reduced form; therefore, its radical character is neutralized and color turns into pale yellow. As DPPH has an absorbance at 517 nm, antioxidant activity of various molecules could be measured spectrophotometrically [117]. From the reduction in the absorbance of DPPH containing solutions at 517 nm, the antioxidant activity was calculated according to following formula:

$$\%\ \text{of DPPH scavenging} = \frac{(A_B - A_S)}{A_B} \times 100$$

where A_B is the absorption of the blank and A_S is the absorption of the sample [118]. The antioxidant activity of QU/β-CD-IC-PAA-films and QU/β-CD-IC-PAA-NFs were 17% and 82%, respectively. Although we applied high electrical potential on QU/β-CD-IC-PAA-NFs during electrospinning process, we

observed that QU maintained its antioxidant activity in QU/β-CD-IC-PAA-NFs, even it was much higher than QU/β-CD-IC-PAA films. In a study on shikonin loaded electrospun composite nanofibers, antioxidant activity of shikonin did not change much after electrospinning as well [114]. Secondly, the much better antioxidant activity of nanofibers compared to films was basically related with high surface area to volume ratio of nanofibers. Similar results were also observed in the literature about antioxidant property of polyaniline nanofibers. Thus, high surface area increases the availability of reaction sites and improves the antioxidant activity [118]. We also observed the changing in the color of solution that is violet in the beginning of the experiment turned into pale yellow at the end of experiment for QU/β-CD-IC-PAA-NFs [118].

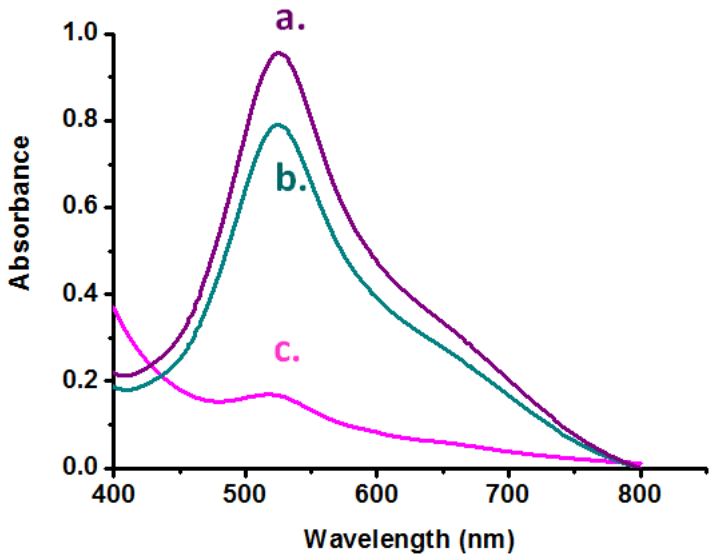

Figure 50. UV-vis spectrum of (a) DPPH, (b) QU/β-CD-IC-PAA-films including DPPH solution, (c) QU/β-CD-IC-PAA-NFs including DPPH solution.

6.8. Conclusion

We successfully produced QU/β-CD-IC-PAA-NFs. Then obtained nanofibers were crosslinked thermally without using any chemical. The structural and thermal characterizations of nanofibers were carried out by SEM, XRD, and TGA. Controlled release was achieved for QU/β-CD-IC-PAA-NFs and QU/β-CD-IC-PAA films both of the samples. However, the release of QU

from QU/β-CD-IC-PAA-NFs was slower than QU/β-CD-IC-PAA films at the initial stage. QU/β-CD-IC-PAA-NFs exhibited quite high antioxidant activity which was 65% more than QU/β-CD-IC-PAA films. As a result, QU/β-CD-IC-PAA-NFs could be used in the release of QU with high antioxidant activity.

CHAPTER VI.

CONCLUSION

In this thesis study, we produced cyclodextrin (CD) functionalized electrospun nanofibers. In the first part, we electrospun hydroxypropyl cellulose (HPC), carboxymethyl cellulose (CMC) and alginate-based nanofibers. In addition, we produced functional electrospun nanofibers from incorporating CD HPC, CMC and alginate nanofibers. These functional electrospun nanofibers have both unique properties of electrospun nanofibers like high surface area to volume ratio, porous structure at nanoscale, and ability of CD molecules to form inclusion complex with many compounds. Hence, they could be used in biomedical applications such as drug delivery, wound healing and tissue engineering.

In the second part, inclusion complex (IC) of sulfisoxazole (SFS) and hydroxypropyl-beta-cyclodextrin (HPβCD) (SFS/HPβCD-IC) incorporating hydroxypropyl cellulose (HPC) nanofibers were produced via electrospinning (SFS/HPβCD-IC-HPC-NFs). The structural and thermal characterizations were done by scanning electron microscopy (SEM), X-ray diffraction (XRD), differential scanning calorimetry (DSC) and thermogravimetric analysis (TGA). The controlled release of SFS was attained with higher release compared to SFS without HPβ-CD including HPC nanofibers. This is related with higher solubility of SFS/HPβ-CD-IC.

In the third part of thesis study, IC of α-tocopherol (α-TC) and beta-cyclodextrin (β-CD) (α-TC/β-CD-IC) was produced, and polycaprolactone (PCL) nanofibers incorporating α-TC/β-CD-IC was obtained by electrospinning (α-TC/β-CD-PCL-NFs). SEM, XRD, DSC and TGA were employed to characterize α-TC/β-CD-PCL-NFs. Controlled release was observed from α-TC/β-CD-PCL-NFs. In addition, α-TC/β-CD-PCL-NFs had higher

photostability and antioxidant activity than α-TC without β-CD including PCL nanofibers.

In the fourth part, we prepared IC of allyl isothiocyanate (AITC) and β-CD (AITC/β-CD-IC), and then AITC/β-CD-IC including polyvinyl alcohol (PVA) solution was electrospun (AITC/β-CD-IC-PVA-NFs). The structural and thermal characterizations of AITC/β-CD-IC-PVA-NFs were performed by SEM, XRD, and TGA. The amount of released AITC from AITC/β-CD-IC-PVA-NFs were considerably higher compared with AITC without β-CD including PVA nanofibers due to the inclusion complex between AITC and β-CD. Moreover, AITC/β-CD-IC-PVA-NFs showed quite high antibacterial activity against Escherichia coli (E.coli) and Staphylococcus aureus (S.aureus).

In the fifth part, IC of quercetin (QU) and β-CD (QU/β-CD-IC) incorporating polyacrylic acid (PAA) nanofibers was produced by electrospinning (QU/β-CD-IC-PAA-NFs). SEM, XRD, and TGA were the methods that we used to characterize QU/β-CD-IC-PAA-NFs. The release of QU from QU/β-CD-IC-PAA-NFs was slower and more controlled manner; whereas the antioxidant activity was significantly higher as compared to QU/β-CD-IC including films.

In brief, we produced CD and CD-IC functionalized biocompatible polymeric nanofibers (SFS/HPβCD-IC-HPC-NFs, α-TC/β-CD-PCL-NFs, AITC/β-CD-IC-PVA-NFs and QU/β-CD-IC-PAA-NFs) by electrospinning. These nanofibers can be used in drug delivery, wound healing and tissue engineering applications. We will continue our studies by incorporating another types of drug-CD-ICs into various polymers.

REFERENCES

[1] S. Ramakrishna, An introduction to electrospinning and nanofibers, World Scientific Pub Co Inc, **2005.**

[2] D. Li and Y. Xia, *Advanced Materials* **2004**, *16*, 1151-1170.

[3] S. Ramakrishna, K. Fujihara, W. E. Teo, T. Yong, Z. Ma and R. Ramaseshan, *Materials Today* **2006**, *9*, 40-50.

[4] X. Lu, C. Wang and Y. Wei, *Small* **2009**, *5*, 2349-2370.

[5] A. Greiner and J. H. Wendorff, *Angewandte Chemie International Edition* **2007**, *46*, 5670-5703.

[6] J. F. Cooley, US 692, 631, **1902.**

[7] W. J. Morton, US 705, 691, **1902.**

[8] J. F. Cooley, US 745, 276, **1903**

[9]. A. Formhals, US 1, 975, 504, **1934.**

[10]. W. Simm, K. Gosling, R. Bonart, B. von Falkai, GB 1346231,**1972.**

[11] J. Doshi and D. H. Reneker, *Journal of electrostatics* **1995**, *35*, 151-160.

[12] G. Srinivasan and D. H. Reneker, *Polymer international* **1995**, *36*, 195-201.

[13]. A. E.Zachariades, R. S. Porter, J. Doshi, G. Srinivasan, D.H. Reneker, *Polymer News* **1995**, 20 (7), 206-207

[14] C. Wang, H. S. Chien, C. H. Hsu, Y. C. Wang, C. T. Wang and H. A. Lu, *Macromolecules* **2007**, *40*, 7973-7983.

[15] G. T. Kim, J. S. Lee, J. H. Shin, Y. C. Ahn, Y. J. Hwang, H. S. Shin, J. K. Lee and C. M. Sung, *Korean Journal of Chemical Engineering* **2005**, *22*, 783-788.

[16] V. Thavasi, G. Singh and S. Ramakrishna, *Energy Environ. Sci.* **2008**, *1*, 205-221.

[17] T. J. Sill and H. A. Von Recum, *Biomaterials* **2008**, *29*, 1989-2006.

[18] P. Zahedi, I. Rezaeian, S. O. Ranaei-Siadat, S. H. Jafari and P. Supaphol, *Polymers for Advanced Technologies* **2010**, *21*, 77-95.

[19]. Biopolymers: making materials nature's way, Washington, DC: U.S. Government Printing Office, September 1993

[20] J. D. Schiffman and C. L. Schauer, *Polymer Reviews* **2008**, *48*, 317-352.

[21] M. J. John and S. Thomas, *Carbohydrate Polymers* **2008**, *71*, 343-364.

[22]. J.H. Gu, G.W. Skinner, W.W. Harcum, P.E. Barnum, *PSTT* **1998**, 1, 254-261.

[23] A. C. Stijnman, I. Bodnar and R. Hans Tromp, *Food Hydrocolloids* **2011**.

[24] A. Mohanty, M. Misra and G. Hinrichsen, *Macromolecular Materials and Engineering* **2000**, *276*, 1-24.

[25] S. Sinha Ray and M. Bousmina, *Progress in Materials Science* **2005**, *50*, 962-1079.

[26] A. Cipitria, A. Skelton, T. Dargaville, P. Dalton and D. Hutmacher, *J. Mater. Chem.* **2011**, *21*, 9419-9453.

[27]. S.H. Bahrami, A.G. Kanani, *Journal of Nanomaterials* **2010**, art. no. 724153

[28] H. Jiang, Y. Hu, Y. Li, P. Zhao, K. Zhu and W. Chen, *Journal of Controlled Release* **2005**, *108*, 237-243.

[29] E. Luong-Van, L. Grøndahl, K. N. Chua, K. W. Leong, V. Nurcombe and S. M. Cool, *Biomaterials* **2006**, *27*, 2042-2050.

[30] Z. M. Huang, C. L. He, A. Yang, Y. Zhang, X. J. Han, J. Yin and Q. Wu, *Journal of Biomedical Materials Research Part A* **2006**, *77*, 169-179.

[31] E. R. Kenawy, F. I. Abdel-Hay, M. H. El-Newehy and G. E. Wnek, *Materials Chemistry and Physics* **2009**, *113*, 296-302.

[32] J. Zeng, A. Aigner, F. Czubayko, T. Kissel, J. H. Wendorff and A. Greiner, *Biomacromolecules* **2005**, *6*, 1484-1488.

[33] P. Taepaiboon, U. Rungsardthong and P. Supaphol, *Nanotechnology* **2006**, *17*, 2317.

[34] E. R. Kenawy, F. I. Abdel-Hay, M. H. El-Newehy and G. E. Wnek, *Materials Science and Engineering: A* **2007**, *459*, 390-396.

[35] N. Charernsriwilaiwat, P. Opanasopit, T. Rojanarata, T. Ngawhirunpat and P. Supaphol, *Carbohydrate Polymers* **2010**, *81*, 675-680.

[36]. A. Chunder, S. Sarkar, Y. Yu, L. Zhai, Colloids and Surfaces B: *Biointerfaces* **2007**, 58, 172–179

[37] X. Shen, D. Yu, L. Zhu and C. Branford-White, **2010**, pp. 1-4.

[38] E. M. Del Valle, *Process Biochemistry* **2004**, *39*, 1033-1046.

[39] J. Szejtli, *Chemical Reviews* **1998**, *98*, 1743-1754.

[40] J. Szejtli, *J. Mater. Chem.* **1997**, *7*, 575-587.

[41] M. Majzoobi, R. Ostovan and A. Farahnaky, *Journal of Texture Studies* **2011**, *42*, 20-30.

[42] J. Johnson, J. Holinej and M. Williams, *International journal of pharmaceutics* **1993**, *90*, 151-159.

[43] T. Fukuyama, S. Sato, Y. Fukase and K. Ito, *Dental materials journal* **2010**, *29*, 160-166.

[44] S. Shukla, E. Brinley, H. J. Cho and S. Seal, *Polymer* **2005**, *46*, 12130-12145.

[45] L. Francis, A. Balakrishnan, K. Sanosh and E. Marsano, *Materials Letters* **2010**, *64*, 1806-1808.

[46] A. Frenot, M. W. Henriksson and P. Walkenström, *Journal of applied polymer science* **2007**, *103*, 1473-1482.

[47] L. Xie, Z. Q. Shao and S. Y. Lv, *Applied Mechanics and Materials* **2012**, *130*, 1266-1269.

[48] J. Song, N. L. Birbach and J. P. Hinestroza, *Cellulose* **2012**, 1-14.

[49] A. Steinbüchel and S. K. Rhee, *Polysaccharides and polyamides in the food industry*, Wiley-VCH, **2005**.

[50] H. Nie, A. He, J. Zheng, S. Xu, J. Li and C. C. Han, *Biomacromolecules* **2008**, *9*, 1362-1365.

[51] N. Bhattarai, Z. Li, D. Edmondson and M. Zhang, *Advanced Materials* **2006**, *18*, 1463-1467.

[52] J. W. Lu, Y. L. Zhu, Z. X. Guo, P. Hu and J. Yu, *Polymer* **2006**, *47*, 8026-8031.

[53] S. Safi, M. Morshed, S. Hosseini Ravandi and M. Ghiaci, *Journal of applied polymer science* **2007**, *104*, 3245-3255.

[54] N. Bhattarai and M. Zhang, *Nanotechnology* **2007**, *18*, 455601.

[55] S. C. Moon, B. Y. Ryu, J. K. Choi, B. W. Jo and R. J. Farris, *Polymer Engineering & Science* **2009**, *49*, 52-59.

[56] Q. S. Kong, Z. S. Yu, Q. Ji and Y. Z. Xia, *Advanced Drug Delivery Reviews* **2009**, pp. 1188-1191.

[57] H. Nie, A. He, W. Wu, J. Zheng, S. Xu, J. Li and C. C. Han, *Polymer* **2009**, *50*, 4926-4934.

[58] G. H. Kim and K. Park, *Polymer Engineering & Science* **2009**, *49*, 2242-2248.

[59]. S.I. Jeong, M.D. Krebs, C.A. Bonino, S .A. Khan, E. Alsberg, Macromolecular Bioscience 2010 10 (8) , 934-943

[60] S. A. Park, K. E. Park and W. D. Kim, *Macromolecular Research* **2010**, *18*, 891-896.

[61] S. I. Jeong, M. D. Krebs, C. A. Bonino, J. E. Samorezov, S. A. Khan and E. Alsberg, *Tissue Engineering Part A* **2010**, *17*, 59-70.

[62] S. H. Huang, T. C. Chien and K. Y. Hung, *Current Nanoscience* **2011**, *7*, 267-274.

[63] C. A. Bonino, M. D. Krebs, C. D. Saquing, S. I. Jeong, K. L. Shearer, E. Alsberg and S. A. Khan, *Carbohydrate Polymers* **2011**.

[64] C. A. Bonino, K. Efimenko, S. I. Jeong, M. D. Krebs, E. Alsberg and S. A. Khan, *Small* 2012.

[65] Y. J. Lee, D. S. Shin, O. W. Kwon, W. H. Park, H. G. Choi, Y. R. Lee, S. S. Han, S. K. Noh and W. S. Lyoo, *Journal of applied polymer science* **2007**, *106*, 1337-1342.

[66]. M.S. Islam, M.R. Karim, *Colloids and Surfaces A: Physicochem. Eng. Aspects* **2010**, 366, 135–140

[67] K. Tarun and N. Gobia, *Indian Journal of Fibre & Textile Research* **2012**, *37*, 127-132.

[68] K. Shalumon, K. Anulekha, S. V. Nair, K. Chennazhi and R. Jayakumar, *International journal of biological macromolecules* **2011**.

[69] D. Fang, Y. Liu, S. Jiang, J. Nie and G. Ma, *Carbohydrate Polymers* **2011**.

[70] T. Uyar, A. Balan, L. Toppare and F. Besenbacher, *Polymer* **2009**, *50*, 475-480.

[71] T. Uyar, R. Havelund, Y. Nur, J. Hacaloglu, F. Besenbacher and P. Kingshott, *Journal of Membrane Science* **2009**, *332*, 129-137.

[72] T. Uyar, R. Havelund, J. Hacaloglu, X. Zhou, F. Besenbacher and P. Kingshott, *Nanotechnology* **2009**, *20*, 125605.

[73] T. Uyar, R. Havelund, J. Hacaloglu, F. Besenbacher and P. Kingshott, *ACS nano* **2010**.

[74] T. Uyar, R. Havelund, Y. Nur, A. Balan, J. Hacaloglu, L. Toppare, F. Besenbacher and P. Kingshott, *Journal of Membrane Science* **2010**, *365*, 409-417.

[75] F. Kayaci and T. Uyar, *Carbohydrate Polymers* **2012**.

[76] F. Kayaci and T. Uyar, *Food Chemistry* **2012**.

[77] C. G. Park, E. Kim, M. Park, J. H. Park, Y. B. Choy, *Journal of Controlled Release* **2011**, 149, 250–257

[78] J. Zeng, X. Xu, X. Chen, Q. Liang, X. Bian, L. Yang and X. Jing, *Journal of Controlled Release* **2003**, *92*, 227-231.

[79] S. Tungprapa, I. Jangchud and P. Supaphol, *Polymer* **2007**, *48*, 5030-5041.

[80] A. Martins, A. R. C. Duarte, S. Faria, A. P. Marques, R. L. Reis and N. M. Neves, *Biomaterials* **2010**, *31*, 5875-5885.

[81] E. R. Kenawy, G. L. Bowlin, K. Mansfield, J. Layman, D. G. Simpson, E. H. Sanders and G. E. Wnek, *Journal of Controlled Release* **2002**, *81*, 57-64.

[82] S. Suganya, T. Senthil Ram, B. Lakshmi and V. Giridev, *Journal of applied polymer science* **2011**.

[83] S. Maretschek, A. Greiner and T. Kissel, *Journal of Controlled Release* **2008**, *127*, 180-187.

[84] I. Liao, S. Chen, J. B. Liu and K. W. Leong, *Journal of Controlled Release* **2009**, *139*, 48-55.

[85] L. Szente and J. Szejtli, *Advanced drug delivery reviews* **1999**, *36*, 17-28.

[86] L. Ghasemi-Mobarakeh, M. P. Prabhakaran, M. Morshed, M. H. Nasr-Esfahani and S. Ramakrishna, *Biomaterials* **2008**, *29*, 4532-4539.

[87] E. Chong, T. Phan, I. Lim, Y. Zhang, B. Bay, S. Ramakrishna and C. Lim, *Acta biomaterialia* **2007**, *3*, 321-330.

[88] G. Y. Y. J. S. Xiaofeng and Z. M. C. Zhinan, *Progress in Chemistry* **2009**, Z2.

[89] A. A. Muthu Prabhu, G. Venkatesh and N. Rajendiran, *Journal of solution chemistry* **2010**, *39*, 1061-1086.

[90] G. Gladys, G. Claudia and L. Marcela, *European journal of pharmaceutical sciences* **2003**, *20*, 285-293.

[91] A. Wei, J. Wang, X. Wang, Q. Wei, M. Ge and D. Hou, *Journal of applied polymer science* **2010**, *118*, 346-352.

[92] C. Wang, H. Tan, Y. Dong and Z. Shao, *Reactive and Functional Polymers* **2006**, *66*, 1165-1173.

[93] X. Y. Li, X. Wang, D. G. Yu, S. Ye, Q. K. Kuang, Q. W. Yi and X. Z. Yao, *Journal of Nanomaterials* **2012**, *2012*, 7.

[94] A. Celebioglu and T. Uyar, *Langmuir* **2011**.

[95] J. Panichpakdee and P. Supaphol, *Carbohydrate Polymers* **2011**.

[96] G. Maa, Y. Liua, C. Penga, D. Fanga, B. Hec, J. Niea, *Carbohydrate Polymers* **2011**, 86, 505–512.

[97] D. C. Bibby, N. M. Davies and I. G. Tucker, *International journal of pharmaceutics* **2000**, *197*, 1-11.

[98] K. Kim, Y. K. Luu, C. Chang, D. Fang, B. S. Hsiao, B. Chu and M. Hadjiargyrou, *Journal of Controlled Release* **2004**, *98*, 47-56.

[99] Q. Wang, Z. Dong, Y. Du and J. F. Kennedy, *Carbohydrate Polymers* **2007**, *69*, 336-343.

[100] J. Szejtli, Cyclodextrin Technology, Chionin Pharmaceutical – chemical works, Budapest, Hungary, Kluwer, the language of science, 1988, 188-191, 337

[101] C. Burger, B. S. Hsiao and B. Chu, *Annu. Rev. Mater. Res.* **2006**, *36*, 333-368.

[102] J. Szejtli and L. Szente, *European journal of pharmaceutics and biopharmaceutics* **2005**, *61*, 115-125.

[103] C. K. Liu, N. P. Latona and M. Ramos, *Journal of applied polymer science* **2011**.

[104] A. Iaconinoto, M. Chicca, S. Pinamonti, A. Casolari, A. Bianchi and S. Scalia, *Die Pharmazie-An International Journal of Pharmaceutical Sciences* **2004**, *59*, 30-33.

[105] A. Iaconinoto, M. Chicca, S. Pinamonti, A. Casolari, A. Bianchi and S. Scalia, *Die Pharmazie-An International Journal of Pharmaceutical Sciences* **2004**, *59*, 30-33.

[106] I. Siró, É. Fenyvesi, L. Szente, B. De Meulenaer, F. Devlieghere, J. Orgoványi, J. Sényi and J. Barta, *Food additives and contaminants* **2006**, *23*, 845-853.

[107] J. L. Koontz, J. E. Marcy, S. F. O'Keefe, S. E. Duncan, T. E. Long and R. D. Moffitt, *Journal of applied polymer science* **2010**, *117*, 2299-2309.

[108] J. Koontz, R. Moffitt, J. Marcy, S. O'Keefe, S. Duncan and T. Long, *Food additives and contaminants* **2010**, *27*, 1598-1607.

[109] T. Uyar, Y. Nur, J. Hacaloglu and F. Besenbacher, *Nanotechnology* **2009**, *20*, 125703.

[110] S. Arora, R. Bagoria and M. Kumar, *Journal of thermal analysis and calorimetry* **2010**, *102*, 375-381.

[111] B. A. Allo, A. S. Rizkalla and K. Mequanint, *Langmuir* **2010**.

[112] L. Cunha-Silva and J. J. C. Teixeira-Dias, *New J. Chem.* **2004**, *28*, 200-206.

[113] M. V. Natu, H. C. De Sousa and M. Gil, *International journal of pharmaceutics* **2010**, *397*, 50-58.

[114] J. Han, T. X. Chen, C. J. Branford-White and L. M. Zhu, *International journal of pharmaceutics* **2009**, *382*, 215-221.

[115] C. M. Sabliov, C. Fronczek, C. Astete, M. Khachaturyan, L. Khachatryan and C. Leonardi, *Journal of the American Oil Chemists' Society* **2009**, *86*, 895-902.

[116]. P.M. Bramley, I. Elmadfa, A. Kafatos, J.F. Kelly, Y. Manios, H.E. Roxborough, W. Schuch, P.J.A. Sheehy, K.H. Wagner, *J Sci Food Agric*. **2000**, 80, 913-938

[117] J. K. Moon and T. Shibamoto, *Journal of agricultural and Food Chemistry* **2009**, *57*, 1655-1666.

[118] S. Banerjee, J. P. Saikia, A. Kumar and B. Konwar, *Nanotechnology* **2010**, *21*, 045101.

[119] C. Jullian, C. Cifuentes, M. Alfaro, S. Miranda, G. Barriga and C. Olea-Azar, *Bioorganic & medicinal chemistry* **2010**, *18*, 5025-5031.

[120] J. Li, M. Zhang, J. Chao and S. Shuang, *Spectrochimica Acta Part A: Molecular and Biomolecular Spectroscopy* **2009**, *73*, 752-756.

[121] M. M. Fir, L. Milivojevic, M. Prosek and A. Smidovnik, *Acta chimica slovenica* **2009**, *56*, 885-891.

[122] K. Shalumon, N. Binulal, N. Selvamurugan, S. Nair, D. Menon, T. Furuike, H. Tamura and R. Jayakumar, *Carbohydrate Polymers* **2009**, *77*, 863-869.

[123] Y. Zhou, D. Yang, X. Chen, Q. Xu, F. Lu and J. Nie, *Biomacromolecules* **2007**, *9*, 349-354.

[124] Q. F. Zhang, Z. T. Jiang and R. Li, *European Food Research and Technology* **2007**, *225*, 407-413.

[125] X. Li, Z. Jin and J. Wang, *Food Chemistry* **2007**, *103*, 461-466.

[126] S. Hayashi, E. Nakamura, Y. Kubo, N. Takahashi, A. Yamaguchi, H. Matsui, S. Hagen and K. Takeuchi, *Acta physiologica Polonica* **2008**, *59*, 691.

[127] S. Hayashi, E. Nakamura, T. Endo, Y. Kubo and K. Takeuchi, *Inflammopharmacology* **2007**, *15*, 218-222.

[128] D. Plackett, A. Ghanbari Siahkali and L. Szente, *Journal of applied polymer science* **2007**, *105*, 2850-2857.

[129] A. C. Vega-Lugo and L. T. Lim, *Food Research International* **2009**, *42*, 933-940.

[130] Y. Ohta, K. Takatani and S. Kawakishi, *Bioscience, biotechnology, and biochemistry* **2000**, *64*, 190-193.

[131] J. H. Park, H. W. Lee, D. K. Chae, W. Oh, J. D. Yun, Y. Deng and J. H. Yeum, *Colloid & Polymer Science* **2009**, *287*, 943-950.

[132] C. C. Rusa, T. A. Bullions, J. Fox, F. E. Porbeni, X. Wang and A. E. Tonelli, *Langmuir* **2002**, *18*, 10016-10023.

[133] M. Ignatova, Z. Petkova, N. Manolova, N. Markova and I. Rashkov, *Macromolecular bioscience* **2012**.

[134] S. Xiao, M. Shen, H. Ma, R. Guo, M. Zhu, S. Wang and X. Shi, *Journal of applied polymer science* **2010**, *116*, 2409-2417.

[135]. H. Jing, Y. Jiang, X. Du,, *Proceedings of SPIE - The International Society for Optical Engineering* **2010,** art. no. 76584B

[136] S. Theron, E. Zussman and A. Yarin, *Polymer* **2004**, *45*, 2017-2030.

[137] K. McKeon Fischer, D. Flagg and J. Freeman, *Journal of Biomedical Materials Research Part A* **2011**.

[138]. Rice-Evans, C., *Free Radical Biology and Medicine* **2004**, 36 (7) , 827-828

[139] T. Pralhad and K. Rajendrakumar, *Journal of pharmaceutical and biomedical analysis* **2004**, *34*, 333-339.

[140] Y. Zheng, I. S. Haworth, Z. Zuo, M. S. S. Chow and A. H. L. Chow, *Journal of pharmaceutical sciences* **2005**, *94*, 1079-1089.

[141] C. Jullian, L. Moyano, C. Yanez and C. Olea-Azar, *Spectrochimica Acta Part A: Molecular and Biomolecular Spectroscopy* **2007**, *67*, 230-234.

[142] T. H. Wu, F. L. Yen, L. T. Lin, T. R. Tsai, C. C. Lin and T. M. Cham, *International journal of pharmaceutics* **2008**, *346*, 160-168.

[143] X. Xu, Y. Yin, X. Ge, H. Wu and Z. Zhang, *Materials Letters* **1998**, *37*, 354-358.

[144] Y. L. Li, Y. Yang, T. C. Bai and J. J. Zhu, *Journal of Chemical & Engineering Data* **2010**.

[145] X. Lu, C. Y. Tan, J. Xu and C. He, *Synthetic metals* **2003**, *138*, 429-440.

[146] P. Thitiwongsawet and P. Supaphol, *Polymers for Advanced Technologies* **2011**, *22*, 1366-1374.